Title

Climate Change and Atmospheric Aerosols: Assessing the Limits of Human Intervention in Curbing Temperature-Dependent Particulate Matter in the United States

Author

Vannucci, Pietro Federico

Publication Date

2023

Peer reviewed|Thesis/dissertation

Climate Change and Atmospheric Aerosols: Assessing the Limits of Human Intervention in Curbing Temperature-Dependent Particulate Matter in the United States

By

Pietro Federico Vannucci

A dissertation submitted in partial satisfaction of the

requirements for the degree of

Doctor of Philosophy

in

Engineering – Civil and Environmental Engineering

in the

Graduate Division

of the

University of California, Berkeley

Committee in charge:

Professor Ronald C. Cohen, Co-chair
Professor Robert A. Harley, Co-chair
Professor Joshua S. Apte

Fall 2023

Climate Change and Atmospheric Aerosols: Assessing the Limits of Human Intervention in Curbing Temperature-Dependent Particulate Matter in the United States

Pietro Federico Vannucci

Abstract

Climate Change and Atmospheric Aerosols: Assessing the Limits of Human Intervention in Curbing Temperature-Dependent Particulate Matter in the United States

by

Pietro Federico Vannucci

Doctor of Philosophy in Civil and Environmental Engineering

University of California, Berkeley

Professor Ronald C. Cohen, Co-chair
Professor Robert A. Harley, Co-chair

Decades of environmental legislation and emission reduction efforts have resulted in remarkable improvements in air quality in the United States, but we continue to find additional benefits to further abating atmospheric concentrations of toxic air pollutants such as particulate matter. This task, however, is becoming increasingly arduous on account of the current climatic transition. The atmospheric warming associated with climate change is dramatically altering the landscape of particulate matter pollution: influencing precursor emission rates, the chemical processes regulating its production, and the meteorology controlling its accumulation and dispersion. This effect is even more pronounced in urban areas, where warming is occurring fastest and where public exposure potential is greatest. Thus, continued air quality improvements in the face of climate change will necessitate a more precise understanding of the drivers of aerosol pollution that do or do not fall under our control. Focusing on summertime in the Eastern U.S., I begin by showing how the current enhancement of particulate matter with temperature is dominated by the behavior of organic aerosols, arguing that this represents a significant regulatory challenge on account of the myriad emission sources responsible for generating this subset of particulate matter. I continue by assessing the role of chemical transport models for investigating the enhancement of organic aerosols with temperature, showing how current model predictions are lacking in the representation of aerosol speciation at high temperatures, and making suggestions for future model evaluation strategies. Finally, I explore the role of meteorology in exacerbating the accumulation of pollutants, illustrating that the connection between ambient temperature and atmospheric stagnation can be exceptionally consistent, representing an amplifying factor to pollution that falls outside of our direct control but within our prognostic capabilities. Through this work, I inform strategies for probing the nature of air pollution in a warmer future, outlining the circumstances in which human intervention will be more or less effective in lessening exposure.

Non vi è sosta se non sulla cima

Acknowledgements

Among the countless people who throughout my life have contributed in some part to my personal and professional wellbeing, I would like to extend my sincere thanks to:

My advisor Ron Cohen, whose consistent guidance and reassurance made it all manageable.

Members of the Cohen group, past and present, whose pleasant company and moral support made me look forward to coming in every day. To Helen, for her mentorship when I first joined the group; to Naomi, for humoring my inane programming questions and for all the tomatoes; to Anna, for pushing me in all my athletic endeavors; to Milan, for his company on site visits and for diligently carrying the BEACO2N PM torch; and to Yishu, for her mastery in all things snack and drink.

The members of my committee, Rob Harley and Josh Apte, for being both excellent lecturers as well as mentors, keeping me in good hands as a I pursued this degree straddled between two departments.

The entire CEE Airheads community, for graciously welcoming me and making me feel at home at Berkeley from the very beginning as a source of academic inspiration and companionship.

My ORISE mentor Havala Pye, who not only elevated and significantly expanded my research efforts, but also personally supported me during my time in North Carolina.

Kristen, Ben, and Christian, among the many researchers at the EPA who kindly dedicated time to contribute to the development and presentation of my work.

Drew Ells, for pushing me to enter this field in the first place and for encouraging me to apply to this program when I refused to believe I might belong here.
Juan Meriles, for watching my back on our excursions and for providing excellent competition on and off the bike.
Gwyne Henke, for her unwavering faith in me as a person which has carried me through so many stages of my life.

My older sister, Bianca, who has led me by example since day one.
My younger sister, Angelica, whose admiration compels me to be the person she thinks I am.
My parents, Andrea and Laura, who made innumerable sacrifices to provide the means for us to attain everything we chose to pursue.

My wife, Dewi, whose love, patience, selflessness, patience, trust, and patience sustained me in every way imaginable and gave me reason to be and to do.

Chapter 1: Introduction

Air pollution is among the greatest global public health hazards, representing the fourth most relevant risk factor for disease and mortality[1]. Exposure to air pollution harms the individual both in the short and long term, leading to cardiovascular, respiratory, and cerebrovascular diseases[2–5]. Exposure to air pollution also negatively impacts society at large, with costs related to healthcare expenses and lost productivity worldwide totaling in the trillions of U.S. dollars annually[6]. Though the risks posed by air pollution are universal, its public health burden is both disproportionately distributed and disparately characterized, with lower-income countries generally facing greater exposure while having fewer means for monitoring air pollution[7]. Therefore, it is imperative that we continue refining our understanding of the sources of air pollution and the drivers of high exposure events with the goal of improving our predictive capabilities and better informing future policy directives that might lead us to a cleaner, healthier, and more equitable world.

Air pollution can take on many forms, but the most relevant species of interest tend to include carbon monoxide (CO), nitrogen dioxide (NO_2), sulfur dioxide (SO_2), ground-level ozone (O_3), a myriad of toxic organic molecules (e.g. benzene), and aerosols, otherwise referred to as particulate matter (PM). These pollutants enter the atmosphere either directly from primary emissions, from secondary formation, or a combination of both. Therefore, we care about these species both for their immediate impact on human health through inhalation as well as the role they might play in promoting the formation of additional pollutants. In this work, I focus primarily on the processes which govern the emissions, formation, accumulation, and removal of PM in our atmosphere, but it is important to note that these processes are profoundly intertwined with the above-mentioned gaseous pollutants, and a broad understanding of the system is necessary to assess the multitude of fates concerning atmospheric aerosols.

A critical consideration with regards to the future of air quality and public health is the current climatic transition. Since the advent of the Industrial Revolution and the widespread adoption of fossil fuels, anthropogenic activities have resulted in a dramatic increase in emissions of both air pollutants and greenhouse gases (GHGs) such as carbon dioxide (CO_2) and methane (CH_4). The GHG emissions injected into our atmosphere have led us down a path of rapid warming and increased climatic variance, a trend that will likely persist, if not worsen, in the coming decades[8]. Facing unprecedented environmental variance and given that climate change and air pollution are intrinsically linked both by their shared sources and by the spatial domain they occupy, it is critical that we consider their synergistic interactions, how rising temperatures might influence pollutant emissions, atmospheric chemistry, and meteorology, and how the compounding effect of climate change on air pollution will impact public health. Several studies have examined this matter, highlighting a multitude of methods in which climate change has the potential to exacerbate future air quality concerns[9–16]. In my research, I have tried to expand on this body of work through the lens of identifying the extent to which management strategies effective for minimizing air pollution will change over time. My goal is to contribute to elucidating the suite of effective policy decisions for abating future air pollutant exposure in the context of a rapidly warming climate.

In this introduction, I will summarize current understanding of connections between climate and PM, highlighting what are considered to be the most relevant factors, identifying knowledge gaps, and describing how my research has contributed to a deeper understanding of

this topic. In my work, I focus principally on summertime phenomena because in future years, as average global temperatures continue to rise, summers will become longer, harsher, and exhibit greater variability[8]. Therefore, understanding the implications of a more extreme summertime on air pollution will become increasingly critical for estimating the overall public health burden. I will begin by briefly characterizing the various types of PM and continue by elaborating on the manner through which climate change and rising temperatures are thought to play a role in modulating their influence, delineating between impacts on emissions, chemistry, and meteorology.

Types of Particulate Matter

Primary PM

Primary PM is the class of aerosols that are emitted directly into the atmosphere. A major subset of primary PM can be thought of as mechanically generated. Natural sources include wind-blown dust, which typically consists of minerals and soils and can be transported thousands of kilometers from the source region[17–19], sea spray aerosols (SSA), which carry both salts and a wide variety of organic species into the atmosphere, impacting coastal air quality and influencing the formation of secondary aerosols as well as clouds[20], and volcanic eruptions, which release significant quantities of sulfurous gases and aerosols[21].

Many anthropogenic activities are also responsible for mechanically-generated PM. Driving, for example, can result in PM emissions from the abrasion of paved surfaces, the resuspension of dust and soil, and from the wear generated on vehicle components such as brakes and tires[22–24]. A wide array of similar activities linked to construction, transportation, farming, and other industries contribute to direct mechanical generation of PM.

Another major subset of primary PM is that which is emitted as a result of combustion processes, both biogenic and anthropogenic. Wildfire emissions, for example, represent a significant biogenic source of both organic carbon (OC) and black carbon (BC) aerosols. Similarly, the deliberate combustion of various types of organic matter, wood, charcoal, coal, oil, and other fossil fuel derivatives for cooking, heating, transportation, waste disposal, and energy generation also release large amounts of organic and inorganic primary PM[25–28].

Secondary PM

Secondary PM is the class of aerosols formed in the atmosphere as a result of chemical processes which transform and aggregate gaseous species into solid and liquid particles. The most common secondary inorganic aerosols (SIA) are sulfate (SO_4^{2-}), nitrate (NO_3^-), and ammonium (NH_4^+), formed from the oxidation of sulfur dioxide (SO_2), nitrogen oxides ($NO_x \equiv NO + NO_2$), and the protonation of ammonia (NH_3), respectively. It is worth noting that SIA can originate both from natural sources (e.g. SO_2 from volcanic emissions or sea spray and NO_x/NH_3 from soil emissions) as well as from anthropogenic sources (e.g. SO_2 from coal combustion, NO_x from a wide variety of combustion sources, and NH_3 from the use of fertilizer in agricultural applications).

Secondary organic aerosols (SOA) can also result from both biogenic and anthropogenic processes, both forms occurring from the oxidation of volatile organic compounds (VOCs)[29–32]. Biogenic VOCs emitted from vegetation such as isoprene and monoterpenes are a major contributor to SOA. Wildfire emissions of organic compounds can also be a source of SOA[33]. Anthropogenic VOCs then represent a wide spectrum of molecules arising from a multitude of

industrial processes. These processes include solvent use, evaporative losses of stored chemicals and fuels, asphalt emissions[34,35], incomplete combustion, emissions of volatile chemical products (VCPs)[36–38] used in personal care and home cleaning, etc.[34,39–42]. It is then the interaction between precursor emissions, availability of oxidizing species, and abundance of preexisting aerosol that determines the SOA formation potential of these molecules.

Decadal Trends in Particulate Matter

We can begin by considering trends in average $PM_{2.5}$ (PM with diameter <= 2.5 microns) concentrations across the continental United States (CONUS) over the last twenty years. I do so by querying observations from the U.S. Environmental Protection Agency Air Quality System (EPA AQS). AQS sites, recording total $PM_{2.5}$ observations on a daily basis and $PM_{2.5}$ speciation observations on a 1-in-3-day schedule, allow us to probe long-term trends in the concentrations of $PM_{2.5}$ and its major components at a glance. In terms of total $PM_{2.5}$, we find that the air pollution control schemes of the last two decades have been successful in reducing average concentrations from ~14 $\mu g/m^3$ in 2000 to ~8.5 $\mu g/m^3$ in 2020. However, investigating trends in individual components is necessary for informing our future control strategies. For example, in Figure 1.1 we see that whereas the bulk of inorganic $PM_{2.5}$ components (sulfate, ammonium, and nitrate aerosols) have been declining steadily from 2000-2020, organic carbon $PM_{2.5}$ shows a different trend, with average concentrations rising again in recent years. This reversal, likely driven by increasing wildfire emissions[43], is a useful representation of the fact that not all types of PM can be regularly controlled via policy and human intervention. Moreover, it suggests that continuing to decrease total $PM_{2.5}$ concentrations in future years will increasingly necessitate targeting organic aerosols.

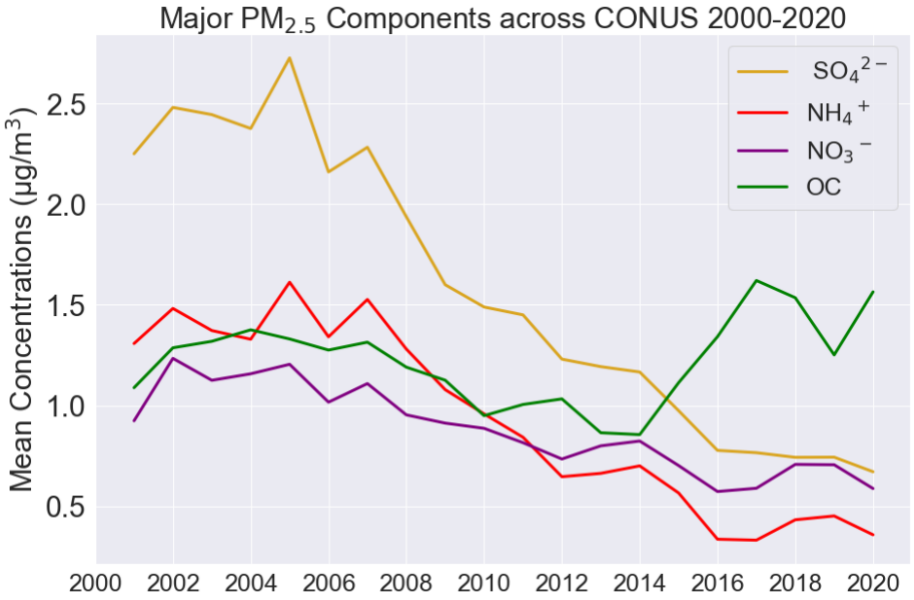

Figure 1.1: Decadal trends in average concentrations of major $PM_{2.5}$ constituents across CONUS, with observations from EPA AQS sites.

Climate Change Impacts on Particulate Matter

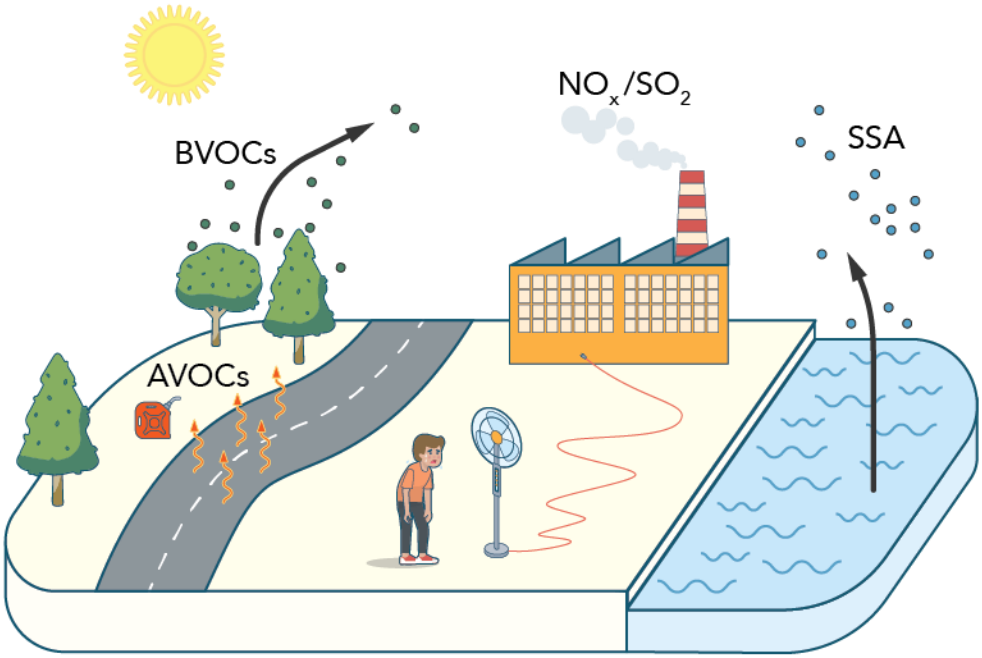

Figure 1.2: Graphic depicting a selection of the many pathways through which a warming climate has the potential to influence aerosol production, by increasing: evaporative emissions of anthropogenic VOCs, asphalt emissions, emissions of biogenic VOCs from vegetation, emissions linked to energy production to meet cooling demand, and direct emissions of sea spray aerosols.

Primary PM

Climate change and rising temperatures have the potential to influence direct emissions of primary PM in a number of ways. First, warmer temperatures exacerbate the risk of wildfires by drying out vegetation and depleting sources of water. In the Western United States, for example, the increased aridity combined with the excess heat greatly exacerbates the frequency and severity of wildfires, a major source of PM that is also expected to continue growing in relevance[44–47].

In addition, while there is still much uncertainty in how global and regional precipitation patterns will evolve as a result of climate change, predictions agree that increases in temperature and rainfall variability as well as extreme events are highly likely[48–50]. As wet deposition is one of the major removal mechanisms for atmospheric aerosols, these changes will no doubt affect aerosol abundance. Also, more frequent droughts will lead to greater uplifting and transport of surface dust. An example of this is the historical event commonly known as the Dust Bowl, where suboptimal farming techniques compounded by droughts in the American Great Plains of the 1930s led to substantial erosion of the topsoil and a subsequent period of severe dust storms. This phenomenon has also been explored more recently on a smaller scales, where elevated temperatures have been found to be associated with greater road dust emissions on account of enhanced surface drying[51].

Finally, shifting focus to marine aerosols, studies have identified a connection between SSA emissions and sea surface temperature[52–54]. This effect was found to be significant and distinct from the relationship between temperature and wind speed, which also regulate the churning of water at the surface and the release of particles. As atmospheric and oceanic temperatures continue to rise[55], emissions of SSA are also expected to grow concurrently.

Secondary PM

Climate change can also drive changes in the emissions of precursor gases leading to secondary PM formation, both directly and indirectly. One direct mechanism is that elevated temperatures will enhance emissions of biogenic VOCs (BVOCs). Isoprene and monoterpenes are emitted ubiquitously from vegetation in large quantities and exhibit a strong response to temperature[29]. Reacting with oxidants in the presence of sunlight to produce both O_3 and PM, BVOCs can thus amplify the pollution from anthropogenic emissions in a temperature dependent manner[56–58]. This enhancement in SOA from BVOC emissions due to warm temperatures has already been identified in observations at regional and urban scales and is projected to increase in magnitude [59]. This is also specifically relevant to human health because SOA are associated with a higher cardiorespiratory disease mortality than other PM components[60].

Another direct manner in which rising temperatures can affect the emissions of secondary PM precursors is through enhanced evaporation of semi-volatile and intermediate-volatility organic compounds such as from motor vehicles[61,62], building products[63], and asphalt[35]. Recent research has shown how the fate of these intermediate volatility species is highly relevant for explaining the abundance of urban SOA; therefore, temperature-dependent increases in volatility and emissions from this sector will be important in influencing air pollutant exposure in cities[64–66]. Additionally, the inclusion of intermediate-volatility organic compounds in emission inventories has been found to impact modeled SOA predictions in a temperature-dependent manner[37].

Additionally, climate change might indirectly lead to greater emissions of secondary PM precursors due to influencing human behavior. For example, emissions from the energy sector can be impacted by temperature due to the incidence of increased air conditioning usage and the subsequent electricity demand on warmer days. This phenomenon has been observed in the Eastern United States, for example, where powerplant emissions of CO_2, SO_2, and NO_x ($NO_x \equiv NO + NO_2$) in the summertime have exhibited robust linear correlations with temperature[67]. Emissions of these pollutants are not only linked to emissions of primary PM but also to the subsequent oxidation of SO_2/NO_x, leading to temperature-dependent enhancements in secondary PM formation[68]. Though decadal improvements in emission control strategies have reduced absolute emissions of these pollutants, the positive response to heightened temperatures has remained consistent. This is also exacerbated by the fact that energy demand in the hottest periods can necessitate the use of "peaker" electricity generating units, facilities that often employ dirtier fuel sources and are regulated through looser air quality guidelines[69]. The persistence of this trend will depend on the sources fueling our electricity generation in order to meet the increased demand. A recent modeling analysis shows how rising temperatures and the associated cooling required would result in significantly increased air pollution and mortality by the middle of this century, emphasizing the need for a transition to cleaner energy sources and greater energy efficiency[70].

Other means through which climate change may impact secondary PM abundance is through the influence of rising temperatures on reaction rates and the chemical transformations

of PM precursors. A notable example in this is the documented relationship between temperature and the rate of oxidation of SO_2 into SO_4^{2-} aerosols[71]. Temperature can also contribute to reductions in aerosol mass, however, as is the case with nitrate aerosols volatilizing back to the gas phase at higher temperatures[11,72]. The relevance of this effect, however, is difficult to constrain, especially relative to the aforementioned ways in which increased vapor pressures are likely to contribute to enhanced secondary PM formation through other channels. Moreover, in the context of a future where anthropogenic emissions of SO_2 and NO_x are increasingly regulated, inorganic secondary aerosols may become less relevant in driving high PM concentration events. Nevertheless, a greater understanding of the impact of rising temperatures on the chemistry driving PM formation and removal will be important for constraining the influence from other factors such as changes in emissions and meteorology.

Climate Change and Meteorology

In delineating the numerous and often intertwined ways in which climate change will impact atmospheric concentrations of pollutants, we cannot ignore potential changes in meteorological patterns. We have already briefly touched on how changes in precipitation patterns are likely to impact aerosol removal mechanisms as well as surface moisture and dust emissions, but future trends in this chaotic system are hard to forecast. There are, however, more predictable consequences of increased summertime temperatures. For example, warm summer days are often associated with stagnation conditions. During periods of atmospheric inversions, when both planetary boundary layer (PBL) height and wind speed are low, the lack of ventilation and dispersion leads to accumulation of pollutants. Various studies conducted in China, Europe, and North America have found significant associations between temperature, stagnation episodes, and elevated concentrations of O_3 and PM[73–77]. The complex nature of the O_3-Temperature relationship is outside the scope of this review, but a study looking specifically at meteorological drivers of this relationship has shown that a large proportion can be explained by temperature-driven atmospheric stagnation[78]. Additionally, modeling analyses indicate that the incidence of stagnation episodes is projected to grow in the coming decades due to climate change[79–81].

Climate Change and Urbanization

The association between a warming climate, air quality, and public health is also significant because we are currently experiencing a rapid population shift from rural areas to urban ones. This densification of both sources of emissions and receptors of pollutants represents a heightened influence of the detrimental effects of poor air quality[82]. Moreover, due to the radiative absorption associated with the built environment, urban spaces generally experience warmer temperatures than the less-developed surroundings, this is commonly referred to as the "urban heat island effect"[83]. This effect can therefore exacerbate the air quality issues plaguing urban areas. We can examine this phenomenon by considering decadal trends in average temperatures over CONUS in rural versus urban areas. In Figure 1.3, I investigate this matter by looking at temperature trends in two regimes: the dense urban domains (defined as areas with a population density greater than 1000 people per square kilometer) and the rural spaces (defined as the least populated settlements with a density of 1-10 people per square kilometer). Utilizing population density data from the NASA Socioeconomic Data and Applications Center[84], I take five-year averages of temperatures in these two regimes sourced from ERA5 reanalysis data provided by the European Centre for Medium-Range Weather Forecasts (ECMWF)[85] and

compare trends from 2000-2020 to the baseline year 2000 level. Comparing these two regimes across the past two decades tells us that on average, urban areas are ~3.3 K warmer than their rural counterparts. Moreover, Figure 1.3 shows how the increase in temperature over the last 20 years has been more pronounced in urban versus rural areas, and that this difference is growing with time. These findings match a recent global analysis which found that on average urban clusters have exhibited ~30% greater warming than the rural background in the last two decades[86]. The continuation of this trend thus suggests that the additional warming over urban spaces will compound the temperature-dependent drivers of air pollution in an increasingly damaging manner. For this reason, large population centers are likely to experience more damaging effects from climate change than regional trends would suggest, an important consideration for public health forecasting.

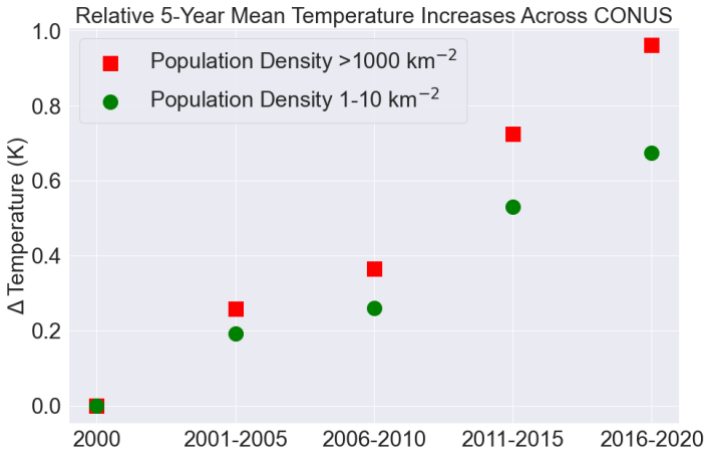

Figure 1.3: Relative increases (from a year 2000 baseline) in average five-year temperatures across CONUS in areas of population density greater than 1000 people per km^2 versus areas with 1-10 people per km^2.

Summary

In this overview, I have described current understanding of climate impacts on aerosols from multiple perspectives. In the following chapters I explore some of these issues in detail.

In Chapter 2, I focus on temperature dependent SO_2 emissions from electricity generating units of the Northeast U.S. As previously outlined, summertime power plant emissions of both NO_x and SO_2 in this domain exhibit a linear response to temperature on account of increased electricity consumption linked to air conditioning usage on warmer days. Through the subsequent conversion of SO_2 to SO_4^{2-} aerosols, this phenomenon has driven a substantial temperature dependent increase in $PM_{2.5}$ across the Northeast U.S. For this reason, the highest summertime $PM_{2.5}$ concentrations have long been associated with the warmest temperatures. Decadal reductions in coal combustion have significantly abated emissions of SO_2. In doing so, we find a concurrent decrease in temperature dependent SO_4^{2-} aerosols. Despite these reductions, average summertime $PM_{2.5}$ concentrations continue to exhibit a robust dependence on temperature. In more recent years, however, this increase is now chiefly attributable to organic aerosols, the formation of which responds to temperature on account of increased BVOC emissions. Therefore, though the drivers of enhanced $PM_{2.5}$ with temperature have shifted, we continue to observe the highest concentrations on the hottest days. This transition presents new challenges in our efforts to continue reducing $PM_{2.5}$, suggesting that combating future high $PM_{2.5}$

concentration events will involve targeting a different class of emissions. Specifically, I present how the growing relevance of organic aerosols in controlling summertime $PM_{2.5}$ necessitates a more precise understanding of their origins and whether the emissions or chemical processes driving this enhancement can be controlled via policy or not.

In Chapter 3, I continue exploring trends in the Eastern U.S. summertime with the goal of further elucidating the present-day drivers of elevated $PM_{2.5}$ with temperature. In this subsequent analysis, I utilize an atmospheric chemical transport model (CTM) to probe the mechanisms relevant for describing the $PM_{2.5}$-temperature response of both SO_4^{2-} and organic aerosols. For the study period of June-August 2019, observations in the Eastern U.S. show a significant temperature response for total $PM_{2.5}$ of ~0.67 $\mu g/m^3/K$, and the Community Multiscale Air Quality (CMAQ) v5.4 regional model predictions closely match this value. However, the model predictions feature component-specific discrepancies with observations. Specifically, the model underestimates SO_4^{2-} concentrations and their increase with temperature while simultaneously overestimating OC concentrations and their increase with temperature. Performing a series of model sensitivity simulations, I identify potential reasons for why model predictions fail to accurately describe the observed trends in both species, probing changes in emissions as well as formation and removal mechanisms. In doing so, I find that the coupling between the SO_4^{2-} and OC systems necessitates a holistic approach to model design, and it is possible to design interventions that simultaneously address the biases in $PM_{2.5}$ components as well as their response to temperature in a synergistic manner. This analysis thus suggests ways to advance CTM performance by improving its capabilities across a wider range of environmental conditions while simultaneously providing insight into species and processes pertinent to describing the summertime SO_4^{2-} and OC response to increasing temperatures. This is relevant because a model that can accurately replicate the observed temperature dependence of $PM_{2.5}$ and its components is essential to having confidence in predicting the future of aerosols in a warmer world and to evaluating policy options for curbing high summertime PM.

In Chapter 4 I turn my attention to enhancements in air pollution driven by temperature-dependent stagnation events. Focusing on the Los Angeles metro area, I build on past work looking at the relationship between elevated NO_x and temperature in this domain[87]. Though this trend was previously identified, no satisfactory causal explanation has been outlined. Here, I demonstrate how the enhancement of NO_x concentrations with temperature is driven by nighttime stagnation episodes that are distinct from daytime trends. Warm nighttime conditions, marked by low planetary boundary layer heights and decreased ventilation, represent greater risks for exposure due to the accumulation of pollutants. High nighttime concentrations therefore have an outsized influence in driving overall daily means. I analyze 20 years of observations from LA to show how relative increases in NO_x with temperature are consistent over time and are therefore independent of the dramatic decadal decreases in emissions. Moreover, by showing that concentrations of carbon monoxide (CO) mirror the same trends, I suggest that a common meteorological factor is influencing the ensemble rather than temperature-dependent chemistry. I conclude by showing how these temperature-dependent stagnation episodes are driving exceedances in daily average NO_2 concentration guidelines. Though exceedances are less prevalent in the present day than they were in past years in absolute terms, their incidence is more strongly correlated with temperature than before, suggesting that the role of temperature as a control for dangerously elevated NO_x concentrations is growing. Though I present an analysis chiefly concerned with NO_x, largely due to data availability considerations, my results are representative of larger trends that extend beyond the city in question and the pollutants

described. This analysis highlights the value of considering the public health burden of air pollution on diurnal time scales, how nighttime may come to dominate over daytime trends, and the ways in which trends in exposure risks may be distinct from trends in air pollutant emissions and formation.

My research has thus advanced understanding of the influence of climate change on air pollution and public health from multiple angles: I have explored the evolution of $PM_{2.5}$ components controlling temperature-dependent high concentration events, noting the implications for the class of emissions meriting increased focus going forward; I have developed a novel lens for evaluating CTM performance, informing model design strategies as well as establishing a basis for identifying atmospherically relevant chemical mechanisms linked to the formation and removal of temperature dependent $PM_{2.5}$; finally, I have highlighted a new perspective regarding the link between rising temperatures and the growing incidence of stagnation episodes, detailing the importance of considering diurnal trends for assessing exceedances in air pollutant guidelines. My analyses thus contribute to the body of work concerned with quantifying the effects of climate change on air pollution and delineating the future strategies that will be more or less effective in mitigating a portion of the environmental threats we are likely to face in the coming years.

Chapter 2: Decadal Trends in the Temperature Dependence of Summertime Urban PM 2.5 in the Northeast United States

This chapter was adapted from: Vannucci, P. F.; Cohen, R. C. Decadal Trends in the Temperature Dependence of Summertime Urban $PM_{2.5}$ in the Northeast United States. *ACS Earth Space Chem.* **2022**, acsearthspacechem.2c00077. https://doi.org/10.1021/acsearthspacechem.2c00077.

Abstract

Temperature has been identified as a key control over particulate matter of diameters smaller than 2.5 microns ($PM_{2.5}$), however, the mechanisms controlling this phenomenon in urban areas have not been definitively elucidated. With increasing urbanization and associated heat-island effects as well as a warming climate, understanding the role that temperature plays in modulating urban aerosol mass is critical. We explore the link between temperature and aerosol mass using observations from seven cities in the Northeast U.S., finding that summertime $PM_{2.5}$ exhibits a strong linear dependence on temperature going back at least two decades. Early in this record, the leading cause of the $PM_{2.5}$ mass increase with temperature was an increase in the ammonium sulfate aerosol mass. We suggest this was due to increased electricity consumption to support air conditioning on warmer days and the associated SO_2 emissions from coal burning power plants. Later in the record and in the present day, the leading cause of the linear correlation of $PM_{2.5}$ mass with temperature is the increase in organic aerosol mass with temperature. Effective policy for curbing high $PM_{2.5}$ events in the future will depend on understanding the factors influencing this temperature-dependent enhancement in organic aerosol specifically; whether they are related to biogenic emissions, anthropogenic emissions, or chemical processes.

Introduction

Particulate matter of a diameter smaller than 2.5 μm ($PM_{2.5}$) is a significant public health hazard; exposure to $PM_{2.5}$ has been linked to elevated occurrences of respiratory and cardiovascular diseases, increases in hospital admissions, and millions of deaths per year[88]. Understanding the drivers of $PM_{2.5}$ is critical for efficient and effective policy guiding reductions in $PM_{2.5}$ and improving public health outcomes. $PM_{2.5}$ can enter the atmosphere in the form of direct emissions from biomass burning, fossil fuel combustion, agricultural activities, volcanic eruptions, sea spray, etc. as well as from secondary processes where chemical reactions transform volatile precursors, both biogenic and anthropogenic, into non-volatile compounds that accrete to existing particles or form new ones. As cities around the world transition towards cleaner sources of energy, improve the energy efficiency of and add emission controls to industrial and transportation systems, primary emissions of $PM_{2.5}$ will continue to decrease.

This is also the case for secondary inorganic aerosols; the two most prevalent components being sulfate and nitrate. Sulfate aerosols, commonly in the form of ammonium sulfate ($(NH_4)_2SO_4$), are formed through oxidation of sulfur dioxide (SO_2) which has its main source in the emissions of coal-fired power plants. SO_2 emissions and sulfate aerosol concentrations have been declining steeply around the world[89–91]. Nitrate aerosols are formed from the oxidation of

nitrogen oxides ($NO_x \equiv NO + NO_2$), and these emissions have also been declining significantly both in the United States[92,93] and globally[94].

Secondary organic aerosols (SOA) stemming from both biogenic and anthropogenic sources typically make up about half of $PM_{2.5}$[95–97]. Anthropogenic volatile organic compound (VOC) emissions have been dramatically reduced through regulations on solvent use, reductions of evaporative emissions associated with fuels, the use of catalytic converters on gasoline powered passenger vehicles, and other emission control systems used on electric generation facilities and diesel vehicles. These reductions have resulted in a notable decrease in associated SOA concentrations[98].

With the reduction of many combustion-related anthropogenic sources of SOA, the role of biogenic emissions and volatile chemical products (VCPs) in urban aerosol formation has taken on more prominence[36]. If biogenic emissions are now a dominant feature in SOA production, then temperature should be playing an increasing role as a control over the frequency of the highest aerosol events. For example, decadal reductions in anthropogenic emissions have changed the nature of $PM_{2.5}$ in the Los Angeles (LA) basin[99]. Whereas in the past, $PM_{2.5}$ in LA did not exhibit a strong dependence on temperature, in more recent times the highest concentrations of $PM_{2.5}$ occur at the highest temperatures and the $PM_{2.5}$ at high temperatures is increasingly organic. Research on VCPs is in an early stage, however to our knowledge no suggestion that VCPs are temperature dependent has been published. If VCP are not temperature dependent, then the observed temperature dependence of organic aerosol strongly points to a biogenic source or to temperature-dependent chemistry that accelerates the conversion of VOC to aerosol as temperature warms.

To explore the role of temperature as a cause of high aerosol events in cities, now, and in the future as anthropogenic emissions of SO_2, NO_2, and VOCs from transportation continue to decrease, it is useful to have a perspective on the response of aerosol to temperature that expands beyond Los Angeles. Here we examine the relationship between temperature and $PM_{2.5}$ in cities in the Northeast United States. The composition of urban $PM_{2.5}$ in the Northeast differed significantly from California because of the much more important role of sulfate over the last 20 years[90,100]. Throughout the last 20 years, a linear increase in $PM_{2.5}$ with temperature is observed. Due to increased cooling demand on warmer days and the consequent energy consumption, met in part by coal-fired power plants, SO_2 emissions in the Eastern U.S. summertime are temperature dependent[67]. Early in the record, the conversion of these emissions to sulfate aerosols explains most of the observed temperature dependence. This explanation for the temperature dependence of $PM_{2.5}$ and sulfate differs from most prior analyses that focused on stagnation and the accelerated conversion of SO_2 to sulfate as temperature warms[101–104].

With the dramatic decrease of SO_2 emissions from the region's coal-fired power plants, sulfate aerosol mass has decreased. Still, we find that a strong, linear temperature dependence of aerosol mass remains. We describe this transition and the current role of organic aerosols (OA) as a primary feature in the temperature dependence of urban aerosol in the region.

Observations

Seven cities in the Northeast U.S. were chosen for analysis of the temperature dependence of $PM_{2.5}$ aerosol: Baltimore, MD; Boston, MA; Buffalo, NY; New York, NY; Philadelphia, PA; Providence, RI; and Washington, D.C. These cities all had relatively complete records (>90% data availability within period of study) of aerosol, aerosol composition, and meteorological observations located near or at the aerosol measurement sites. The observations

were obtained from the United States Environmental Protection Agency Air Quality System (US EPA AQS) and the associated Chemical Speciation Network (CSN). The period studied spans the months of June to August for the years 2000 to 2020. $PM_{2.5}$ mass, NO_x concentrations, and temperature are used in this analysis. Some observations are available hourly, others as 24-hour averages recorded daily and others as 24-hour averages on 3-day intervals. $PM_{2.5}$ speciation values were available as noted in Appendix A, Table A.1 along with identifying information pertaining to the specific AQS sites in each city. Where one site was not sufficient to describe the full period of speciation data, a nearby site also located within the same urban region was used to supplement the record. All $PM_{2.5}$ values were recorded at a fixed relative humidity and therefore do not reflect the effects of hygroscopic growth. Finally, organic carbon (OC) speciation data was only available from June-August 2016-2020.

Data was first screened for negative values and obvious outliers (values two to three orders of magnitude greater than adjacent points), and then grouped by subperiod (2000-2005, 2006-2010, 2011-2015, 2016-2020). Data availability varies across cities and subperiods (with more recent data usually being more complete) and we see this reflected in the higher variance associated with observations from the earlier subperiods.

At the beginning of the millennium (2000-2005), ammonium sulfate (ASO_4) comprised on average 51% of summertime $PM_{2.5}$ mass across the seven cities, with total $PM_{2.5}$ concentrations averaging around 16.9 $\mu g/m^3$. In more recent times (2016-2020), ASO_4 comprises only about 16% of summertime $PM_{2.5}$, with total $PM_{2.5}$ concentrations averaging 8.0 $\mu g/m^3$. We find that the mass of NH_4 reported is a stoichiometric match to the sulfate mass and thus report ASO_4 as the sum of the two without further adjustment.

At the same time as the total $PM_{2.5}$ mass and the sulfate fraction decreased, the temperature dependence of $PM_{2.5}$ also decreased. In the seven cities, summertime $PM_{2.5}$ mass and ASO_4 mass shows a strong linear correlation with temperature throughout the record. Figure 2.1 shows the example of Washington, D.C. Early in the record, the slope of $PM_{2.5}$ mass vs. temperature was 2.0 ± 0.5 $\mu g/m^3/°C$, whereas in the most recent subperiod the slope was 0.6 ± 0.2 $\mu g/m^3/°C$. For ASO_4, early in the record, the slope vs. temperature was 1.3 ± 0.4 $\mu g/m^3/°C$, whereas in the most recent subperiod the slope was 0.2 ± 0.05 $\mu g/m^3/°C$. Parameters describing the linear fits to observations for all seven cities in each of the four time periods aggregated in Figure 2.1 are listed in Table 2.1. Sets of figures showing this relationship for the other six cities not featured here are displayed in Figures A.1 and A.2 of Appendix A.

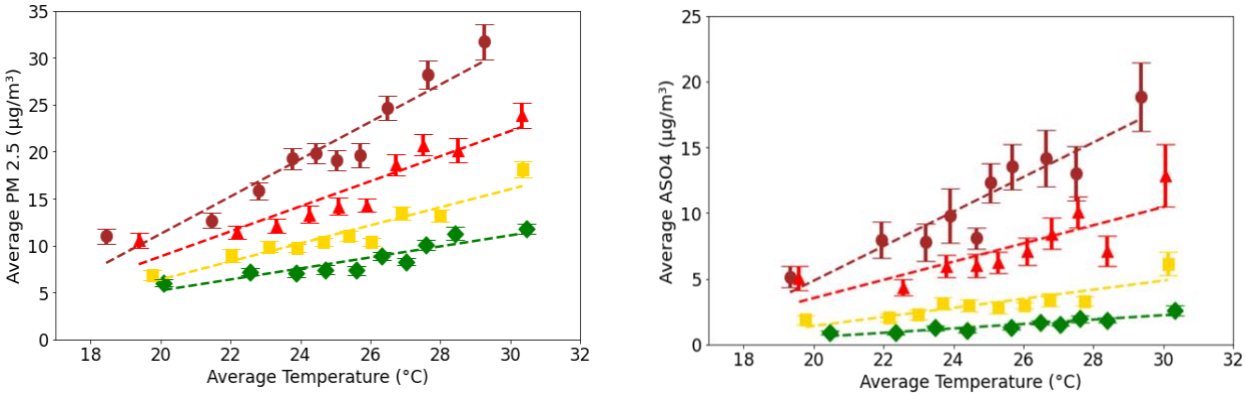

Figure 2.1: (Left) $PM_{2.5}$ and (Right) ASO_4 mass concentrations vs. temperature for Washington, D.C. ● : 2000-2005; ▲: 2006-2010; ■ : 2011-2015; ◆ : 2016-2020. The range shown at each point represents the central 66% of the distribution in that bin.

To confirm that this phenomenon is not a result of the correlation of stagnation with warmer temperatures, we examined the temperature dependence of nitrogen dioxide (NO_2). Figure 2.2 shows that there is a slight increase in the NO_2 concentration that is correlated with temperature early in the record, but the slope is much, much less than observed for ASO_4 or $PM_{2.5}$. Later in the record the slope is near zero. Nitrate aerosol mass (also investigated but not shown), decreases linearly with temperature early in the record, presumably because of displacement by sulfate. Later in the record, the nitrate temperature relationship follows that of NO_2.

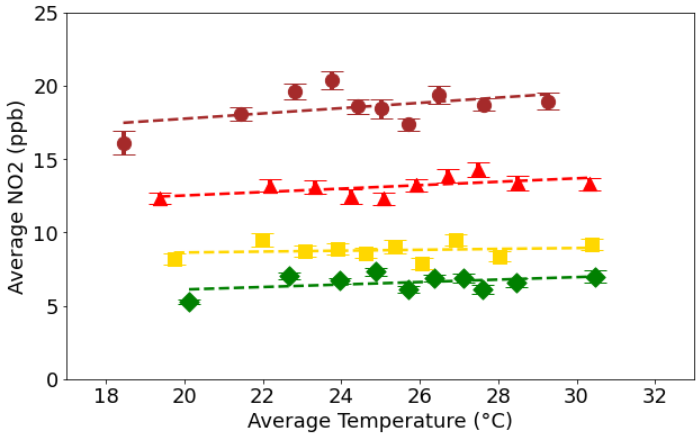

Figure 2.2: NO_2 concentrations vs. temperature for Washington, D.C. ● : 2000-2005; ▲: 2006-2010; ■ : 2011-2015; ◆ : 2016-2020. The range shown at each point represents the central 66% of the distribution in that bin.

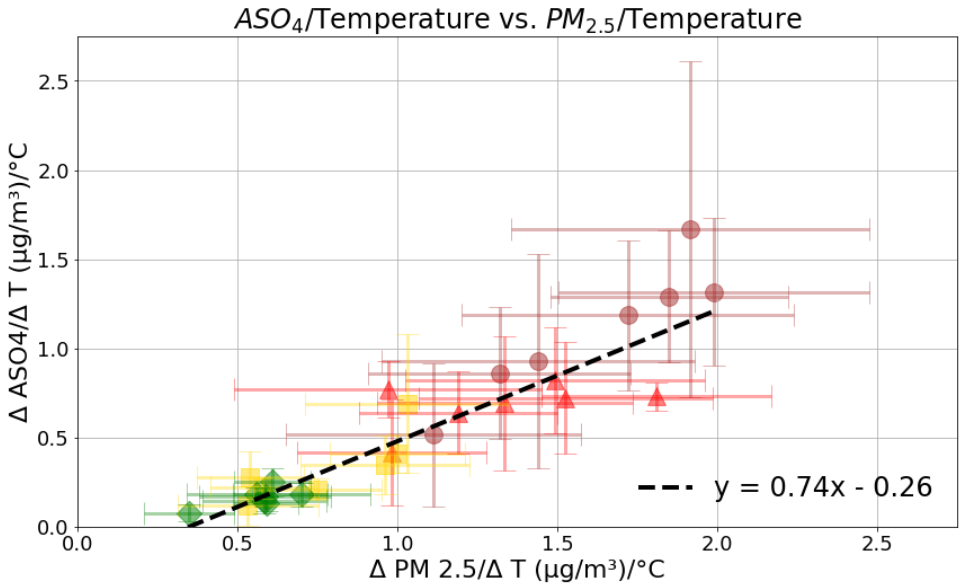

Figure 2.3: Slopes of ASO_4 mass vs. temperature vs. the slopes of total $PM_{2.5}$ vs. temperature for the seven cities featured in this study. The x and y ranges shown at each point represent the central 95% of the distribution for each slope estimate. ● : 2000-2005; ▲ : 2006-2010; ■ : 2011-2015; ◆ : 2016-2020.

Figure 2.3 shows the correlation of ASO_4 mass with temperature vs. the correlation of total $PM_{2.5}$ with temperature. A slope of 1 would suggest that ASO_4 explains the entire temperature dependent increase in $PM_{2.5}$. Fitting the data to a line and taking into account the uncertainty in both x and y (using a weighted least squares fit as described by York et al. 2004)[105] gives the slope shown of 0.74 ± 0.1 [µg $ASO_4/m^3/°C$]/[µg $PM_{2.5}/m^3/°C$]. This indicates that ASO_4 was the dominant source (~75%) of the $PM_{2.5}$ temperature dependence in these seven locations over this period. The x-intercept of roughly 0.35 µg $PM_{2.5}/m^3/°C$ then represents the portion of the $PM_{2.5}$ temperature dependence that is unrelated to ASO_4.

This residual is likely linked to OA. Though the EPA AQS does not measure OA directly, it measures organic carbon (OC), and literature suggests that an appropriate value for the ratio of OA to OC in the Northeast U.S. summertime is roughly 2.2[106,107]. Figure 2.4A shows OA (OC*2.2) vs. temperature in Washington D.C. for the most recent subperiod (2016-2020). The other six cities are shown in Figure A.3 of Appendix A. The slope derived from Figure 2.4A is 0.32 ± 0.14 $µg/m^3/°C$. The magnitude of this correlation and that for the other three cities are roughly in line with the x-intercept shown in Figure 2.3, representing the fraction of $PM_{2.5}$ temperature dependence explainable by organic aerosols. This idea is supported by Figure 2.4B, which is constructed similarly to Figure 2.3. The slope of the correlation of OA with temperature vs. the slope of the correlation of total $PM_{2.5}$ with temperature for these seven cities between 2016-2020 is roughly three fifths of the observed temperature dependence of $PM_{2.5}$. In Table 2.1, we list the temperature dependence of ASO_4 and OA for the four 5-year periods we have analyzed.

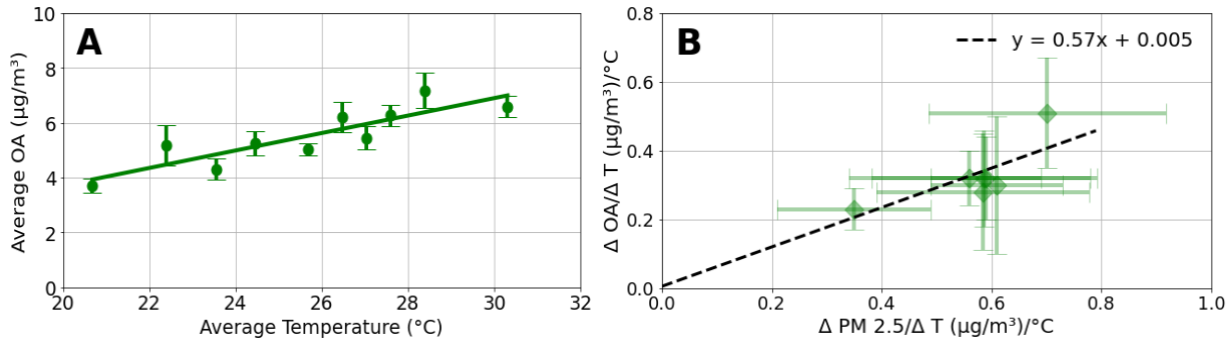

Figure 2.4: A: Relationship between OA and temperature in Washington, D.C. between 2016 and 2020. The range shown at each point represents the central 66% of the distribution in that bin. B: Slopes of OM vs. temperature vs. the slopes of total $PM_{2.5}$ vs. temperature for the seven cities featured in this study. The x and y ranges shown at each point represent the central 95% of the distribution for each slope estimate.

Table 2.1. Slopes of $PM_{2.5}$, ASO_4, and OM versus temperature as well as the ratio of the slopes of ASO_4 and $PM_{2.5}$ across all cities and subperiods along with their 95% confidence intervals. Slope units are in µg/m³/°C.

City	Data	2000-2005	2006-2010	2011-2015	2016-2020
Baltimore	**$PM_{2.5}$ Slope**	1.85 ± 0.37	1.81 ± 0.36	1.00 ± 0.21	0.56 ± 0.22
	ASO_4 Slope	1.29 ± 0.37	0.73 ± 0.08	0.41 ± 0.11	0.18 ± 0.04
	OM Slope	-	-	-	0.32 ± 0.08
	$m_{ASO4}/m_{PM\ 2.5}$	0.70	0.40	0.41	0.32
Boston	**$PM_{2.5}$ Slope**	1.11 ± 0.46	0.98 ± 0.30	0.53 ± 0.22	0.35 ± 0.14
	ASO_4 Slope	0.52 ± 0.40	0.42 ± 0.29	0.12 ± 0.11	0.08 ± 0.05
	OM Slope	-	-	-	0.23 ± 0.06
	$m_{ASO4}/m_{PM\ 2.5}$	0.46	0.42	0.22	0.22
Buffalo	**$PM_{2.5}$ Slope**	1.91 ± 0.56	1.53 ± 0.46	0.54 ± 0.17	0.58 ± 0.19
	ASO_4 Slope	1.67 ± 0.94	0.72 ± 0.31	0.28 ± 0.15	0.14 ± 0.07
	OM Slope	-	-	-	0.28 ± 0.17
	$m_{ASO4}/m_{PM\ 2.5}$	0.87	0.47	0.52	0.24
New York	**$PM_{2.5}$ Slope**	1.72 ± 0.52	1.49 ± 0.47	0.58 ± 0.16	0.70 ± 0.22
	ASO_4 Slope	1.19 ± 0.42	0.82 ± 0.30	0.22 ± 0.06	0.18 ± 0.07
	OM Slope	-	-	-	0.51 ± 0.16
	$m_{ASO4}/m_{PM\ 2.5}$	0.69	0.55	0.38	0.26
Philadelphia	**$PM_{2.5}$ Slope**	1.32 ± 0.41	0.97 ± 0.48	1.03 ± 0.32	0.61 ± 0.12
	ASO_4 Slope	0.86 ± 0.37	0.77 ± 0.16	0.69 ± 0.39	0.25 ± 0.08
	OM Slope	-	-	-	0.30 ± 0.20
	$m_{ASO4}/m_{PM\ 2.5}$	0.65	0.79	0.67	0.41
Providence	**$PM_{2.5}$ Slope**	1.44 ± 0.49	1.19 ± 0.31	0.75 ± 0.20	0.59 ± 0.10
	ASO_4 Slope	0.93 ± 0.6	0.64 ± 0.23	0.21 ± 0.06	0.13 ± 0.04

	OM Slope	-	-	-	0.32 ± 0.12
	$m_{ASO4}/m_{PM\ 2.5}$	0.65	0.54	0.28	0.22
Washington, D.C.	**$PM_{2.5}$ Slope**	1.99 ± 0.49	1.34 ± 0.40	0.96 ± 0.26	0.59 ± 0.21
	ASO_4 Slope	1.32 ± 0.42	0.69 ± 0.38	0.35 ± 0.16	0.17 ± 0.05
	OM Slope	-	-	-	0.32 ± 0.14
	$m_{ASO4}/m_{PM\ 2.5}$	0.66	0.52	0.36	0.29

Early in this record (2000-2005), ASO_4 represented ~67% of the temperature dependence of $PM_{2.5}$. OC measurements are not available during this time period. However, if we assume the behavior of organic aerosol has been constant and use the values from 2016-2020, then the observed temperature dependence is explained almost completely by these two components (Figure 2.5, top). In 2016-2020, ASO_4 represents only ~28% of the $PM_{2.5}$ temperature dependence across our seven cities while organic components now represent ~57% (Figure 2.5, bottom). Again, the overall temperature dependence is almost entirely explained by the temperature dependence of these two terms, but the relative importance is reversed.

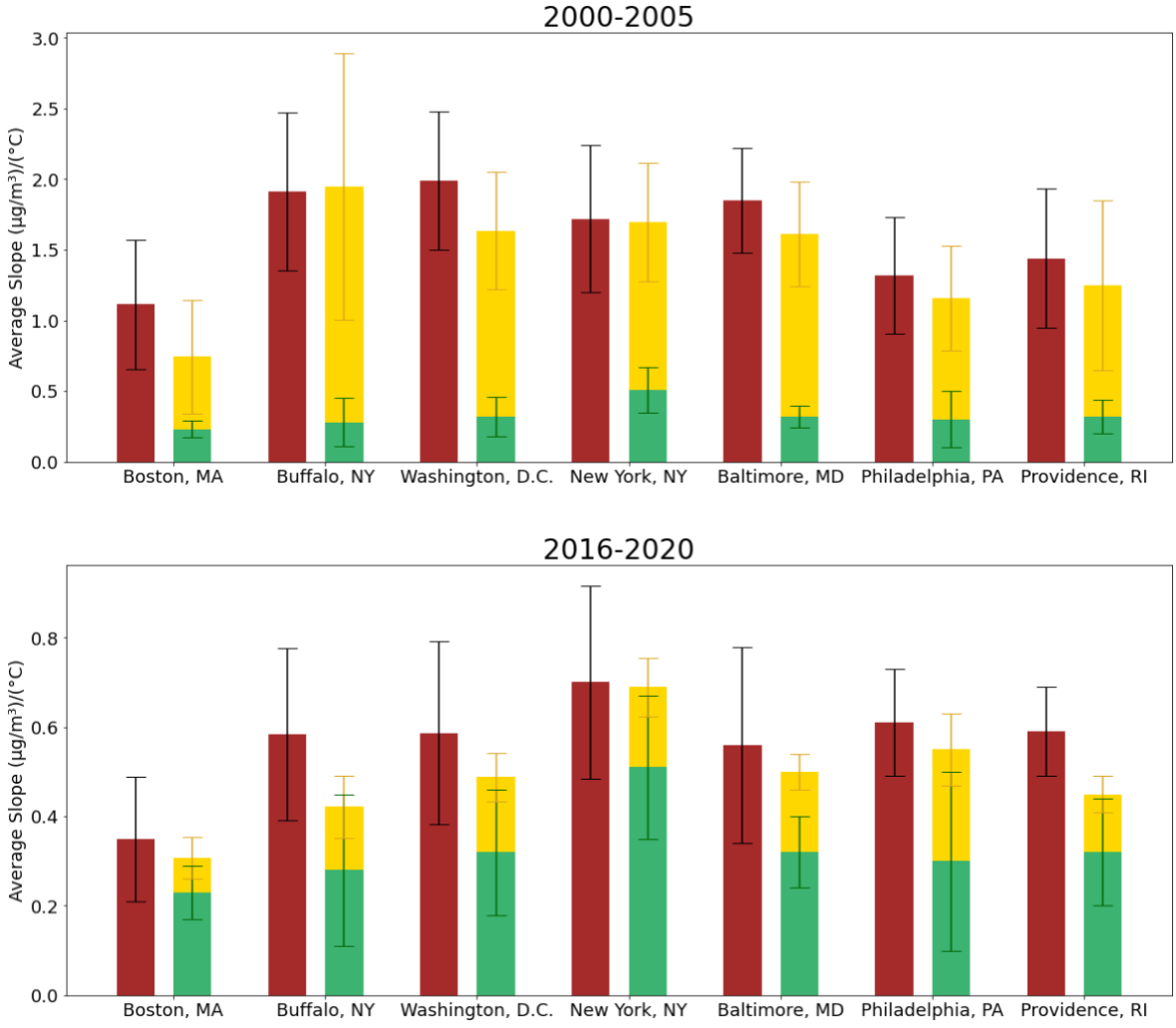

Figure 2.5: The temperature dependence of $PM_{2.5}$ and its components in 2000-2005 (Top) and 2016-2020 (Bottom). OM correlation values from 2016-2020 are displayed in both. Error bars shown correspond to the 95% confidence interval for each slope. ■ : Total $PM_{2.5}$ vs. T; ■ : ASO_4 vs. T; ■ : OM vs. T.

Discussion

In the Northeast U.S., summertime $PM_{2.5}$ has been changing dramatically over the last 20 years. Air quality initiatives have resulted in a reduction in primary emissions of sulfur dioxide and nitrogen oxides. As SO_2 emissions were successfully curbed, sulfate aerosol concentrations tumbled[90]. Due to the positive correlation between summertime temperatures, energy demand for cooling, and SO_2 emissions associated with energy production[67], these reductions were reflected in the temperature dependence of ASO_4 aerosol concentrations. The abatement of SO_2 emissions has had the dual effect of reducing overall $PM_{2.5}$ concentrations as well as the dependence of summertime $PM_{2.5}$ concentrations on temperature. Across the Northeast U.S., the enhancement in $PM_{2.5}$ due to temperature shrunk significantly comparing 2016-2020 to 2000-2005; the difference in $PM_{2.5}$ concentrations between the top and bottom temperature deciles decreased by

10 – 17 μg/m^3. The World Health Organization (WHO) recommends that 24-hour average $PM_{2.5}$ concentrations should not exceed 15 μg/m^3 more than 3-4 days per year (https://www.who.int/news-room/fact-sheets/detail/ambient-(outdoor)-air-quality-and-health). In the years 2000-2005, the percent of summer days with average $PM_{2.5}$ concentrations exceeding this WHO standard was 58% in Baltimore; 46% in Boston; 43% in Buffalo; 54% in New York; 56% in Philadelphia; 29% in Providence; and 63% in Washington, D.C. More recently, in the years 2016-2020, the percent of summer days exceeding the standard was below 5% in all seven of the cities we analyzed. Days exceeding the standard are exclusively the warmest days. By this metric, the emission reduction efforts of the last 20 years have had tremendous success in improving air quality in the cities of the Northeast U.S. Recent studies have shown how the negative health impacts of $PM_{2.5}$ exposure can begin to manifest below this threshold of 15 μg/m^3 [4,108,109]. For this reason, understanding the pathways towards continued decreases of aerosol mass on the hottest days remains important.

Warmer temperatures are still driving high aerosol events through their connection to enhanced OA (Figures 2.4B and 2.5). Strategies for reducing the occurrence of high aerosol events will vary depending on the cause of the temperature dependence of urban OA. Biogenic VOC emissions are strongly temperature dependent[110]. If the aerosol source is from biogenic emissions outside of cities, then there may be few policy options. However, if the biogenic emissions are within cities, then the types of trees planted will likely be important. Planting of trees is viewed as an important strategy for mitigating the urban heat island effect. Alternatively, if VCPs or temperature-dependent chemistry are responsible for increased aerosol mass at high temperatures, then a number of policies for control might be available.

Chapter 3: Temperature-dependent composition of summertime $PM_{2.5}$ in observations and model predictions across the Eastern U.S.

This chapter was adapted from: Vannucci, P. F.; Foley, K.; Murphy, B. N.; Hogrefe, C.; Cohen, R. C.; Pye, H.O.T. Temperature-dependent composition of summertime $PM_{2.5}$ in observations and model predictions across the Eastern U.S. *Under review – pending publication.*

Abstract

Throughout the U.S., summertime fine particulate matter ($PM_{2.5}$) exhibits a strong temperature (T) dependence. Reducing the $PM_{2.5}$ enhancement with T could reduce the public health burden of $PM_{2.5}$ now and in a warmer future. Atmospheric models are a critical tool for probing the processes and components driving observed behaviors. In this work, we describe how observed and modeled aerosol abundance and composition varies with T in the present-day Eastern U.S. with specific attention to the two major $PM_{2.5}$ components: sulfate (SO_4^{2-}) and organic carbon (OC). Observations in the Eastern U.S. show an average measured summertime $PM_{2.5}$-T sensitivity of 0.67 $\mu g/m^3/K$, with CMAQ v5.4 regional model predictions closely matching this value. Observed SO_4^{2-} and OC also increase with T; however, the model has component-specific discrepancies with observations. Specifically, the model underestimates SO_4^{2-} concentrations and their increase with T while overestimating OC concentrations and their increase with T. Here, we explore a series of model interventions aimed at correcting these deviations. We conclude that the $PM_{2.5}$-T relationship is driven by inorganic and organic systems that are highly coupled, and it is possible to design model interventions to simultaneously address biases in $PM_{2.5}$ component concentrations as well as their response to T.

Introduction

Exposure to airborne particulate matter, specifically that of a diameter smaller than 2.5 mm ($PM_{2.5}$), has been linked to numerous deleterious health effects[88]. Efforts to decrease $PM_{2.5}$ in the United States have reduced average annual concentrations by 37% since the start of the millennium, reaching a national mean of ~8.5 $\mu g/m^3$ in 2021[111]. A growing number of studies suggest that negative health impacts of $PM_{2.5}$ exposure occur at even lower concentrations[4,108,109], and in 2021, the World Health Organization suggested an annual mean $PM_{2.5}$ guideline of 5 $\mu g/m^3$ [112]. Strategies for achieving reductions to meet such stringent standards will involve controls on multiple sources of $PM_{2.5}$ and likely require a speciated approach[113]

The most common $PM_{2.5}$ components by mass in the U.S. are organic aerosols (OA), sulfate (SO_4^{2-}), ammonium (NH_4^+), and nitrate (NO_3^-). Since 2002, U.S. emissions of nitrogen oxides (NO_x) have decreased by 63%, and emissions of sulfur dioxide (SO_2) by 86%[114], leading to reductions in aerosol nitrate and sulfate. Reductions in OA have been slower. Myriad volatile organic compounds (VOCs), both biogenic and anthropogenic, are aerosol precursors and only a subset of the precursors are known to be controllable. In addition, primary emissions of OA from wildfires are not directly controllable. Since primary OA is only a fraction of total OA[95] and

inorganic aerosol components continue to decrease, reducing OA precursors and their conversion to secondary OA represent potentially meaningful avenues for further abating $PM_{2.5}$[114].

Ambient temperature has been identified as having a prominent role in promoting elevated summertime $PM_{2.5}$ concentrations in diverse regions of the United States such as the Northeast, the Southeast, and Southern California[58,68,99,115,116]. The summertime temperature dependence of OA is primarily driven by an increase in biogenic emissions, whereas for SO_4^{2-} it is driven by temperature dependent SO_2 emissions[67,117] and further modulated by temperature dependent solubility and conversion of SO_2 to SO_4^{2-} [101]. In addition, SO_4^{2-} can mediate OA production by regulating both particle-phase acidity as well as aerosol liquid water content which modulate the formation of OA by promoting uptake of isoprene epoxydiols (IEPOX) to the particle phase[57,118]. Therefore, a fraction of OA responds to temperature by virtue of chemical coupling between sulfate and temperature dependent biogenic emissions.

Vannucci and Cohen show that temperature-dependent inorganic emissions controlled the behavior of $PM_{2.5}$ in the Northeast in the early 2000s[68]. However, in recent years organic compounds were the primary driver of the observed temperature dependent increase in aerosol mass. Going forward, as our climate continues to warm, understanding the complex interactions between temperature and $PM_{2.5}$ will be of critical importance so that future air quality can be properly estimated[119]. Here, we characterize the observed relationship between temperature and total sulfur ($SO_2 + SO_4^{2-}$), aerosol SO_4^{2-}, and organic aerosols in the U.S. and compare it to that predicted by the most recent version of the Community Multiscale Air Quality model (CMAQ)[120] with the Community Regional Atmospheric Chemistry Multiphase Mechanism (CRACMM)[121]. In addition, we explore how modeled temperature sensitivities can be impacted by changing select model processes with the goal of improving agreement with observations.

Methods

Observed concentrations of ambient SO_2 as well as total and speciated $PM_{2.5}$ were obtained from the Environmental Protection Agency Air Quality System (EPA AQS). For a complete list of AQS sites and final values utilized in this study, refer to the supporting data archive. $PM_{2.5}$ concentrations were usually reported as daily 24-hour averages. For speciated $PM_{2.5}$, concentrations were usually reported as 24-hour averages every third day. Observations of gaseous SO_2 were reported hourly and resampled here as 24-hour averages for comparison to the $PM_{2.5}$ data. Analysis focused on the sulfate and organic carbon (OC) components of $PM_{2.5}$, both of which demonstrate a consistent positive temperature dependence. Sulfate reported in the AQS was measured through ion chromatography and does not include organic sulfate; it does, however, include sulfate in the form of hydroxymethane sulfonate (HMS), which is not included in the model's chemical mechanism[122,123]. Ammonium $PM_{2.5}$ was found to track sulfate $PM_{2.5}$ in the observations, indicating that it serves primarily as a counter ion and does not offer meaningfully independent information on aerosol mass. Observed nitrate $PM_{2.5}$ was small compared to SO_4^{2-} and OC in summer and thus not considered for analysis as an independent component.

CMAQ version 5.4, running with CRACMM version 1.0[121,124] was used to predict atmospheric composition for the contiguous U.S. (CONUS) at 12 km horizontal resolution with 35 vertical layers (though only the bottom layer, 0-20 meters, was used in this analysis) during the Summer of 2019 (June to August with 10 days of spin-up in May). Meteorological fields were simulated with the Weather Research & Forecasting Model (WRF) version 4.1.1 and

processed for use in CMAQ through the Meteorology-Chemistry Interface Processor (MCIP)[125,126]. For representing aerosol dry deposition, we used the STAGE-Emerson mechanism[127]. For anthropogenic emissions, emissions from the EQUATES project were processed through the Sparse Matrix Object Kernel Emission (SMOKE) framework[128,129], and for biogenic emissions, we used the Biogenic Emission Inventory System (BEIS) within CMAQ[130].

Model predictions of $PM_{2.5}$ and its components were matched in time and space to AQS observations using the EPA Atmospheric Model Evaluation Tool[131]. Model predictions of OA were converted to OC using factors specific to each OA species in CRACMM. The ratio of OA to OC typically ranges between 1.8 and 2.1 throughout our domain of interest[132] and spatiotemporal variations in this value are therefore unlikely to affect observed trends in the OC-T relationship.

Only sites with datasets that were more than two-thirds complete were retained in the analyses (at least 60 days out of the 92-day period for daily observations, and at least 20 days of observations for measurements made every 3rd day). Model performance statistics in the form of mean bias/error, normalized mean bias/error, and Pearson correlation coefficients were generated based on modeled and observed concentrations for our species of interest (see supporting information for definitions of the metrics).

In addition, we define a $PM_{2.5}$-T sensitivity in units of $\mu g/m^3$ per K as the slope of $PM_{2.5}$ (or its constituent) versus modeled average daily temperature calculated using Theil-Sen estimators at each site. This method involves finding the median value of slopes determined by evaluating all pairs of points[133] and was chosen to minimize the influence of outliers given the paucity of samples at individual AQS sites (especially for $PM_{2.5}$ speciation observations). For the purposes of comparing modeled and observed T-sensitivities as shown later in Figures 3.4 and 3.6, calculated slope values were only retained if the absolute value of the Spearman rank correlation coefficient was greater than 0.25 to eliminate outlying trends we are less confident in. Modeled temperature values were used to generate both observed and modeled $PM_{2.5}$-T sensitivities because temperature measurements were not always available at sites with $PM_{2.5}$ observations. Where temperature observations were available, they were found to be in good agreement with the modeled values, with an average bias of 0.14 K across all observations (Figure B.1 in Appendix B).

Base Case Results

$PM_{2.5}$ concentrations measured at AQS sites during the summer of 2019 across CONUS (Figure 3.1A) are broadly higher in the eastern U.S. compared to the western U.S. with California being a notable exception of high concentrations in the West. We find positive correlations between $PM_{2.5}$ and temperature across much of CONUS with, on average, higher concentrations and a stronger sensitivity to temperature east of the Texas panhandle (Figure 3.1B). In the Eastern U.S., the average $PM_{2.5}$-T sensitivity is ~0.67 $\mu g/m^3/K$, and the temperature response is particularly high along the Gulf Coast, where the average $PM_{2.5}$-T sensitivity is ~1.4 $\mu g/m^3/K$. This region is likely to exhibit such a strong response to temperature because of its proximity to large swathes of vegetation and BVOC emissions, heightened SO_2 emissions from the shipping sector, and the overall warmer temperatures compared to the rest of the Eastern U.S. In addition, a notable departure from broad regional trends is found at a few sites in Southern California where elevated $PM_{2.5}$ at low temperatures drives the overall negative sensitivity to temperature (not including the Los Angeles urban core, which instead features a positive

relationship between $PM_{2.5}$ and temperature, as observed by Nussbaumer & Cohen[99]). Finally, the response of $PM_{2.5}$ to temperature is weak in the Southwestern desert despite the high temperatures, likely due in part to lower biogenic VOC emissions as well as a higher contribution of desert dust to $PM_{2.5}$.

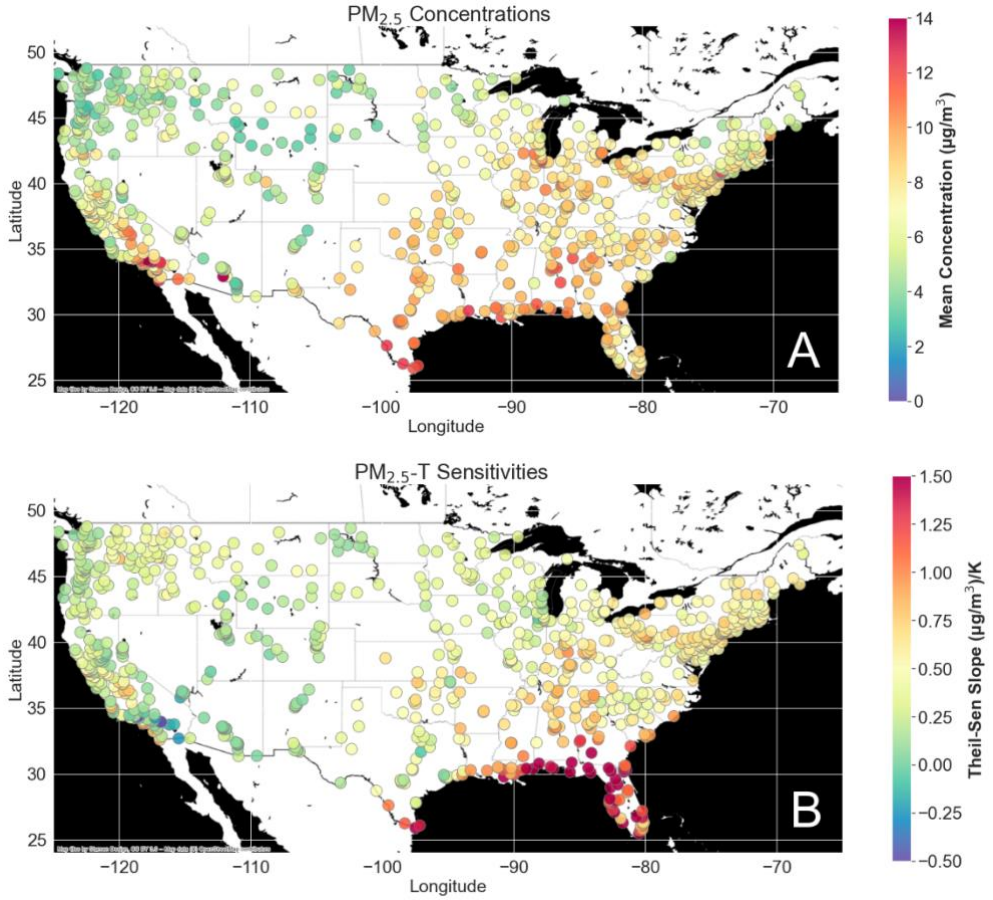

Figure 3.1: A: Mean concentrations of total $PM_{2.5}$ mass at AQS sites. B: Sensitivity of observed $PM_{2.5}$ to temperature at AQS sites (see Methods section for details).

OC and SO_4^{2-} components of $PM_{2.5}$ are also found to have a widespread sensitivity to temperature. As with total $PM_{2.5}$, both OC and SO_4^{2-} show the strongest positive relationships with temperature in the Eastern U.S. with average sensitivities of ~0.11 and ~0.12 $\mu g/m^3/K$ respectively. Adding ammonium as a counter ion for sulfate and the non-carbon fraction of OA associated with OC brings the total sensitivity of $PM_{2.5}$ vs T captured by OC and SO_4^{2-} to 0.37 $\mu g/m^3/K$, within one standard deviation of the total $PM_{2.5}$ vs T sensitivity for co-located, temporally coincident $PM_{2.5}$ (0.60 +/- 0.25 $\mu g/m^3/K$, a slight reduction from the value calculated utilizing all available $PM_{2.5}$ observations). In work by Vannucci & Cohen[68] the authors find that when utilizing select AQS sites with ample data availability (and averaged over five-year subperiods instead of a single year), the sum of the T sensitivities of OC and SO_4^{2-} is adequate for convincingly explaining the total $PM_{2.5}$-T sensitivity in the Eastern U.S. summertime. We thus focus on OC and SO_4^{2-} as they account for the majority of the $PM_{2.5}$-T sensitivity.

We then assess model performance by considering the model bias and error in total $PM_{2.5}$. Across all total $PM_{2.5}$ observations throughout CONUS, we find a normalized mean bias of -17% and a normalized mean error of 36% for an average observed concentration of 7.29 $\mu g/m^3$ (Table B.1 in Appendix B). We also find the $PM_{2.5}$-T sensitivity relationship in the model corresponds well with observed trends. Across all AQS sites there is only a slight underestimation of -0.07 $\mu g/m^3/K$ on average between modeled and observed $PM_{2.5}$-T relationships (Table B.10 in Appendix B).

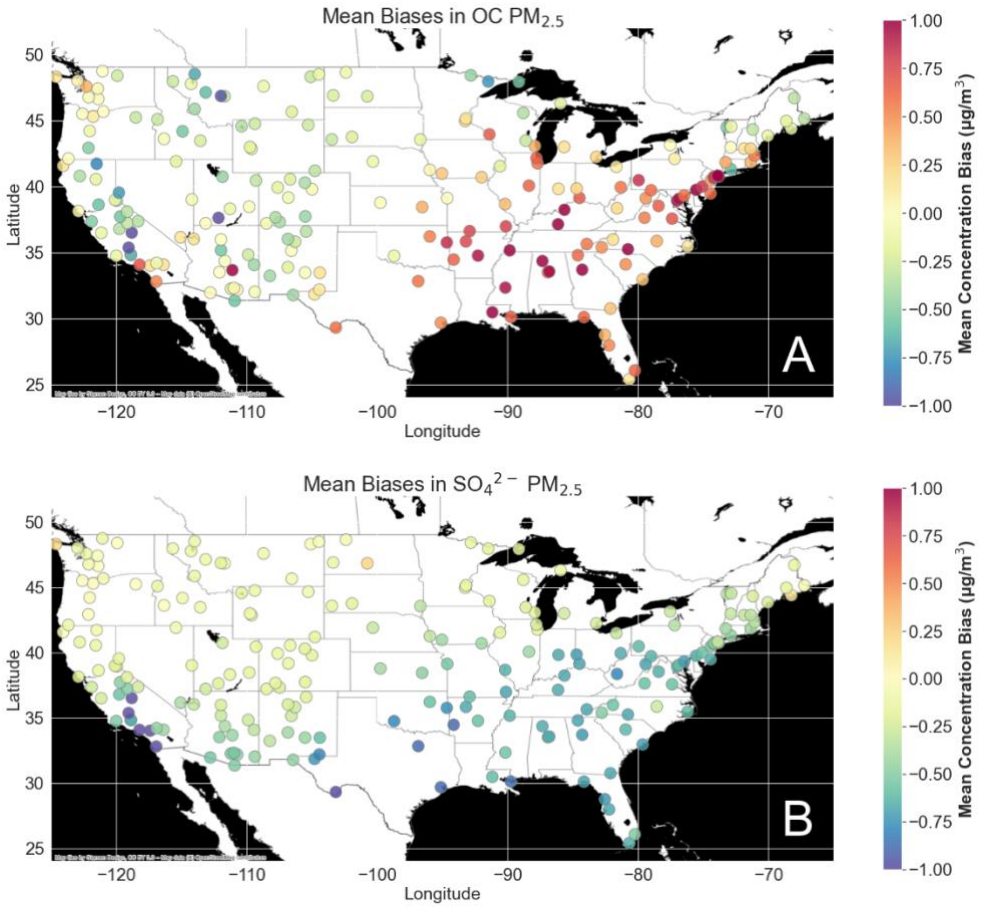

Figure 3.2: A: Mean difference between modeled and observed concentrations of OC $PM_{2.5}$. B: The same for SO_4^{2-} $PM_{2.5}$.

Despite the relatively good agreement between predicted and observed total $PM_{2.5}$, model representations of OC and SO_4^{2-} exhibit significant and compensating biases with broad regional features (Figure 3.2, Table B.2 in Appendix B). Figure 3.2A shows that modeled OC is overestimated by ~0.5 $\mu g/m^3$ in much of the Eastern U.S. (east of -100° longitude). Figure 3.2B shows that modeled SO_4^{2-} is underestimated by ~0.5 $\mu g/m^3$ over the same broad region where OC is overestimated. Outside the eastern U.S., biases are more localized. For example, there is a large (> 1 $\mu g/m^3$) difference between model predictions and observations of both OC and SO_4^{2-} in Southern California. In much of the rest of the country, model and observations are a close match. For this reason, we use the longitude of -100° as a dividing line and focus on the Eastern

half of the continent where the biases are widespread and largely homogenous for the remainder of our analysis. The southeastern U.S. is also of particular interest as it is projected to experience the greatest regional increase in $PM_{2.5}$-attributable deaths due to climate change by 2095[16].

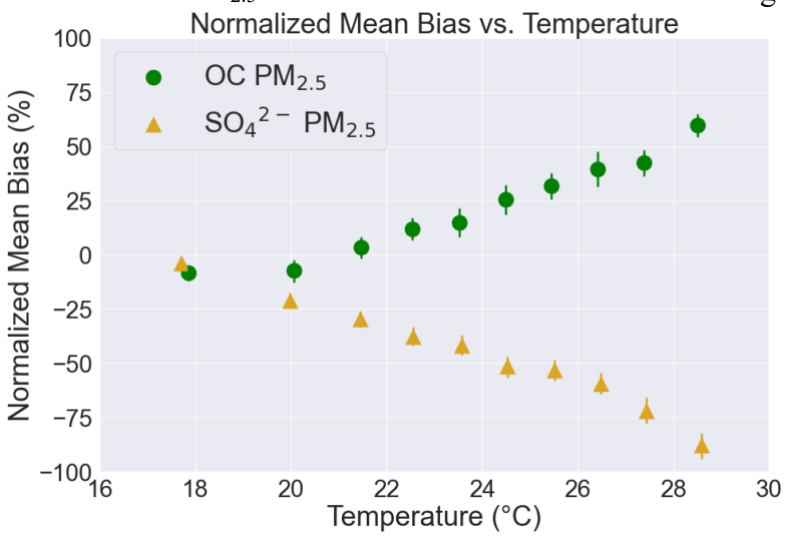

Figure 3.3: Normalized mean bias of model predictions compared to observations (see supporting information for details) for both OC and SO_4^{2-} concentrations split into equally-sized bins representing temperature deciles. We include all available daily observations from the Eastern U.S. (Longitude > -100°) June-August 2019. Error bars represent the bootstrapped 95% confidence interval for the median of each bin.

We find that normalized mean bias of predicted OC and SO_4^{2-} $PM_{2.5}$ compared to observations is not only ubiquitous but also dependent on temperature. Both OC overestimations and SO_4^{2-} underestimations grow with temperature (Figure 3.3). At the low end of the temperature range, normalized mean bias is within ~10% for both OC and SO_4^{2-}. As temperature grows, biases in both OC and SO_4^{2-} grow linearly in opposite directions. At the top decile of temperatures, bias in OC grows to more than +60% (with an average observed OC $PM_{2.5}$ concentration of 2.0 $\mu g/m^3$) and bias in SO_4^{2-} grows to nearly -90% (with an average observed SO_4^{2-} $PM_{2.5}$ concentration of 1.75 $\mu g/m^3$). As concentrations of both components grow with temperature, normalized biases consistently grow as well. This is also the case when looking at normalized mean error (Figure B.2 in Appendix B) which grows linearly with temperature for both constituents at a similar rate.

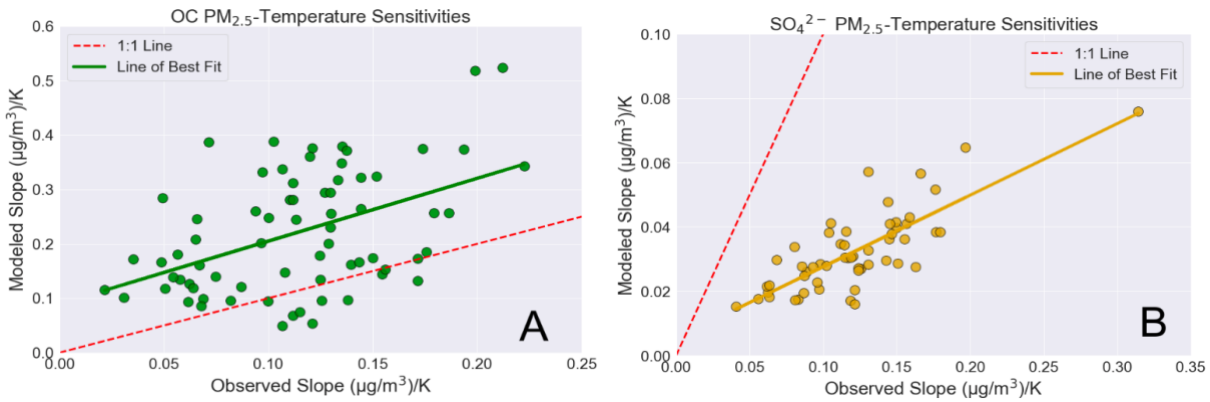

Figure 3.4: **Modeled versus observed sensitivities of OC $PM_{2.5}$ versus temperature (A) and SO_4^{2-} $PM_{2.5}$ versus temperature (B) at AQS sites in the Eastern U.S. (Longitude >-100°). Data shown only for sites meeting filtering criteria as described in the Methods section.**

Figure 3.4 shows the contrast between modeled and observed $PM_{2.5}$-T sensitivities of OC and SO_4^{2-} $PM_{2.5}$ in the Eastern U.S. For organic carbon, the model overestimates the temperature response by a roughly constant 0.1 µg/m^3/K (Figure 3.4A). This error is largely consistent across sites, and it does not scale with the observed sensitivity of OC to temperature. On average throughout the Eastern U.S., the modeled sensitivity of OC to temperature is 2x greater than observed. In contrast, the model underestimates the relationship between sulfate and temperature across the board and appears to have a multiplicative error rather than an offset error (Figure 3.4B). On average throughout the Eastern U.S., the modeled sensitivity of SO_4^{2-} to temperature is 3.5x smaller than observed.

Model Sensitivity Simulations

In this section, we explore model simulations to modify the relationship between $PM_{2.5}$ constituents and temperature with the goal of improving agreement with observations. Mean bias, error, and Pearson correlation coefficients for $PM_{2.5}$, OC, and SO_4^{2-} in the sensitivity simulations are provided in Tables B3-B8 in Appendix B for CONUS and the Eastern U.S.

Sulfate

Two factors drive the abundance of aerosol sulfate: the total sulfur emitted and the conversion of emitted sulfur to sulfate. To ensure that spatial mismatches in sampling locations do not influence our assessment, we restrict this portion of the analysis to AQS sites reporting both gaseous SO_2 as well as aerosol SO_4^{2-} concentrations (for the exact subset see the supporting data archive).

The bias in model-predicted total sulfur (SO_2 + SO_4^{2-}) at the lowest temperatures hovers around -10%, whereas at the highest temperature the bias grows closer to -40% (Figure 3.5A). This suggests that the model is missing sulfur across the temperature range, but especially so on the hottest days (Figure 3.5A). Figure 3.5B shows how the observed conversion of SO_2 to SO_4^{2-} is higher at high temperatures, increasing from ~35% to ~55% from 291 to 302 K (18 to 29 °C). By contrast, the modeled conversion of SO_2 to SO_4^{2-} decreases as temperature rises, going from ~55% to ~40% over this temperature range. These panels suggest both that the model could be

missing one or more sources of sulfur and that the modeled conversion of SO_2 into SO_4^{2-} needs to be revised to produce slower oxidation at low temperatures and faster oxidation at high ones.

Note that neither the AQS observations nor the modeled concentrations for sulfate shown here include organosulfates. Therefore, model-observation disagreements in the proportion of inorganic to organic sulfate might also drive discrepancies here. For example, if the model features greater-than-observed conversion of inorganic to organic sulfate at higher temperatures, this might also manifest as a lower modeled ratio of SO_4^{2-} to $SO_4^{2-}+SO_2$ because the organics are not being considered. Another confounding factor could be discrepancies in temperature-dependent emissions of primary sulfate, but most of the summertime SO_4^{2-} is expected to be secondary in nature[134].

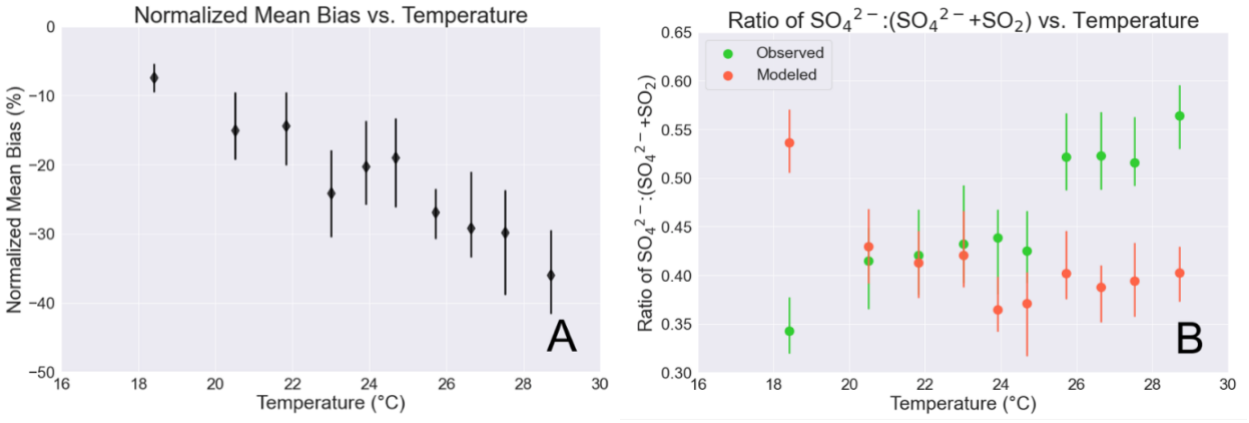

Figure 3.5: A: Normalized model bias with respect to total SO_2 + SO_4^{2-} in µg/m³. B: Modeled and observed ratios of SO_4^{2-} to (SO_2+SO_4^{2-}). In both panels, data are represented as medians of ten bins with equal numbers of observations per bin from the Eastern U.S. (Longitude > -100°) June-August 2019. Error bars represent the bootstrapped 95% confidence interval for the median of each bin.

To correct the model bias in total sulfur, we first test the effects of increasing sulfur emissions by utilizing the CMAQ Detailed Emissions Scaling, Isolation and Diagnostic (DESID) module[135] to implement a constant scale factor aimed at bringing the modeled and observed total sulfur into agreement. Given that normalized bias in total sulfur varies from -10 to -40%, we conduct an assessment at the upper bound by increasing sulfur dioxide emissions by 40% (intervention #1). We conduct this intervention as a hypothetical simulation to probe how the model might handle a large increase in SO_2 and whether that would result in substantially greater SO_4^{2-} $PM_{2.5}$ production. This emission increase results in a smaller normalized bias in total sulfur, moving it from an average of -20% to an average of +8%. However, we find that this emission increase does little to address the temperature-dependent model bias in sulfate as it does not affect the distribution of sulfur among phases. The normalized mean bias in SO_4^{2-} $PM_{2.5}$ changes from -46% in the base case to -36% with the increased emissions, and the normalized mean error changes from 50% to 44%. Though we achieve modest improvements in absolute concentrations of sulfate, we do not sufficiently alter the representation of the SO_4^{2-}—T

relationship, as shown in Figure 3.6B, indicating that we are still not targeting the major atmospheric process causing bias.

Given the need for additional conversion to SO_4^{2-} in the model, we then separately tested the ability of adding chemical processes to increase sulfate (intervention #2). The CMAQ model oxidizes SO_2 to form sulfate in the gas-phase and in cloud droplets but not in aqueous particles. This aqueous aerosol-mediated pathway is estimated to produce significant amounts of sulfate as well[136]. We introduce an uptake coefficient to bring SO_2 into aqueous particles as sulfate, selecting a value of 10^{-2}, at the high-end of what has been suggested in the literature[137]. Including aqueous aerosol uptake has a notable effect on sulfate concentrations, resulting in a new normalized mean bias for SO_4^{2-} $PM_{2.5}$ of +5% and a new normalized mean error of 57%. Though this intervention significantly improves mean biases, it results in greater variance in model-observation agreement and worsens model error. This is also readily apparent when considering the degradation of the Pearson correlation coefficient between model predictions and observations, from 0.62 in the base case to 0.38 in intervention #2 (Table B.8 in Appendix B). However, this intervention results in a dramatic enhancement in the modeled SO_4^{2-}—T relationship (Figure 3.6B). Overall, while this intervention shows mixed results, it underscores the relevance of this pathway for SO_4^{2-} production and invites further consideration in future analyses.

To reiterate, the black line in Figure 3.6B (identical to the best fit line in Figure 3.4B) shows how our base case model representation of the sulfate temperature dependence was limited, showing a growing deviation from the 1:1 line of agreement as observed SO_4^{2-}—T sensitivities increase. The dashed orange line then represents the line of best fit through the modeled versus observed SO_4^{2-}—T sensitivities following intervention #1, demonstrating how boosting SO_2 emissions had only a minor effect in correcting this relationship. However, the dotted blue line representing the implementation of aerosol SO_2 uptake (intervention #2) shows remarkable improvement in model-observation agreement, highlighting the efficacy of the aqueous particle formation pathway for producing sulfate and doing so in a temperature-dependent manner. Since the SO_2 uptake was implemented without a strong temperature dependence (a 10 K temperature increase enhances the uptake by ~2%), this effect is likely due to increased conversion of already temperature-dependent SO_2 emissions or to increased aqueous aerosol surface area at higher temperatures.

Organic Carbon

Overestimations in the temperature dependence of OA could be due to errors in VOC emissions, VOC oxidation to SOA, and/or a lack of SOA removal processes. We explored a different representation of biogenic emissions (MEGAN[138]) and determined that BVOC emissions impact OC predictions and the OC-T sensitivity significantly (Figure B.3 in Appendix B). When utilizing the MEGAN inventory, we find that overestimations in OC are higher than when using BEIS and that the growth of biases with temperature is even more pronounced; at the highest temperatures (top 10%), the normalized mean bias for modeled OC is 3x higher comparing MEGAN to BEIS. We thus proceed here with BEIS emissions given they produced a lower bound on total OC and OC sensitivity to temperature resulting in lower model error and bias. Here we explore three model modifications aimed at reducing OC and its sensitivity to temperature.

Reductions in IEPOX aerosol uptake, a major source of SOA, are likely to be effective at improving model-observation agreement. We decrease the condensed phase rate constant for the

HSO_4^--catalyzed uptake of IEPOX to a more realistic value of 1.31×10^{-5} moles^{-2} L^2 s^{-1} (CRACMM v1.0 overestimated the rate by assuming the same value for HSO_4^- as for H^+). Altering this pathway (intervention #3) affects both OC as well as SO_4^{2-} concentrations as organosulfates are a major product (the coupling will be further discussed in the following section). As a result, this analysis probes the question of how overestimates in IEPOX SOA can affect the $PM_{2.5}$-T sensitivity of both PM constituents. Reducing SOA from IEPOX in this manner improves the modeled representation of OC, with the normalized mean bias for the Eastern U.S. in OC $PM_{2.5}$ falling from +22% to +8% and the normalized mean error falling from 42% to 35%. The response of OC to temperature is also improved significantly (Figure 3.6A; purple dotted line).

Our second OC model intervention focuses on photolytic destruction of OA. Photolytic aerosol removal pathways that are competitive with deposition and represent a significant portion of the fate of tropospheric OA have been demonstrated in laboratory settings and found to improve model predictions of OA[139–143]. Monoterpenes in particular are a major source of OA ubiquitous throughout the eastern U.S.[144,145]. Monoterpene oxidation products found in aerosol include labile peroxides[146] and nitrates, and photolysis loss of monoterpene OA has been observed in laboratory experiments[142,147]. We set the photolysis rate of monoterpene-derived OA at 1% of the NO_2 photolysis rate, corresponding to average rate values reported in literature[143], giving a lifetime of approximately 3 hours for monoterpene aerosol during the daytime (intervention #4). Adding this photolytic process significantly reduces the normalized mean bias in OC to –2% and the normalized mean error to 35%. We also see improvements in the modeled OC-T sensitivity, with the gold dotted line in Figure 3.6A showing the trendline much closer to approaching the 1:1 line of agreement. A similar scheme, implementing the photolysis of monoterpene SOA set at 2% of the NO_2 photolysis rate has been recently explored by Liu et al. who also found the change to have a positive effect in achieving model-observation agreement for OA[59].

Our next model intervention aimed at OC $PM_{2.5}$ explores monoterpene-derived organic nitrates (ONs), which can be found in the gas or particle phase and whose fate has implications for both SOA and ozone. The SOA formation potential of nitrate radicals reacting with select monoterpene species is high and described in several recent studies[148–150]. The loss of ONs by hydrolysis can contribute to SOA, but parameterizing the reaction is difficult due to the number of ON structures with different rates[151–154]. Our base case assumed gas-phase monoterpene ONs either deposited or reacted to form highly functional species that condensed as SOA. Here, we lower the yield of SOA from gas-phase ON reactions to 50% to reflect a broad array of structures[155] and introduce particle-phase uptake and hydrolysis as a competitive removal mechanism for the ONs following Pye et al.[153] (intervention #5). With these modifications to the monoterpene ON fate, there are significant reductions in OC $PM_{2.5}$ throughout the Eastern U.S., with normalized mean bias falling to +7% and normalized mean error falling to 36%. The magnitude of the reductions suggest that the fate of ONs is highly relevant in modulating OC concentrations and that correctly representing their formation and removal in a manner consistent with our current understanding of the chemistry involved will be an important improvement in model design. Figure 3.6A demonstrates how each of the three OC model interventions outlined has a positive effect in moving the modeled slopes closer to agreement with observations but that none of them individually eliminate model bias. Rather than a providing a definitive resolution to model bias, the impact of these interventions on the OC-T relationship motivates further consideration in future analyses.

Cross-system Coupling

Evaluating model performance for OC or SO_4^{2-} in isolation is not recommended because the two systems are coupled and model interventions aimed at targeting one can influence the other. This coupling primarily stems from the role of sulfate in particle-phase acidity and aerosol liquid water content which cause increases in SO_4^{2-} concentrations to lead to an enhancement in OC as well. We observe this effect in both model interventions aimed at tackling low sulfate (interventions #1 and #2). For the case of boosting SO_2 emissions, the normalized mean bias in OC increases slightly from +22% to +26%, and the normalized mean error increases from 42% to 45%. In the case of introducing aerosol uptake of SO_2, we see even more dramatic results, with normalized mean bias rising to 42% and normalized mean error to 58%. Furthermore, these model interventions also worsen the OC-T sensitivity (Figure 3.6A; orange dashed line and blue dotted line). This suggests that correcting the model's representation of SO_4^{2-} requires concurrently introducing measures to counter the resulting worsening of the overestimations in OC.

For the model interventions aimed at improving the representation of monoterpene OC (#4 and #5), we find no meaningful feedback on the sulfate system, as expected. On the other hand, changing the rate constant of the HSO_4^--catalyzed IEPOX reaction does affect inorganic sulfate, this time slightly improving both average concentrations of SO_4^{2-} as well as the modeled SO_4^{2-}-T sensitivity (Figure 3.6B, purple dotted line). Here, the normalized mean bias for SO_4^{2-} in the Eastern U.S. falls from -46% in the base case to –30%, and the normalized mean error falls from 50% to 38%. Moreover, we also see a notable improvement in the Pearson correlation coefficient, going from 0.62 in the base case to 0.70 here as a result of intervention #3 (Table B.8 in Appendix B). These results suggest that the IEPOX pathway for OC production is also an important mechanism for converting inorganic sulfate to organic sulfate, the latter of which is not routinely measured.

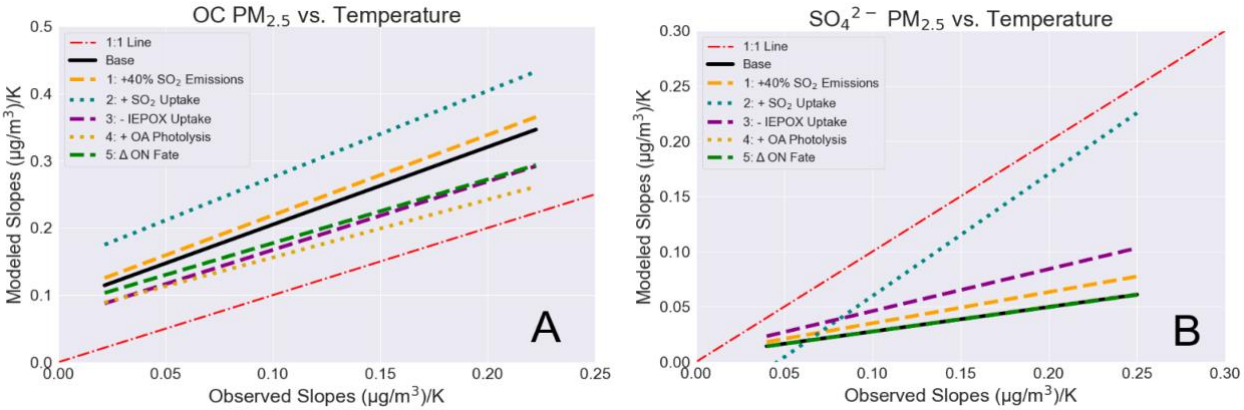

Figure 3.6: Analogous to Figure 3.4, showing only lines of best fit for clarity, restricted to the subset of AQS sites meeting the filtering criteria described in the Methods section for all interventions. A: Trends between modeled and observed sensitivities of OC $PM_{2.5}$ to temperature in the base case and after our five model modifications. B: the same for SO_4^{2-} $PM_{2.5}$. Note the different axis limits. Also note that the lines of best fit for interventions #4 and #5 for SO_4^{2-} $PM_{2.5}$ are identical to the base case.

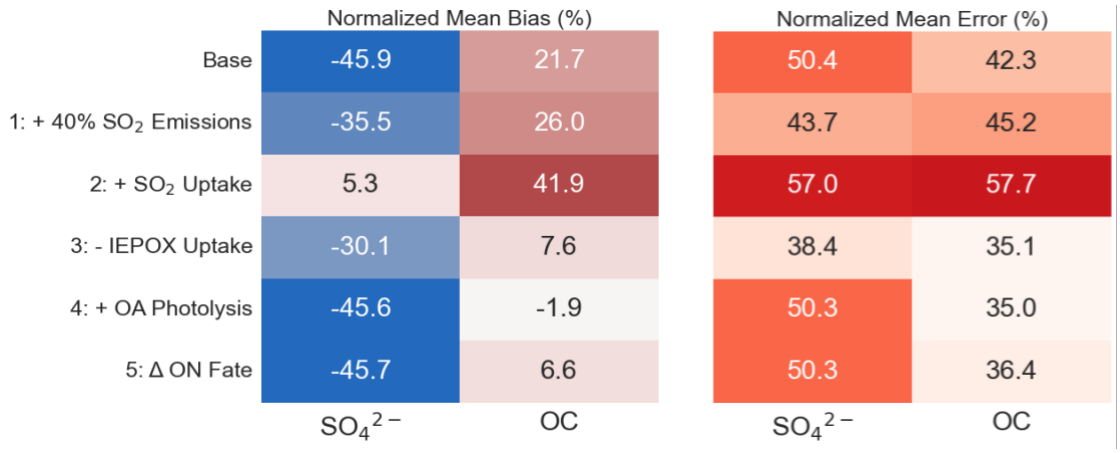

Figure 3.7: Left: Percent normalized mean bias in model predictions of SO_4^{2-} and OC $PM_{2.5}$ concentrations in the Eastern U.S. summertime in the base case and after the five model modifications pursued in this study. Right: The same but for percent normalized mean error.

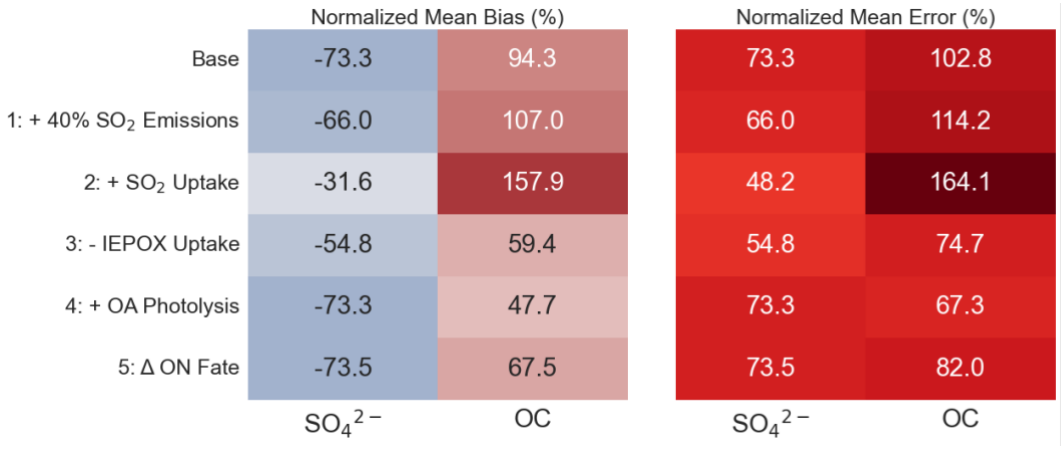

Figure 3.8: Left: Percent normalized bias in model predictions of the $PM_{2.5}$-T sensitivity for OC and SO_4^{2-} in the Eastern U.S. summertime in the base case and after the five model modifications pursued in this study. Right: The same but for percent normalized error.

Discussion

Figure 3.7 represents tabulated results for how normalized mean bias and error in $PM_{2.5}$ component concentrations vary from the base case throughout our five model design interventions. Figure 3.8 then represents the normalized mean bias and error in the modeled representations of the SO_4^{2-}-T and OC-T relationships (see also Tables B.9-B.10 in Appendix B). The comparison of Figures 3.7 and 3.8 shows how model-observation agreement for the T sensitivity of OC and SO_4^{2-} across our interventions mirrors model-observation agreement in absolute concentrations. We thus find that model biases in $PM_{2.5}$ component mass concentrations are linked to biases in their temperature dependence, and model modifications to improve $PM_{2.5}$

component mass predictions can address both biases simultaneously. Five model modifications were tested to evaluate their efficacy for improving the representation of how $PM_{2.5}$ components change with temperature: two enhanced SO_4^{2-} production, two targeted OC removal and fate, and one addressed both SO_4^{2-} and OC. We note that these model interventions were not specifically aimed at temperature, and temperature is one indicator of meteorology. Meteorological biases in the model could affect the $PM_{2.5}$-T relationship. However, SO_4^{2-} and OC temperature-dependent biases were in opposite directions, suggesting that a common meteorological driver is not primarily responsible for biases. Nevertheless, this work does not preclude errors in meteorological drivers from contributing to model bias. For example, if our WRF fields underestimate cloud cover at high temperatures, this might limit the aqueous-phase oxidation of SO_2 into SO_4^{2-} in clouds.

In attempting to address the model's low bias with respect to sulfate aerosols, we find that increasing SO_2 emissions by 40% broadly improves modeled SO_4^{2-} concentrations, but it does not improve the modeled response of SO_4^{2-} to temperature sufficiently. Summertime SO_2 emissions have been shown to be sensitive to temperature on account of heightened electricity demand to meet cooling needs on the hottest days and the coal combustion utilized to meet that demand[67,117]. While SO_2 emissions from power plants are generally monitored and thus well characterized, exploring missing sources of temperature dependent SO_2 emissions such as from "peaker" plants and behind-the-meter electricity generators that may be more active during periods of high summertime temperatures and electricity demand may be a future avenue to more specifically target model performance at high temperatures[69].

Introducing an aerosol uptake coefficient for generating particle-phase SO_4^{2-} consistent with the upper limits established in literature substantially reduces the model's low bias in SO_4^{2-} $PM_{2.5}$ but increases model error and variance, indicating that this intervention does not work equally well across all AQS sites probed. However, this model intervention significantly improves agreement between modeled and observed SO_4^{2-}-T sensitivity at AQS sites in the Eastern U.S., highlighting the relevance of particle phase oxidation or other chemical conversion of SO_2 for SO_4^{2-} formation. A more detailed representation of SO_2 uptake to the aerosol phase, modulated by temperature-dependent solubility, transition metal abundance, particle acidity, and water content could add spatial nuance and a more complete representation of this chemistry to better reflect these atmospheric processes as we currently understand them[156]. Future analyses should investigate how such schemes may impact model predictions.

In attempting to address the model's high bias with respect to OC $PM_{2.5}$, we find that model modifications based on laboratory experiments concerning OC production and removal processes are highly effective in reducing concentrations and improving both bias and error. However, no individual modification that we explored removes all bias. Implementing some combination of changes to model chemistry could yield even better agreement. Introducing both photolysis of monoterpene OC as well as updating the fate of organic nitrates had a large impact on average OC concentrations across the Eastern U.S. Nevertheless, the remaining discrepancies between modeled and observed slopes of OC versus temperature suggest the need for further model adjustments such as introducing additional temperature-dependent removal processes, less temperature-dependent biogenic VOC emissions, and/or a less temperature-dependent conversion of VOCs to OC. Additionally, the increase in OC bias as SO_4^{2-} is corrected demonstrates how these two major $PM_{2.5}$ components are best addressed together. We see this in our third model intervention, where we introduce a lower rate constant for HSO_4^--catalyzed uptake and find notable improvements in both OC and SO_4^{2-} modeled concentrations and

temperature response. This linkage may become even more important going forward, especially in the Eastern U.S., as organosulfates are expected to increase in abundance relative to inorganic sulfate[157].

We conclude that achieving an accurate model representation of $PM_{2.5}$ and its sensitivity to temperature will require addressing the processes governing the formation and removal of individual components as well as their synergistic interactions. Evaluating model performance through this lens provides additional insight into model chemistry and the processes which are most atmospherically relevant. With more accurate descriptions of the nature of $PM_{2.5}$, models of future scenarios will offer more robust predictions across a wider range of environmental conditions, an ever-growing concern in our warming climate. In addition, through the added insight into the chemistry resulting in high summertime $PM_{2.5}$, models will be better able to evaluate possible policies aimed at reducing high aerosol events, a crucial aspect of our continued efforts towards curbing exposure and the adverse health effects of aerosol pollution.

Chapter 4: Temperature-dependent nighttime stagnation episodes driving decadal air pollutant exceedances in Los Angeles

This chapter was adapted from: Vannucci, P. F.; Cohen, R. C. Temperature-dependent nighttime stagnation episodes driving decadal air pollutant exceedances in Los Angeles**.** *Under review – pending publication.*

Abstract

Nitrogen dioxide (NO_2) is a toxic air pollutant originating primarily from anthropogenic combustion processes. Because NO_2 is linked to adverse health outcomes and increased mortality, understanding its drivers and limiting exposure to high concentrations remains a key objective. Focusing on the Los Angeles metro area, previous studies have identified a relationship between NO_x ($NO_x \equiv NO + NO_2$) concentrations and temperature, but did not convincingly explain its drivers. We expand on past work, demonstrating how the relationship between enhanced NO_2 concentrations and temperature is driven by nighttime stagnation episodes that are distinct from daytime trends. Warm nighttime conditions, marked by low planetary boundary layer heights and decreased ventilation, lead to the accumulation of pollutants. The high nighttime concentrations therefore have an outsized influence in driving overall daily means. Here, we analyze 20 years of observations to show how relative increases in NO_2 with temperature are consistent over time and are therefore independent of the dramatic decadal decreases in emissions. Moreover, by showing that concentrations of carbon monoxide (CO) mirror the same trends, we suggest that a common meteorological factor is influencing the ensemble rather than temperature-dependent chemistry. We conclude by showing how these temperature-dependent stagnation episodes are driving exceedances in daily average NO_2 concentration guidelines. Though in absolute terms exceedances are less prevalent today than in past years, their incidence is now more strongly correlated with temperature, suggesting that the role of temperature as a control for dangerously elevated NO_x concentrations is growing.

Introduction

Nitrogen dioxide (NO_2) is a widely recognized atmospheric pollutant that represents a significant burden to public health[158]. As such, assessing and understanding the drivers of exposure to high NO_2 concentrations is an important objective. In the context of a warming climate, understanding how increases in NO_2 may be linked to temperature is relevant for predicting metrics of exposure in the future. NO_2 occurs in the atmosphere primarily as a result of the chemical conversion of nitric oxide (NO) to NO_2 by reaction with ozone and peroxy radicals. The sum of $NO+NO_2$ is commonly referred to as NO_x. Here, we consider trends in summertime NO_2 and NO_x in order to better elucidate its behavior at the warmest temperatures.

This spatial focus of this study is Los Angeles (LA), California. The greater LA area is a domain of interest for air quality given its large population and unique geography: a central basin bounded by mountains on all sides excepting the coast. The role of temperature with respect to NO_x and O_3 in the LA basin has previously been explored. For example, Nussbaumer and Cohen[87] observed a spatially heterogenous relationship between summertime NO_x and temperature; at one location NO_x concentrations appeared to increase linearly with temperature,

and at others, NO_x concentrations peaked at the middle of the temperature range before decreasing. In this previous study, a satisfactory explanation for why NO_x concentrations should increase with temperature was not suggested, given that the large majority of NO_x emissions in the LA basin are from temperature-independent mobile sources[159,160]. The relationships previously observed consisted of daily average values derived from hourly observations taken between the hours of 10:00-14:00. Here, we expand on this work by considering the relationship between NO_x and temperature at all hours of the day to better understand the phenomena that might influence the enhancement of NO_x on warmer days. Given the wide array of chemical reactions NO_x can participate in, we also consider the behavior of carbon monoxide (CO) with temperature. Because CO reacts at much slower timescales than NO_x, we use it as a pseudo-tracer species to track its enhancement with temperature as independent of chemistry— also with the assumption that CO emissions are independent of temperature.

Methods

We use hourly observations of NO_2, NO_x, and CO from the Environmental Protection Agency Air Quality System (EPA AQS) for the months of May-September and the years 2000-2019. A complete list of AQS sites used in this analysis are shown in Table C.1 of Appendix C. Site selection within the greater LA area was based on the locations featuring complete data records for the three species of interest throughout the entire period of analysis. For each species, we create three sets of daily averages, one utilizing only the hours of 10:00-17:00, one utilizing only the hours of 22:00-05:00, and one utilizing every hour of the day (00:00-23:00). In this way, we probe how trends differ when considering daytime versus nighttime trends. We then pair each daily average concentration with a daily average temperature. Because not all AQS sites report temperature observations, we utilize temperature values from the ERA5 reanalysis provided by the Copernicus Climate Data Store of the European Centre for Medium-Range Weather Forecasts (ECMWF)[161]. Temperatures are synchronized to each AQS site on a daily basis and spatially by the average grid-cell value within 0.2 degrees of latitude and longitude. Doing so allows us to consider every AQS observation available and not exclude sites which do not report temperature readings.

We then split our observations into four five-year periods: 2000-2004, 2005-2009, 2010-2014, and 2015-2019. We do so to gauge decadal trends and also to ensure fair comparisons within each period given the dramatic decline in absolute concentrations of these pollutants over the two decades. For a list of average concentrations of NO_2/NO_x/CO at each AQS site in each period, see Table C.2 of Appendix C. We utilize these average concentrations to normalize all observations by their five-year average at each respective AQS site. This allows us to compare relative increases in these pollutants with temperature despite spatial and temporal variations in concentrations. By then binning these relative enhancements in NO_2/NO_x/CO by temperature deciles, we assess how average concentrations vary at each AQS site for each five-year period as a function of temperature.

Results

We first consider how daily average concentrations of NO_2 correlate with temperature when resampled from all hours of the day. For each five-year period, NO_2 observations are divided by the average concentration at their respective AQS site during that time and then binned by daily mean temperature deciles. Figure 4.1A shows how this results in a remarkably consistent linear relationship between normalized NO_2 concentrations and temperature. Across

the period 2000-2019, the lowest decile of temperatures is associated with NO_2 concentrations of roughly 70% of the mean, and the highest decile of temperatures is associated with NO_2 concentrations of roughly 130% of the mean. Even as absolute concentrations of NO_2 have fallen dramatically from 26.1 to 11.4 ppb (Table C.2 in Appendix C), this relationship between relative enhancement and temperature has remained robust. Figures 4.1B and 4.1C then replicate this analysis for daily averages calculated from either (B) only daytime hours and (C) only nighttime hours.

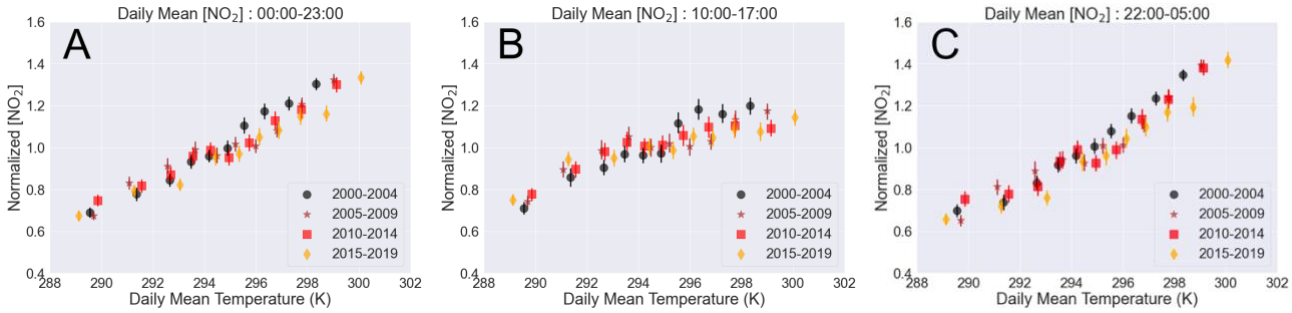

Figure 4.1: Mean daily normalized concentrations of NO_2 binned by temperature decile resampled from either (A) all hours of the day, (B) 10:00-17:00, and (C) 22:00-5:00. Error bars represent the bootstrapped 95% confidence interval for the median of each bin.

The daytime enhancement in NO_2 with temperature is weaker than the 24-hour enhancement, with a range of ~80-110% of the respective means across the full temperature range (Figure 4.1B). However, the nighttime enhancement of NO_2 with temperature closely tracks the 24-hour enhancement (Figure 4.1C). Given that nighttime conditions feature lower planetary boundary layer (PBL) heights, and therefore represent a greater potential for accumulation and generally higher concentrations, it is not surprising that nighttime trends dominate the 24-hour average. This persistent nighttime increase in NO_2 with temperature is indicative that atmospheric stagnation is important. On warmer days, we could expect lower wind speeds and atmospheric inversions that result in lower PBL heights and a consequent accumulation of primary pollution. The unique topography of LA also facilitates this phenomenon by trapping air in its basin. Other potential explanatory variables for this enhancement might be temperature dependent chemical processes or emissions. Given that the lion's share of NO_x emissions in LA are from temperature-independent mobile sources, emissions are unlikely to be driving the observed behavior. In addition, the fact that the relative increase in NO_2 with temperature remains virtually unchanged despite reductions in absolute NO_2 concentrations of more than a factor of two during the study period suggests that temperature dependent emissions are unlikely to play a role. To then investigate the potential role of chemistry, we repeat the analysis conducted in Figure 4.1 for the species of NO_x and CO. Given the strong similarities between the analyses conducted on NO_2 vis-à-vis NO_x concentrations, we relegate the plots showing the decadal increases in normalized NO_x concentrations versus temperature to Appendix C (Figure C.1). The plots for CO are then shown in Figure 4.2.

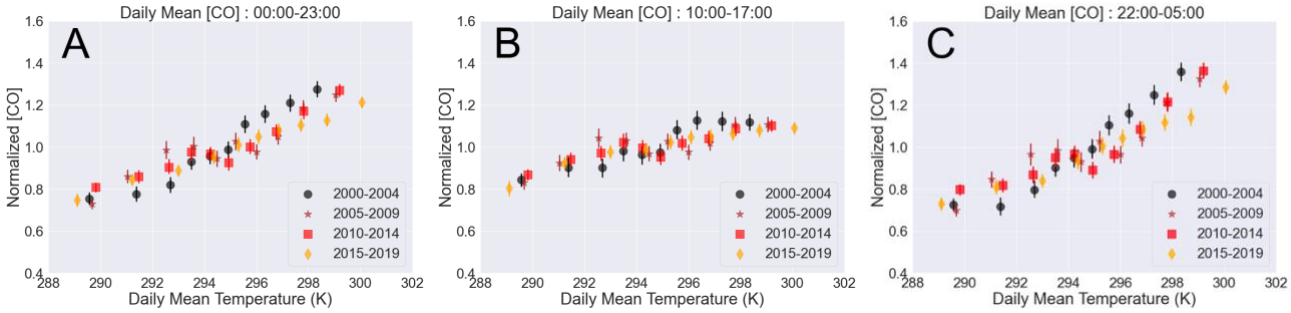

Figure 4.2: Mean daily normalized concentrations of CO binned by temperature decile resampled from either (A) all hours of the day, (B) 10:00-17:00, and (C) 22:00-5:00. Error bars represent the bootstrapped 95% confidence interval for the median of each bin.

Figures C.1 and C.2 in Appendix C demonstrate how the trends we observe in NO_2 are mirrored when considering both NO_x and CO. Here too we see normalized concentrations of 60-80% of the mean at the lowest decile of temperatures and 120-140% of the mean at the highest decile of temperatures. The fact that the normalized concentrations of these three species increase in the same linear fashion with temperature, especially at nighttime, suggests that a common factor is controlling the ensemble. Chemical processes are unlikely to be a factor here, given that we don't expect CO to participate in substantial transformations at this timescale, especially at night when photochemical sources should be negligible. In addition, we observe little distinction between the temperature-dependent enhancement in CO relative to NO_2/NO_x, again suggesting that temperature-dependent chemistry is not influencing one species differently than the other. Also, given that the daytime concentrations of CO and NO_x are much less responsive to temperature, we do not expect these trends to significantly affect the temperature dependence of daytime ozone and aerosols.

Another useful analysis is to consider how this temperature dependent enhancement is contributing to exceedances of air quality standards. The World Health Organization (WHO) suggests a guideline 24-hour mean concentration for NO_2 of 25 $\mu g/m^3$ (~13 ppb)[162] and this threshold is routinely crossed throughout the period of study (May-September, 2000-2019). Figure 4.3 shows the probability of mean daily NO_2 concentrations exceeding the guideline binned by temperature decile in each five-year period. Panel A represents the probabilities of exceedances considering only weekdays and panel B considering only weekends.

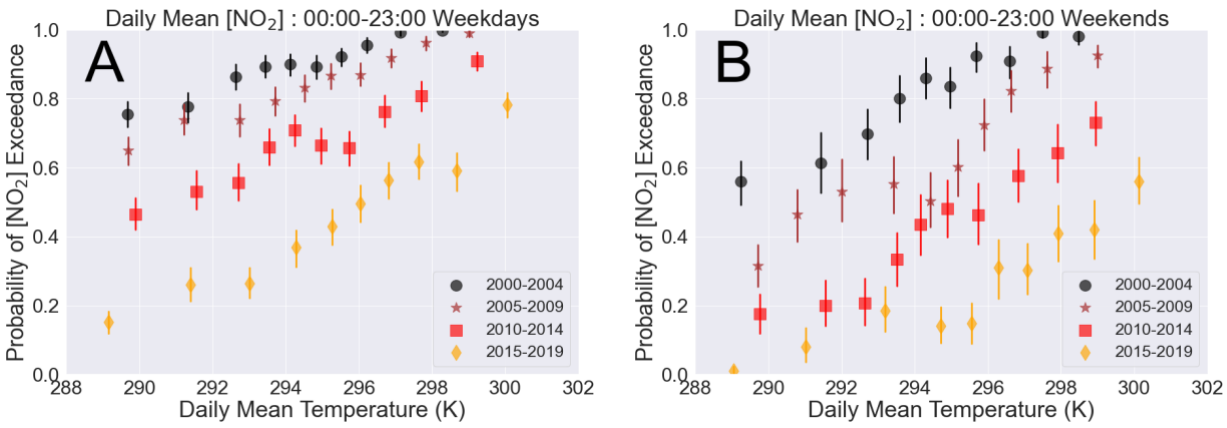

Figure 4.3: Probability of exceeding WHO 24-hour NO_2 guideline binned by temperature decile during (A) weekdays only and (B) weekends only. Error bars represent the bootstrapped 95% confidence interval for the median of each bin.

Figure 4.3 shows how in absolute terms, we are much less likely to exceed the NO_2 guideline value in recent years. Across all days of the week between 2000-2004, NO_2 concentrations were in exceedance of the guideline 87% of the time, whereas between 2015-2019, this value is just under 40%. Comparing then between weekdays (Figure 4.3A) and weekends (Figure 4.3B), we find that weekdays feature higher probabilities of exceeding NO_2 standards across the board. This is consistent with lessened NO_2 emissions during the weekends due to there being fewer cars and trucks on the road. However, across all time periods and days of the week, we find that the probability of exceedance grows with temperature, and this increase in exceedances with temperature is becoming starker. In recent years, the coldest decile of days saw a ~8% probability of exceeding the NO_2 guideline (~12% on weekdays and <1% on weekends), whereas the probability at the hottest decile of days was ~75% (~82% on weekdays and ~57% on weekends). This highlights how temperature is becoming a very strong control for predicting summertime NO_2 exceedances in LA. Though Figure 4.3 is constructed from daily averages resampled utilizing all hours of the day, Figure 4.1 tells us that it is specifically the nighttime trends that are driving these exceedances. In this way, nighttime stagnation and accumulation of NO_2 on warm days currently represents the greatest exposure risk during LA summers.

Discussion

During summertime in LA, we find that daily average NO_2 concentrations are strongly temperature dependent, and this dependence is dominated by nighttime accumulation. Similarities in the enhancements of total NO_x and CO show how this effect is not unique to NO_2 and likely meteorological. Even in recent years, we continue to exceed NO_2 guidelines on a regular basis. Considering that each point in Figure 4.3 represents a tenth of the time range, we see that half the weekdays had a 50% chance or better of exceeding NO_2 standards. We can also deduce that every 1 K increase in mean daily temperature is associated with a ~5% increase in probability of exceeding standards.

Emission control schemes have been largely successful in decreasing NO_x concentrations in LA; from 1994 to 2019, observations from downtown LA have seen reductions of nearly 80%[87], but there are additional public health benefits to continuing to bring down concentrations. In the 2022 Air Quality Management Plan (AQMP) prepared by the local South Coast Air Quality Management District[163], the authors assert that current regulation strategies are projected to decrease NO_x emissions by 47% comparing 2018 to 2037. If we imagine that these emission reductions will result in a comparable decrease in NO_2 concentrations, this abatement should be successful in keeping NO_2 concentrations below WHO guidelines ~95% of the time. However, an increase in air pollutant accumulation due to stagnation would jeopardize this progress. Therefore, this analysis shows that a major source of uncertainty for forecasting future exposure risks in LA remains the extent to which climate change worsens the frequency and severity of stagnation episodes. This is concerning because it represents a hazard that is difficult to predict and even more difficult to control via policy.

Another important consideration is the matter of nighttime exposure. A growing number of studies are finding that exposure to air pollution, both ambient and indoor, is a contributor to adverse sleep health[164] and NO_2 exposure specifically has been linked to sleep disorders in both children and adults[165,166]. The link between temperature, summertime air pollution, and stagnation has been investigated in past research[73–78,80], but this analysis is novel in scope in demonstrating how it is nighttime stagnation specifically that is contributing to present-day air quality guideline exceedances (and doing so in a temperature-dependent manner). In addition, past studies have focused primarily on stagnation as a driver of aerosol and O_3 accumulation, and to our knowledge, no study has shown NO_x concentrations to be temperature dependent as a result of stagnation. In this way, we build on previous findings by Nussbaumer & Cohen[87] and highlight the importance of considering nighttime trends specifically for accurately assessing exposure risk. Correctly modeling and predicting future air quality in LA will thus necessitate a more complete understanding of the meteorological mechanisms through which stagnation events occur.

Chapter 5: Conclusions

Among the countless unforeseen consequences of climate change, the influence of rising temperatures on air quality represents a uniquely compelling factor to consider. This is because rising ambient temperatures will shift the landscape of biological processes, human behavior, atmospheric chemistry, and meteorology in unprecedented ways. Throughout my work, I have considered both the direct impact of rising temperatures on drivers of air pollution as well as the ways in which temperature may act as a proxy for other explanatory variables. In both instances, however, the power of temperature as a predictor for poor air quality is made evident. To frame the problem through this lens is thus useful not only for understanding the underlying mechanisms enhancing air pollution, but also to inform public health strategies in order to minimize exposure. Here, I outline the principal conclusions of my research in this matter, elucidating potential directions for future work as well as considering the implications these findings may have on future policies.

Major Findings

In Chapter 2, I present an analysis of a regime transitioning from a summertime $PM_{2.5}$-temperature dependence dominated by sulfate aerosols to one instead regulated by organic aerosols. This transition underscores a profound improvement in air quality as a result of decadal reductions in coal combustion in the region. However, the drastic elimination of sulfate aerosols also signifies that the benefits of curbing SO_2 emissions are diminishing. Whereas targeting this fraction of $PM_{2.5}$ has been relatively straightforward on account of the limited sources of SO_2 emissions, addressing the broader class of organic aerosols will necessitate a multifaceted approach. This is not only because a much wider array of precursors can contribute towards forming organic aerosols, but also because a large fraction of these precursors is biogenic and thus lies largely outside of our control. This challenge is then further complicated by the fact that emission rates of both biogenic and anthropogenic OA precursors are expected to increase with temperature, as discussed in Chapter 1. In a warmer future, the highest summertime exposure risks in this region will continue to be associated with the highest ambient temperatures, but unlike in our sulfate-modulated past, we will have to contend with myriad drivers of enhanced $PM_{2.5}$. Though the region of study is notable in that it represents a domain unobfuscated by temperature-independent primary $PM_{2.5}$, allowing us to readily glimpse the trends in secondary formation, these processes are not unique to the Northeast U.S. The enhanced production of organic aerosols with temperature will occur even in regions where it is not the dominant feature of total $PM_{2.5}$. This analysis thus highlights the necessity of considering detailed $PM_{2.5}$ speciation when designing and evaluating policies to curb high aerosol concentrations, a task that is set to become increasingly complicated in the coming years.

In Chapter 3, I explore how atmospheric chemical transport models can aid us in delineating the sources of enhanced $PM_{2.5}$ with temperature. Using model predictions to evaluate the impact of shifting precursor emissions or evolving meteorological conditions on aerosol formation can be particularly informative. However, to meaningfully guide our understanding of the drivers of enhanced $PM_{2.5}$, predictions must be correct in both magnitude and composition. In this investigation of summertime $PM_{2.5}$, a comparison of model predictions to regulatory-grade observations across the Eastern U.S. yields good agreement in both mass concentrations as well as the response of total $PM_{2.5}$ to temperature. However, this agreement masks competing biases

in the two major temperature-dependent $PM_{2.5}$ components, sulfate and organic aerosols, underestimating the former and its response to temperature, and overestimating the latter and its response to temperature. Adjusting model parameters to address these biases is problematic because of the significant coupling between the two systems, where sulfate abundance promotes organic aerosol production. Nevertheless, by introducing additional pathways for sulfate formation in tandem with organic aerosol removal mechanisms, it is possible to address both biases simultaneously. These interventions, though inspired by recent literature advances, may not necessarily represent a complete picture of the atmospherically relevant processes at play. Future model simulations may reveal further ways in which to tune these parameters, among others, to achieve even better agreement with observations and theory. Still, this work presents a valuable framework for examining model performance through a novel lens, suggesting that upcoming assessments of aerosol predictions should consider the composition-specific temperature dependence. This aspect will be crucial for designing models able to thoroughly capture the landscape of aerosols in a warmer future, allowing us to better answer our original question of what precursors and chemical processes are primarily responsible for driving enhanced organic aerosol production with temperature, and what strategies may be more or less successful for its curtailment. Being able to accurately forecast $PM_{2.5}$ speciation will also be an important factor for predicting the damaging effects of future aerosol pollution, because designing effective PM mitigation strategies will comport considering not only total concentrations but also the characteristics of the inhaled particles and their specific health consequences.

In Chapter 4, I focus on the role of meteorology in controlling air pollutant concentrations, examining the interactions between temperature and atmospheric stagnation. High temperatures drive stagnation because they are associated with atmospheric inversions and lower wind speeds, limiting ventilation of pollutants. In this study, I show how despite significant decadal reductions in primary emissions, the temperature-driven relative enhancement of air pollutants in Los Angeles summers follows a steady trend over the last twenty years. The lowest temperatures are consistently associated with the lowest concentrations, and increases in temperature are linearly associated with increases in concentrations across the full temporal and spatial range of this study. Moreover, I show how it is specifically nighttime stagnation that is driving these trends. At night, when planetary boundary layer heights are at their lowest, the potential for accumulation is highest. Here, I focus on NO_2 and CO as the primary pollutants of interest because their concentrations are reported at the hourly level going back 20+ years. However, the atmospheric processes regulating their accumulation are certainly impacting aerosol concentrations as well (among several other factors previously described). A warmer future with greater periods of atmospheric stagnation thus represents an increased risk of exposure for a variety of air pollutants irrespective of enhancements in emissions or the acceleration of chemical processes. This study emphasizes the importance of taking spatially and temporally dense PM observations for elucidating these trends. A simple daily average measurement can disguise diurnal trends that are highly relevant for estimating exposures and making public health recommendations. Finally, though the effects outlined in this work are certainly exacerbated by the unique topography of Los Angeles, the association between temperature and stagnation is not unique to the region in question, and a warmer future impels us to consider temperature-driven nighttime stagnation as a distinct exposure hazard beyond this domain.

Future Research

Given the rising role of organic aerosols in governing summertime $PM_{2.5}$, a major avenue to explore in future work will be to more precisely delineate the relative contributions of various types of precursors. It will be necessary to understand what fraction of OA can be attributed to biogenic VOCs, anthropogenic VOCs, VCPs, etc. Moreover, we should also seek to understand how this source profile varies with temperature, and what precursors will be most influenced by a warmer climate. Exploring this matter will necessitate looking at aerosol formation from multiple perspectives; we will need greater resolution in aerosol speciation measurements as well as more sophisticated models able to consider an ever-expanding field of molecules and interactions we discover to be atmospherically relevant. Initiatives such as the Atmospheric Science and Chemistry Measurement Network (ASCENT)[167], a network currently in development at 12 sites across the U.S. which aims to provide high temporal resolution measurements of fine aerosol abundance, composition, and size distribution, will be critical in filling these knowledge gaps. Being able to speciate $PM_{2.5}$ with increased frequency and fidelity will make corroborating model predictions a more accessible task. Additionally, being able to compare organic aerosol abundance in urban and rural areas with different vegetation profiles, population densities, traffic patterns, and industries will also inform our understanding of the most pertinent factors influencing aerosol production. Expanding the class of molecules that we consider organic aerosol precursors is therefore an important angle to future model development. Another relevant angle is to continue refining model representations of the sulfate-OA coupling. In my work, I find that aerosol-phase oxidation of SO_2 is massively impactful in regulating total sulfate concentrations. However, the formation pathway I implement in the analysis featured in Chapter 3 is exceedingly simplistic. An important direction for future research in this space is to represent particle phase SO_2 oxidation in a manner more reflective of the actual atmospheric processes at play, mediated by particle acidity, water content, and transition metal abundance, among other factors. Despite the diminishing role of sulfate aerosols in influencing air quality in the present-day U.S., nailing model representations of sulfate will be crucial for properly predicting OA concentrations. Constraining the influence of sulfate on OA production will thus allow us to better understand the numerous other parameters influencing OA formation and removal. Achieving greater confidence in our modeled representation of OA will then allow us to better answer the original question of which fraction of aerosol we may hope to control via policy directives going forward.

Policy Implications

The state of air quality in urban areas across the United States is approaching an inflection point. Over the past several decades, environmental legislation has been largely effective in reducing atmospheric concentrations of many dangerous pollutants[168]. Still, our growing understanding of the true societal burdens associated with poor air quality suggests that there are additional public health benefits to be gained in continuing to limit exposure. For this reason, we are continuously reassessing what should constitute an acceptable level of exposure[169]. However, our methods for judging adherence to these standards are fundamentally biased, and we continue to find spatial, racial, and socioeconomic inequalities in urban exposure risks across the nation[170]. We are therefore impelled to revisit our strategies both with regards to abating air pollutants as well as evaluating the results of our efforts. The success of the policies of the past decades demonstrates the power of concerted action in throttling vehicular and power plant emissions, for example, but these approaches may start to yield diminishing returns.

Continuing to work towards a cleaner and more egalitarian future for U.S. cities will necessitate adopting dynamic policies that can respond to rapidly evolving environmental conditions. As our understanding of what sources present the greatest exposure threat at any given time progresses, so must our control strategies.

For example, a recent analysis of air pollution drivers in Los Angeles outlines the growing prevalence of biogenic VOCs in regulating both ozone and SOA formation potential[171]. Though a large fraction of biogenic VOC emissions remains squarely outside of our control, this study suggests that we should exercise more agency in how we manage our urban forests. Given the close proximity of urban vegetation to both anthropogenic oxidants (necessary to convert VOCs to SOA or ozone) as well as to the receptors vulnerable to air pollutant exposure, we need to consider their characteristics judiciously. Specifically, in our urban greening efforts we should favor the planting of species of vegetation with low VOC emission profiles. We should also seek out species whose emissions will respond less intensely to environmental stressors such as rising temperatures and aridity. The benefits of urban reforestation with respect to mitigating surface heating and preserving ecosystems impel us to continue exploring best practices for introducing additional vegetation to urban areas in ways that minimize the negative impact on air pollution, now, and in a warmer future.

Another way we can frame our policy strategies is in how to best adapt to environmental threats we cannot hope to control. For example, there is no sensible direct action we can take to disrupt an episode of atmospheric stagnation. However, what I outline in Chapter 4 is that the regularity of the response of stagnation events to temperature can help us design proactive measures. If we know that the incidence of stagnation is robustly correlated with temperature, and that the effect will be felt most strongly at nighttime, then we know we must prioritize the cessation of emissions in those periods. Policy strategies in this space might thus involve providing incentives to limit vehicular, industrial, and power plant emissions during the warmest days and especially the warmest nights. Additionally, we should continue investing in technologies that would allow us to store electrical energy produced in periods of high renewable generation availability to offset later periods of high demand and low renewable availability. By tying the extent of these emission reduction incentives to a tangible measurement like ambient temperature, we can better predict short-term constraints and simplify enforcement of such policies.

Finally, though the bulk of the analyses presented here focus on secondary OA formation, it is important to reiterate the importance of primary OA originating from wildfires in controlling $PM_{2.5}$ abundance and air quality guideline exceedances. $PM_{2.5}$ concentrations seen under wildfire events greatly exceed secondary OA production on even the hottest days. Therefore, and given that the frequency of wildfire events will continue to grow in coming years, we must continue pursuing active forest management as a means for preventing the degradation of both ecosystems and regional air quality. Internalizing the true societal costs of wildfire events and supporting collaboration across jurisdictions to implement precautionary efforts will be a key aspect of our policy strategies in this regard.

I conclude by considering the privilege that I have had in focusing my attention on the United States, a domain that can boast of substantial successes both in air quality monitoring and management over the past decades. The public health risks that I identify for U.S. cities are profoundly different in magnitude and nature than the challenges present in other nations. Though climate change promises to complicate future efforts in air pollution control, we are fortunate still to be able to pose these questions and contemplate if the limit of human

intervention on improving air quality is on the horizon. If this is an attainable future, for the U.S. and for other nations as they transition away from regimes dominated by primary anthropogenic emissions, then I hope the considerations I have brought forth will prove useful in informing the continued pursuit of clean air for all.

References

(1) Murray, C. J. L. et al.; Global Burden of 87 Risk Factors in 204 Countries and Territories, 1990–2019: A Systematic Analysis for the Global Burden of Disease Study 2019. *The Lancet* **2020**, *396* (10258), 1223–1249. https://doi.org/10.1016/S0140-6736(20)30752-2.

(2) Brunekreef, B.; Strak, M.; Chen, J.; Andersen, Z. J.; Atkinson, R.; Bauwelinck, M.; Bellander, T.; Boutron, M.-C.; Brandt, J.; Carey, I.; Cesaroni, G.; Forastiere, F.; Fecht, D.; Gulliver, J.; Hertel, O.; Hoffmann, B.; de Hoogh, K.; Houthuijs, D.; Hvidtfeldt, U.; Janssen, N.; Jørgensen, J.; Katsouyanni, K.; Ketzel, M.; Klompmaker, J.; Krog, N. H.; Liu, S.; Ljungman, P.; Mehta, A.; Nagel, G.; Oftedal, B.; Pershagen, G.; Peters, A.; Raaschou-Nielsen, O.; Renzi, M.; Rodopoulou, S.; Samoli, E.; Schwarze, P.; Sigsgaard, T.; Stafoggia, M.; Vienneau, D.; Weinmayr, G.; Wolf, K.; Hoek, G. Mortality and Morbidity Effects of Long-Term Exposure to Low-Level $PM_{2.5}$, BC, NO2, and O3: An Analysis of European Cohorts in the ELAPSE Project. *Res. Rep. Health Eff. Inst.* **2021**, *2021*, 208.

(3) Chen, J.; Hoek, G. Long-Term Exposure to PM and All-Cause and Cause-Specific Mortality: A Systematic Review and Meta-Analysis. *Environ. Int.* **2020**, *143*, 105974. https://doi.org/10.1016/j.envint.2020.105974.

(4) Di, Q.; Dai, L.; Wang, Y.; Zanobetti, A.; Choirat, C.; Schwartz, J. D.; Dominici, F. Association of Short-Term Exposure to Air Pollution With Mortality in Older Adults. *JAMA* **2017**, *318* (24), 2446. https://doi.org/10.1001/jama.2017.17923.

(5) Orellano, P.; Reynoso, J.; Quaranta, N.; Bardach, A.; Ciapponi, A. Short-Term Exposure to Particulate Matter (PM10 and $PM_{2.5}$), Nitrogen Dioxide (NO2), and Ozone (O3) and All-Cause and Cause-Specific Mortality: Systematic Review and Meta-Analysis. *Environ. Int.* **2020**, *142*, 105876. https://doi.org/10.1016/j.envint.2020.105876.

(6) *The cost of air pollution : strengthening the economic case for action*. World Bank. https://documents.worldbank.org/en/publication/documents-reports/documentdetail/781521473177013155/The-cost-of-air-pollution-strengthening-the-economic-case-for-action (accessed 2023-08-09).

(7) *WHO Ambient Air Quality Database, 2022 Update: Status Report.*; World Health Organization: Geneva, 2023.

(8) Calvin, K.; Dasgupta, D.; Krinner, G.; Mukherji, A.; Thorne, P. W.; Trisos, C.; Romero, J.; Aldunce, P.; Barrett, K.; Blanco, G.; Cheung, W. W. L.; Connors, S.; Denton, F.; Diongue-Niang, A.; Dodman, D.; Garschagen, M.; Geden, O.; Hayward, B.; Jones, C.; Jotzo, F.; Krug, T.; Lasco, R.; Lee, Y.-Y.; Masson-Delmotte, V.; Meinshausen, M.; Mintenbeck, K.; Mokssit, A.; Otto, F. E. L.; Pathak, M.; Pirani, A.; Poloczanska, E.; Pörtner, H.-O.; Revi, A.; Roberts, D. C.; Roy, J.; Ruane, A. C.; Skea, J.; Shukla, P. R.; Slade, R.; Slangen, A.; Sokona, Y.; Sörensson, A. A.; Tignor, M.; Van Vuuren, D.; Wei, Y.-M.; Winkler, H.; Zhai, P.; Zommers, Z.; Hourcade, J.-C.; Johnson, F. X.; Pachauri, S.; Simpson, N. P.; Singh, C.; Thomas, A.; Totin, E.; Arias, P.; Bustamante, M.; Elgizouli, I.; Flato, G.; Howden, M.; Méndez-Vallejo, C.; Pereira, J. J.; Pichs-Madruga, R.; Rose, S. K.; Saheb, Y.; Sánchez Rodríguez, R.; Ürge-Vorsatz, D.; Xiao, C.; Yassaa, N.; Alegría, A.; Armour, K.; Bednar-Friedl, B.; Blok, K.; Cissé, G.; Dentener, F.; Eriksen, S.; Fischer, E.; Garner, G.; Guivarch, C.; Haasnoot, M.; Hansen, G.; Hauser, M.; Hawkins, E.; Hermans, T.; Kopp, R.; Leprince-Ringuet, N.; Lewis, J.; Ley, D.; Ludden, C.; Niamir, L.; Nicholls, Z.; Some, S.; Szopa, S.; Trewin, B.; Van Der Wijst, K.-I.; Winter, G.; Witting, M.; Birt, A.; Ha, M.; Romero, J.; Kim, J.; Haites, E. F.; Jung, Y.; Stavins, R.; Birt, A.; Ha, M.; Orendain, D. J. A.; Ignon, L.; Park, S.; Park, Y.;

Reisinger, A.; Cammaramo, D.; Fischlin, A.; Fuglestvedt, J. S.; Hansen, G.; Ludden, C.; Masson-Delmotte, V.; Matthews, J. B. R.; Mintenbeck, K.; Pirani, A.; Poloczanska, E.; Leprince-Ringuet, N.; Péan, C. *IPCC, 2023: Climate Change 2023: Synthesis Report. Contribution of Working Groups I, II and III to the Sixth Assessment Report of the Intergovernmental Panel on Climate Change [Core Writing Team, H. Lee and J. Romero (Eds.)]. IPCC, Geneva, Switzerland.*, First.; Intergovernmental Panel on Climate Change (IPCC), 2023. https://doi.org/10.59327/IPCC/AR6-9789291691647.

(9) Tagaris, E.; Manomaiphiboon, K.; Liao, K.-J.; Leung, L. R.; Woo, J.-H.; He, S.; Amar, P.; Russell, A. G. Impacts of Global Climate Change and Emissions on Regional Ozone and Fine Particulate Matter Concentrations over the United States. *J. Geophys. Res.* **2007**, *112* (D14), D14312. https://doi.org/10.1029/2006JD008262.

(10) Ebi, K. L.; McGregor, G. Climate Change, Tropospheric Ozone and Particulate Matter, and Health Impacts. *Environ. Health Perspect.* **2008**, *116* (11), 1449–1455. https://doi.org/10.1289/ehp.11463.

(11) Pye, H. O. T.; Liao, H.; Wu, S.; Mickley, L. J.; Jacob, D. J.; Henze, D. K.; Seinfeld, J. H. Effect of Changes in Climate and Emissions on Future Sulfate-nitrate-ammonium Aerosol Levels in the United States. *J. Geophys. Res. Atmospheres* **2009**, *114* (D1), 2008JD010701. https://doi.org/10.1029/2008JD010701.

(12) Fang, Y.; Mauzerall, D. L.; Liu, J.; Fiore, A. M.; Horowitz, L. W. Impacts of 21st Century Climate Change on Global Air Pollution-Related Premature Mortality. *Clim. Change* **2013**, *121* (2), 239–253. https://doi.org/10.1007/s10584-013-0847-8.

(13) Fuzzi, S.; Baltensperger, U.; Carslaw, K.; Decesari, S.; Denier Van Der Gon, H.; Facchini, M. C.; Fowler, D.; Koren, I.; Langford, B.; Lohmann, U.; Nemitz, E.; Pandis, S.; Riipinen, I.; Rudich, Y.; Schaap, M.; Slowik, J. G.; Spracklen, D. V.; Vignati, E.; Wild, M.; Williams, M.; Gilardoni, S. Particulate Matter, Air Quality and Climate: Lessons Learned and Future Needs. *Atmospheric Chem. Phys.* **2015**, *15* (14), 8217–8299. https://doi.org/10.5194/acp-15-8217-2015.

(14) Silva, R. A.; West, J. J.; Lamarque, J.-F.; Shindell, D. T.; Collins, W. J.; Faluvegi, G.; Folberth, G. A.; Horowitz, L. W.; Nagashima, T.; Naik, V.; Rumbold, S. T.; Sudo, K.; Takemura, T.; Bergmann, D.; Cameron-Smith, P.; Doherty, R. M.; Josse, B.; MacKenzie, I. A.; Stevenson, D. S.; Zeng, G. Future Global Mortality from Changes in Air Pollution Attributable to Climate Change. *Nat. Clim. Change* **2017**, *7* (9), 647–651. https://doi.org/10.1038/nclimate3354.

(15) Park, S.; Allen, R. J.; Lim, C. H. A Likely Increase in Fine Particulate Matter and Premature Mortality under Future Climate Change. *Air Qual. Atmosphere Health* **2020**, *13* (2), 143–151. https://doi.org/10.1007/s11869-019-00785-7.

(16) Fann, N. L.; Nolte, C. G.; Sarofim, M. C.; Martinich, J.; Nassikas, N. J. Associations Between Simulated Future Changes in Climate, Air Quality, and Human Health. *JAMA Netw. Open* **2021**, *4* (1), e2032064. https://doi.org/10.1001/jamanetworkopen.2020.32064.

(17) Liaskoni, M.; Huszar, P.; Bartík, L.; Prieto Perez, A. P.; Karlický, J.; Vlček, O. Modelling the European Wind-Blown Dust Emissions and Their Impact on Particulate Matter (PM) Concentrations. *Atmospheric Chem. Phys.* **2023**, *23* (6), 3629–3654. https://doi.org/10.5194/acp-23-3629-2023.

(18) Liu, S.; Xing, J.; Sahu, S. K.; Liu, X.; Liu, S.; Jiang, Y.; Zhang, H.; Li, S.; Ding, D.; Chang, X.; Wang, S. Wind-Blown Dust and Its Impacts on Particulate Matter Pollution in

Northern China: Current and Future Scenarios. *Environ. Res. Lett.* **2021**, *16* (11), 114041. https://doi.org/10.1088/1748-9326/ac31ec.
(19) Park, S. H.; Gong, S. L.; Gong, W.; Makar, P. A.; Moran, M. D.; Zhang, J.; Stroud, C. A. Relative Impact of Windblown Dust versus Anthropogenic Fugitive Dust in PM $_{2.5}$ on Air Quality in North America. *J. Geophys. Res.* **2010**, *115* (D16), D16210. https://doi.org/10.1029/2009JD013144.
(20) Cochran, R. E.; Ryder, O. S.; Grassian, V. H.; Prather, K. A. Sea Spray Aerosol: The Chemical Link between the Oceans, Atmosphere, and Climate. *Acc. Chem. Res.* **2017**, *50* (3), 599–604. https://doi.org/10.1021/acs.accounts.6b00603.
(21) Mather, T. A.; Pyle, D. M.; Oppenheimer, C. Tropospheric Volcanic Aerosol. In *Geophysical Monograph Series*; Robock, A., Oppenheimer, C., Eds.; American Geophysical Union: Washington, D. C., 2003; Vol. 139, pp 189–212. https://doi.org/10.1029/139GM12.
(22) Penkała, M.; Ogrodnik, P.; Rogula-Kozłowska, W. Particulate Matter from the Road Surface Abrasion as a Problem of Non-Exhaust Emission Control. *Environments* **2018**, *5* (1), 9. https://doi.org/10.3390/environments5010009.
(23) Kuhns, H.; Gillies, J.; Etyemezian, V.; Nikolich, G.; King, J.; Zhu, D.; Uppapalli, S.; Engelbrecht, J.; Kohl, S. Effect of Soil Type and Momentum on Unpaved Road Particulate Matter Emissions from Wheeled and Tracked Vehicles. *Aerosol Sci. Technol.* **2010**, *44* (3), 187–196. https://doi.org/10.1080/02786820903516844.
(24) Fussell, J. C.; Franklin, M.; Green, D. C.; Gustafsson, M.; Harrison, R. M.; Hicks, W.; Kelly, F. J.; Kishta, F.; Miller, M. R.; Mudway, I. S.; Oroumiyeh, F.; Selley, L.; Wang, M.; Zhu, Y. A Review of Road Traffic-Derived Non-Exhaust Particles: Emissions, Physicochemical Characteristics, Health Risks, and Mitigation Measures. *Environ. Sci. Technol.* **2022**, *56* (11), 6813–6835. https://doi.org/10.1021/acs.est.2c01072.
(25) Haslett, S. L.; Thomas, J. C.; Morgan, W. T.; Hadden, R.; Liu, D.; Allan, J. D.; Williams, P. I.; Keita, S.; Liousse, C.; Coe, H. Highly Controlled, Reproducible Measurements of Aerosol Emissions from Combustion of a Common African Biofuel Source. *Atmospheric Chem. Phys.* **2018**, *18* (1), 385–403. https://doi.org/10.5194/acp-18-385-2018.
(26) Li, X.; Wang, S.; Duan, L.; Hao, J.; Nie, Y. Carbonaceous Aerosol Emissions from Household Biofuel Combustion in China. *Environ. Sci. Technol.* **2009**, *43* (15), 6076–6081. https://doi.org/10.1021/es803330j.
(27) Presto, A. A.; Gordon, T. D.; Robinson, A. L. Primary to Secondary Organic Aerosol: Evolution of Organic Emissions from Mobile Combustion Sources. *Atmospheric Chem. Phys.* **2014**, *14* (10), 5015–5036. https://doi.org/10.5194/acp-14-5015-2014.
(28) Mohr, C.; Huffman, J. A.; Cubison, M. J.; Aiken, A. C.; Docherty, K. S.; Kimmel, J. R.; Ulbrich, I. M.; Hannigan, M.; Jimenez, J. L. Characterization of Primary Organic Aerosol Emissions from Meat Cooking, Trash Burning, and Motor Vehicles with High-Resolution Aerosol Mass Spectrometry and Comparison with Ambient and Chamber Observations. *Environ. Sci. Technol.* **2009**, *43* (7), 2443–2449. https://doi.org/10.1021/es8011518.
(29) Guenther, A. B.; Zimmerman, P. R.; Harley, P. C.; Monson, R. K.; Fall, R. Isoprene and Monoterpene Emission Rate Variability: Model Evaluations and Sensitivity Analyses. *J. Geophys. Res.* **1993**, *98* (D7), 12609. https://doi.org/10.1029/93JD00527.
(30) Henze, D. K.; Seinfeld, J. H. Global Secondary Organic Aerosol from Isoprene Oxidation. *Geophys. Res. Lett.* **2006**, *33* (9), L09812. https://doi.org/10.1029/2006GL025976.

(31) Carlton, A. G.; Wiedinmyer, C.; Kroll, J. H. A Review of Secondary Organic Aerosol (SOA) Formation from Isoprene. *Atmospheric Chem. Phys.* **2009**, *9* (14), 4987–5005. https://doi.org/10.5194/acp-9-4987-2009.
(32) Mutzel, A.; Rodigast, M.; Iinuma, Y.; Böge, O.; Herrmann, H. Monoterpene SOA – Contribution of First-Generation Oxidation Products to Formation and Chemical Composition. *Atmos. Environ.* **2016**, *130*, 136–144. https://doi.org/10.1016/j.atmosenv.2015.10.080.
(33) Tomaz, S.; Cui, T.; Chen, Y.; Sexton, K. G.; Roberts, J. M.; Warneke, C.; Yokelson, R. J.; Surratt, J. D.; Turpin, B. J. Photochemical Cloud Processing of Primary Wildfire Emissions as a Potential Source of Secondary Organic Aerosol. *Environ. Sci. Technol.* **2018**, *52* (19), 11027–11037. https://doi.org/10.1021/acs.est.8b03293.
(34) Khare, P.; Gentner, D. R. Considering the Future of Anthropogenic Gas-Phase Organic Compound Emissions and the Increasing Influence of Non-Combustion Sources on Urban Air Quality. *Atmospheric Chem. Phys.* **2018**, *18* (8), 5391–5413. https://doi.org/10.5194/acp-18-5391-2018.
(35) Khare, P.; Machesky, J.; Soto, R.; He, M.; Presto, A. A.; Gentner, D. R. Asphalt-Related Emissions Are a Major Missing Nontraditional Source of Secondary Organic Aerosol Precursors. *Sci. Adv.* **2020**, *6* (36), eabb9785. https://doi.org/10.1126/sciadv.abb9785.
(36) McDonald, B. C.; de Gouw, J. A.; Gilman, J. B.; Jathar, S. H.; Akherati, A.; Cappa, C. D.; Jimenez, J. L.; Lee-Taylor, J.; Hayes, P. L.; McKeen, S. A.; Cui, Y. Y.; Kim, S.-W.; Gentner, D. R.; Isaacman-VanWertz, G.; Goldstein, A. H.; Harley, R. A.; Frost, G. J.; Roberts, J. M.; Ryerson, T. B.; Trainer, M. Volatile Chemical Products Emerging as Largest Petrochemical Source of Urban Organic Emissions. *Science* **2018**, *359* (6377), 760–764. https://doi.org/10.1126/science.aaq0524.
(37) Pennington, E. A.; Seltzer, K. M.; Murphy, B. N.; Qin, M.; Seinfeld, J. H.; Pye, H. O. T. Modeling Secondary Organic Aerosol Formation from Volatile Chemical Products. *Atmospheric Chem. Phys.* **2021**, *21* (24), 18247–18261. https://doi.org/10.5194/acp-21-18247-2021.
(38) Sasidharan, S.; He, Y.; Akherati, A.; Li, Q.; Li, W.; Cocker, D.; McDonald, B. C.; Coggon, M. M.; Seltzer, K. M.; Pye, H. O. T.; Pierce, J. R.; Jathar, S. H. Secondary Organic Aerosol Formation from Volatile Chemical Product Emissions: Model Parameters and Contributions to Anthropogenic Aerosol. *Environ. Sci. Technol.* **2023**, *57* (32), 11891–11902. https://doi.org/10.1021/acs.est.3c00683.
(39) Wu, W.; Zhao, B.; Wang, S.; Hao, J. Ozone and Secondary Organic Aerosol Formation Potential from Anthropogenic Volatile Organic Compounds Emissions in China. *J. Environ. Sci.* **2017**, *53*, 224–237. https://doi.org/10.1016/j.jes.2016.03.025.
(40) Tuet, W. Y.; Chen, Y.; Xu, L.; Fok, S.; Gao, D.; Weber, R. J.; Ng, N. L. Chemical Oxidative Potential of Secondary Organic Aerosol (SOA) Generated from the Photooxidation of Biogenic and Anthropogenic Volatile Organic Compounds. *Atmospheric Chem. Phys.* **2017**, *17* (2), 839–853. https://doi.org/10.5194/acp-17-839-2017.
(41) Piccot, S. D.; Watson, J. J.; Jones, J. W. A Global Inventory of Volatile Organic Compound Emissions from Anthropogenic Sources. *J. Geophys. Res. Atmospheres* **1992**, *97* (D9), 9897–9912. https://doi.org/10.1029/92JD00682.
(42) Gentner, D. R.; Jathar, S. H.; Gordon, T. D.; Bahreini, R.; Day, D. A.; El Haddad, I.; Hayes, P. L.; Pieber, S. M.; Platt, S. M.; De Gouw, J.; Goldstein, A. H.; Harley, R. A.; Jimenez, J. L.; Prévôt, A. S. H.; Robinson, A. L. Review of Urban Secondary Organic

Aerosol Formation from Gasoline and Diesel Motor Vehicle Emissions. *Environ. Sci. Technol.* **2017**, *51* (3), 1074–1093. https://doi.org/10.1021/acs.est.6b04509.
(43) Burke, M.; Childs, M. L.; De La Cuesta, B.; Qiu, M.; Li, J.; Gould, C. F.; Heft-Neal, S.; Wara, M. The Contribution of Wildfire to $PM_{2.5}$ Trends in the USA. *Nature* **2023**. https://doi.org/10.1038/s41586-023-06522-6.
(44) Burke, M.; Driscoll, A.; Heft-Neal, S.; Xue, J.; Burney, J.; Wara, M. The Changing Risk and Burden of Wildfire in the United States. *Proc. Natl. Acad. Sci.* **2021**, *118* (2), e2011048118. https://doi.org/10.1073/pnas.2011048118.
(45) Jaffe, D. A.; O'Neill, S. M.; Larkin, N. K.; Holder, A. L.; Peterson, D. L.; Halofsky, J. E.; Rappold, A. G. Wildfire and Prescribed Burning Impacts on Air Quality in the United States. *J. Air Waste Manag. Assoc.* **2020**, *70* (6), 583–615. https://doi.org/10.1080/10962247.2020.1749731.
(46) Liu, J. C.; Mickley, L. J.; Sulprizio, M. P.; Dominici, F.; Yue, X.; Ebisu, K.; Anderson, G. B.; Khan, R. F. A.; Bravo, M. A.; Bell, M. L. Particulate Air Pollution from Wildfires in the Western US under Climate Change. *Clim. Change* **2016**, *138* (3–4), 655–666. https://doi.org/10.1007/s10584-016-1762-6.
(47) Abatzoglou, J. T.; Williams, A. P. Impact of Anthropogenic Climate Change on Wildfire across Western US Forests. *Proc. Natl. Acad. Sci.* **2016**, *113* (42), 11770–11775. https://doi.org/10.1073/pnas.1607171113.
(48) Dore, M. H. I. Climate Change and Changes in Global Precipitation Patterns: What Do We Know? *Environ. Int.* **2005**, *31* (8), 1167–1181. https://doi.org/10.1016/j.envint.2005.03.004.
(49) Trenberth, K. Changes in Precipitation with Climate Change. *Clim. Res.* **2011**, *47* (1), 123–138. https://doi.org/10.3354/cr00953.
(50) O'Gorman, P. A. Precipitation Extremes Under Climate Change. *Curr. Clim. Change Rep.* **2015**, *1* (2), 49–59. https://doi.org/10.1007/s40641-015-0009-3.
(51) Berger, J.; Denby, B. A Generalised Model for Traffic Induced Road Dust Emissions. Model Description and Evaluation. *Atmos. Environ.* **2011**, *45* (22), 3692–3703. https://doi.org/10.1016/j.atmosenv.2011.04.021.
(52) Callaghan, A. H.; Stokes, M. D.; Deane, G. B. The Effect of Water Temperature on Air Entrainment, Bubble Plumes, and Surface Foam in a Laboratory Breaking-Wave Analog. *J. Geophys. Res. Oceans* **2014**, *119* (11), 7463–7482. https://doi.org/10.1002/2014JC010351.
(53) Grythe, H.; Ström, J.; Krejci, R.; Quinn, P.; Stohl, A. A Review of Sea-Spray Aerosol Source Functions Using a Large Global Set of Sea Salt Aerosol Concentration Measurements. *Atmospheric Chem. Phys.* **2014**, *14* (3), 1277–1297. https://doi.org/10.5194/acp-14-1277-2014.
(54) Liu, S.; Liu, C.-C.; Froyd, K. D.; Schill, G. P.; Murphy, D. M.; Bui, T. P.; Dean-Day, J. M.; Weinzierl, B.; Dollner, M.; Diskin, G. S.; Chen, G.; Gao, R.-S. Sea Spray Aerosol Concentration Modulated by Sea Surface Temperature. *Proc. Natl. Acad. Sci.* **2021**, *118* (9), e2020583118. https://doi.org/10.1073/pnas.2020583118.
(55) Sutton, R. T.; Dong, B.; Gregory, J. M. Land/Sea Warming Ratio in Response to Climate Change: IPCC AR4 Model Results and Comparison with Observations. *Geophys. Res. Lett.* **2007**, *34* (2), L02701. https://doi.org/10.1029/2006GL028164.
(56) Shrivastava, M.; Andreae, M. O.; Artaxo, P.; Barbosa, H. M. J.; Berg, L. K.; Brito, J.; Ching, J.; Easter, R. C.; Fan, J.; Fast, J. D.; Feng, Z.; Fuentes, J. D.; Glasius, M.; Goldstein, A. H.; Alves, E. G.; Gomes, H.; Gu, D.; Guenther, A.; Jathar, S. H.; Kim, S.; Liu, Y.; Lou, S.;

Martin, S. T.; McNeill, V. F.; Medeiros, A.; de Sá, S. S.; Shilling, J. E.; Springston, S. R.; Souza, R. A. F.; Thornton, J. A.; Isaacman-VanWertz, G.; Yee, L. D.; Ynoue, R.; Zaveri, R. A.; Zelenyuk, A.; Zhao, C. Urban Pollution Greatly Enhances Formation of Natural Aerosols over the Amazon Rainforest. *Nat. Commun.* **2019**, *10* (1), 1046. https://doi.org/10.1038/s41467-019-08909-4.

(57) Xu, L.; Guo, H.; Boyd, C. M.; Klein, M.; Bougiatioti, A.; Cerully, K. M.; Hite, J. R.; Isaacman-VanWertz, G.; Kreisberg, N. M.; Knote, C.; Olson, K.; Koss, A.; Goldstein, A. H.; Hering, S. V.; de Gouw, J.; Baumann, K.; Lee, S.-H.; Nenes, A.; Weber, R. J.; Ng, N. L. Effects of Anthropogenic Emissions on Aerosol Formation from Isoprene and Monoterpenes in the Southeastern United States. *Proc. Natl. Acad. Sci.* **2015**, *112* (1), 37–42. https://doi.org/10.1073/pnas.1417609112.

(58) Goldstein, A. H.; Koven, C. D.; Heald, C. L.; Fung, I. Y. Biogenic Carbon and Anthropogenic Pollutants Combine to Form a Cooling Haze over the Southeastern United States. *Proc. Natl. Acad. Sci.* **2009**, *106* (22), 8835–8840. https://doi.org/10.1073/pnas.0904128106.

(59) Liu, Y.; Dong, X.; Emmons, L. K.; Jo, D. S.; Liu, Y.; Shrivastava, M.; Yue, M.; Liang, Y.; Song, Z.; He, X.; Wang, M. Exploring the Factors Controlling the Long-Term Trend (1988–2019) of Surface Organic Aerosols in the Continental United States by Simulations. *J. Geophys. Res. Atmospheres* **2023**, *128* (9), e2022JD037935. https://doi.org/10.1029/2022JD037935.

(60) Pye, H. O. T.; Ward-Caviness, C. K.; Murphy, B. N.; Appel, K. W.; Seltzer, K. M. Secondary Organic Aerosol Association with Cardiorespiratory Disease Mortality in the United States. *Nat. Commun.* **2021**, *12* (1), 7215. https://doi.org/10.1038/s41467-021-27484-1.

(61) Rubin, J. I.; Kean, A. J.; Harley, R. A.; Millet, D. B.; Goldstein, A. H. Temperature Dependence of Volatile Organic Compound Evaporative Emissions from Motor Vehicles. *J. Geophys. Res.* **2006**, *111* (D3), D03305. https://doi.org/10.1029/2005JD006458.

(62) Li, J.; Ge, Y.; Wang, X.; Zhang, M. Evaporative Emission Characteristics of High-Mileage Gasoline Vehicles. *Environ. Pollut.* **2022**, *303*, 119127. https://doi.org/10.1016/j.envpol.2022.119127.

(63) Wolkoff, P. Impact of Air Velocity, Temperature, Humidity, and Air on Long-Term Voc Emissions from Building Products. *Atmos. Environ.* **1998**, *32* (14–15), 2659–2668. https://doi.org/10.1016/S1352-2310(97)00402-0.

(64) Tang, R.; Guo, S.; Lu, Q.; Song, K.; Gong, Y.; Tan, R.; Liu, K.; Wang, H.; Yu, Y.; Shen, R.; Chen, S.; Zeng, L.; Jorga, S. D.; Robinson, A. L. Unexpected Moderate Contribution of Intermediate Volatility Organic Compounds from Gasoline Vehicle Emission to Secondary Organic Aerosol Formation in Summer of Beijing. *Atmospheric Res.* **2023**, *295*, 106990. https://doi.org/10.1016/j.atmosres.2023.106990.

(65) Zhang, Y.; Fan, J.; Song, K.; Gong, Y.; Lv, D.; Wan, Z.; Li, T.; Zhang, C.; Lu, S.; Chen, S.; Zeng, L.; Guo, S. Secondary Organic Aerosol Formation from Semi-Volatile and Intermediate Volatility Organic Compounds in the Fall in Beijing. *Atmosphere* **2022**, *14* (1), 94. https://doi.org/10.3390/atmos14010094.

(66) Song, K.; Guo, S.; Gong, Y.; Lv, D.; Zhang, Y.; Wan, Z.; Li, T.; Zhu, W.; Wang, H.; Yu, Y.; Tan, R.; Shen, R.; Lu, S.; Li, S.; Chen, Y.; Hu, M. Impact of Cooking Style and Oil on Semi-Volatile and Intermediate Volatility Organic Compound Emissions from Chinese

Domestic Cooking. *Atmospheric Chem. Phys.* **2022**, *22* (15), 9827–9841. https://doi.org/10.5194/acp-22-9827-2022.
(67) Abel, D.; Holloway, T.; Kladar, R. M.; Meier, P.; Ahl, D.; Harkey, M.; Patz, J. Response of Power Plant Emissions to Ambient Temperature in the Eastern United States. *Environ. Sci. Technol.* **2017**, *51* (10), 5838–5846. https://doi.org/10.1021/acs.est.6b06201.
(68) Vannucci, P. F.; Cohen, R. C. Decadal Trends in the Temperature Dependence of Summertime Urban $PM_{2.5}$ in the Northeast United States. *ACS Earth Space Chem.* **2022**, acsearthspacechem.2c00077. https://doi.org/10.1021/acsearthspacechem.2c00077.
(69) Farkas, C. M.; Moeller, M. D.; Felder, F. A.; Henderson, B. H.; Carlton, A. G. High Electricity Demand in the Northeast U.S.: PJM Reliability Network and Peaking Unit Impacts on Air Quality. *Environ. Sci. Technol.* **2016**, *50* (15), 8375–8384. https://doi.org/10.1021/acs.est.6b01697.
(70) Abel, D. W.; Holloway, T.; Harkey, M.; Meier, P.; Ahl, D.; Limaye, V. S.; Patz, J. A. Air-Quality-Related Health Impacts from Climate Change and from Adaptation of Cooling Demand for Buildings in the Eastern United States: An Interdisciplinary Modeling Study. *PLOS Med.* **2018**, *15* (7), e1002599. https://doi.org/10.1371/journal.pmed.1002599.
(71) Rae, J. G. L.; Johnson, C. E.; Bellouin, N.; Boucher, O.; Haywood, J. M.; Jones, A. Sensitivity of Global Sulphate Aerosol Production to Changes in Oxidant Concentrations and Climate: GLOBAL SULPHATE AEROSOL PRODUCTION. *J. Geophys. Res. Atmospheres* **2007**, *112* (D10). https://doi.org/10.1029/2006JD007826.
(72) Aw, J. Evaluating the First-Order Effect of Intraannual Temperature Variability on Urban Air Pollution. *J. Geophys. Res.* **2003**, *108* (D12), 4365. https://doi.org/10.1029/2002JD002688.
(73) Wang, L.; Li, M.; Wang, Q.; Li, Y.; Xin, J.; Tang, X.; Du, W.; Song, T.; Li, T.; Sun, Y.; Gao, W.; Hu, B.; Wang, Y. Air Stagnation in China: Spatiotemporal Variability and Differing Impact on $PM_{2.5}$ and O3 during 2013–2018. *Sci. Total Environ.* **2022**, *819*, 152778. https://doi.org/10.1016/j.scitotenv.2021.152778.
(74) Garrido-Perez, J. M.; Ordóñez, C.; García-Herrera, R.; Schnell, J. L. The Differing Impact of Air Stagnation on Summer Ozone across Europe. *Atmos. Environ.* **2019**, *219*, 117062. https://doi.org/10.1016/j.atmosenv.2019.117062.
(75) Garrido-Perez, J. M.; Ordóñez, C.; García-Herrera, R.; Barriopedro, D. Air Stagnation in Europe: Spatiotemporal Variability and Impact on Air Quality. *Sci. Total Environ.* **2018**, *645*, 1238–1252. https://doi.org/10.1016/j.scitotenv.2018.07.238.
(76) Kerr, G. H.; Waugh, D. W. Connections between Summer Air Pollution and Stagnation. *Environ. Res. Lett.* **2018**, *13* (8), 084001. https://doi.org/10.1088/1748-9326/aad2e2.
(77) Schnell, J. L.; Prather, M. J. Co-Occurrence of Extremes in Surface Ozone, Particulate Matter, and Temperature over Eastern North America. *Proc. Natl. Acad. Sci.* **2017**, *114* (11), 2854–2859. https://doi.org/10.1073/pnas.1614453114.
(78) Porter, W. C.; Heald, C. L. *The Mechanisms and Meteorological Drivers of the Ozone–Temperature Relationship*; preprint; Gases/Atmospheric Modelling/Troposphere/Chemistry (chemical composition and reactions), 2019. https://doi.org/10.5194/acp-2019-140.
(79) Maddison, J. W.; Abalos, M.; Barriopedro, D.; García-Herrera, R.; Garrido-Perez, J. M.; Ordóñez, C.; Simpson, I. R. Assessing the Projected Changes in European Air Stagnation Due to Climate Change. *J. Clim.* **2023**, *36* (3), 917–930. https://doi.org/10.1175/JCLI-D-22-0180.1.

(80) Caserini, S.; Giani, P.; Cacciamani, C.; Ozgen, S.; Lonati, G. Influence of Climate Change on the Frequency of Daytime Temperature Inversions and Stagnation Events in the Po Valley: Historical Trend and Future Projections. *Atmospheric Res.* **2017**, *184*, 15–23. https://doi.org/10.1016/j.atmosres.2016.09.018.
(81) Horton, D. E.; Harshvardhan; Diffenbaugh, N. S. Response of Air Stagnation Frequency to Anthropogenically Enhanced Radiative Forcing. *Environ. Res. Lett.* **2012**, *7* (4), 044034. https://doi.org/10.1088/1748-9326/7/4/044034.
(82) *Urbanization, Biodiversity and Ecosystem Services: Challenges and Opportunities*; Elmqvist, T., Fragkias, M., Goodness, J., Güneralp, B., Marcotullio, P. J., McDonald, R. I., Parnell, S., Schewenius, M., Sendstad, M., Seto, K. C., Wilkinson, C., Eds.; Springer Netherlands: Dordrecht, 2013. https://doi.org/10.1007/978-94-007-7088-1.
(83) Sangiorgio, V.; Fiorito, F.; Santamouris, M. Development of a Holistic Urban Heat Island Evaluation Methodology. *Sci. Rep.* **2020**, *10* (1), 17913. https://doi.org/10.1038/s41598-020-75018-4.
(84) Center For International Earth Science Information Network-CIESIN-Columbia University. Gridded Population of the World, Version 4 (GPWv4): Population Density, 2016. https://doi.org/10.7927/H4NP22DQ.
(85) Hersbach, H., Bell, B., Berrisford, P., Biavati, G., Horányi, A., Muñoz Sabater, J., Nicolas, J., Peubey, C., Radu, R., Rozum, I., Schepers, D., Simmons, A., Soci, C., Dee, D., Thépaut, J-N. ERA5 Hourly Data on Single Levels from 1940 to Present. Copernicus Climate Change Service (C3S) Climate Data Store (CDS), 2023. https://doi.org/10.24381/cds.adbb2d47.
(86) Liu, Z.; Zhan, W.; Bechtel, B.; Voogt, J.; Lai, J.; Chakraborty, T.; Wang, Z.-H.; Li, M.; Huang, F.; Lee, X. Surface Warming in Global Cities Is Substantially More Rapid than in Rural Background Areas. *Commun. Earth Environ.* **2022**, *3* (1), 219. https://doi.org/10.1038/s43247-022-00539-x.
(87) Nussbaumer, C. M.; Cohen, R. C. The Role of Temperature and NOx in Ozone Trends in the Los Angeles Basin. *Environ. Sci. Technol.* **2020**, *54* (24), 15652–15659. https://doi.org/10.1021/acs.est.0c04910.
(88) Kim, K.-H.; Kabir, E.; Kabir, S. A Review on the Human Health Impact of Airborne Particulate Matter. *Environ. Int.* **2015**, *74*, 136–143. https://doi.org/10.1016/j.envint.2014.10.005.
(89) Manktelow, P. T.; Mann, G. W.; Carslaw, K. S.; Spracklen, D. V.; Chipperfield, M. P. Regional and Global Trends in Sulfate Aerosol since the 1980s. *Geophys. Res. Lett.* **2007**, *34* (14), L14803. https://doi.org/10.1029/2006GL028668.
(90) Hand, J. L.; Schichtel, B. A.; Malm, W. C.; Pitchford, M. L. Particulate Sulfate Ion Concentration and SO2 Emission Trends in the United States from the Early 1990s through 2010. *Atmospheric Chem. Phys.* **2012**, *12* (21), 10353–10365. https://doi.org/10.5194/acp-12-10353-2012.
(91) Krotkov, N. A.; McLinden, C. A.; Li, C.; Lamsal, L. N.; Celarier, E. A.; Marchenko, S. V.; Swartz, W. H.; Bucsela, E. J.; Joiner, J.; Duncan, B. N.; Boersma, K. F.; Veefkind, J. P.; Levelt, P. F.; Fioletov, V. E.; Dickerson, R. R.; He, H.; Lu, Z.; Streets, D. G. *Aura OMI Observations of Regional SO2 and NO2 Pollution Changes from 2005 to 2014*; preprint; Gases/Remote Sensing/Troposphere/Chemistry (chemical composition and reactions), 2015. https://doi.org/10.5194/acpd-15-26555-2015.

(92) McDonald, B. C.; Dallmann, T. R.; Martin, E. W.; Harley, R. A. Long-Term Trends in Nitrogen Oxide Emissions from Motor Vehicles at National, State, and Air Basin Scales: LONG-TERM TRENDS IN NITROGEN OXIDE EMISSIONS. *J. Geophys. Res. Atmospheres* **2012**, *117* (D21), n/a-n/a. https://doi.org/10.1029/2012JD018304.
(93) Silvern, R. F.; Jacob, D. J.; Mickley, L. J.; Sulprizio, M. P.; Travis, K. R.; Marais, E. A.; Cohen, R. C.; Laughner, J. L.; Choi, S.; Joiner, J.; Lamsal, L. N. Using Satellite Observations of Tropospheric NO2 Columns to Infer Long-Term Trends in US NO2 Emissions: The Importance of Accounting for the Free Tropospheric NO2 Background. *Atmospheric Chem. Phys.* **2019**, *19* (13), 8863–8878. https://doi.org/10.5194/acp-19-8863-2019.
(94) Duncan, B. N.; Lamsal, L. N.; Thompson, A. M.; Yoshida, Y.; Lu, Z.; Streets, D. G.; Hurwitz, M. M.; Pickering, K. E. A Space-Based, High-Resolution View of Notable Changes in Urban NOx Pollution around the World (2005-2014): NOTABLE CHANGES IN URBAN NOx POLLUTION. *J. Geophys. Res. Atmospheres* **2016**, *121* (2), 976–996. https://doi.org/10.1002/2015JD024121.
(95) Jimenez, J. L.; Canagaratna, M. R.; Donahue, N. M.; Prevot, A. S. H.; Zhang, Q.; Kroll, J. H.; DeCarlo, P. F.; Allan, J. D.; Coe, H.; Ng, N. L.; Aiken, A. C.; Docherty, K. S.; Ulbrich, I. M.; Grieshop, A. P.; Robinson, A. L.; Duplissy, J.; Smith, J. D.; Wilson, K. R.; Lanz, V. A.; Hueglin, C.; Sun, Y. L.; Tian, J.; Laaksonen, A.; Raatikainen, T.; Rautiainen, J.; Vaattovaara, P.; Ehn, M.; Kulmala, M.; Tomlinson, J. M.; Collins, D. R.; Cubison, M. J.; E.; Dunlea, J.; Huffman, J. A.; Onasch, T. B.; Alfarra, M. R.; Williams, P. I.; Bower, K.; Kondo, Y.; Schneider, J.; Drewnick, F.; Borrmann, S.; Weimer, S.; Demerjian, K.; Salcedo, D.; Cottrell, L.; Griffin, R.; Takami, A.; Miyoshi, T.; Hatakeyama, S.; Shimono, A.; Sun, J. Y.; Zhang, Y. M.; Dzepina, K.; Kimmel, J. R.; Sueper, D.; Jayne, J. T.; Herndon, S. C.; Trimborn, A. M.; Williams, L. R.; Wood, E. C.; Middlebrook, A. M.; Kolb, C. E.; Baltensperger, U.; Worsnop, D. R. Evolution of Organic Aerosols in the Atmosphere. *Science* **2009**, *326* (5959), 1525–1529. https://doi.org/10.1126/science.1180353.
(96) Hand, J. L.; Schichtel, B. A.; Pitchford, M.; Malm, W. C.; Frank, N. H. Seasonal Composition of Remote and Urban Fine Particulate Matter in the United States: COMPOSITION OF REMOTE AND URBAN AEROSOLS. *J. Geophys. Res. Atmospheres* **2012**, *117* (D5), n/a-n/a. https://doi.org/10.1029/2011JD017122.
(97) Shrivastava, M.; Cappa, C. D.; Fan, J.; Goldstein, A. H.; Guenther, A. B.; Jimenez, J. L.; Kuang, C.; Laskin, A.; Martin, S. T.; Ng, N. L.; Petaja, T.; Pierce, J. R.; Rasch, P. J.; Roldin, P.; Seinfeld, J. H.; Shilling, J.; Smith, J. N.; Thornton, J. A.; Volkamer, R.; Wang, J.; Worsnop, D. R.; Zaveri, R. A.; Zelenyuk, A.; Zhang, Q. Recent Advances in Understanding Secondary Organic Aerosol: Implications for Global Climate Forcing. *Rev. Geophys.* **2017**, *55* (2), 509–559. https://doi.org/10.1002/2016RG000540.
(98) Ridley, D. A.; Heald, C. L.; Ridley, K. J.; Kroll, J. H. Causes and Consequences of Decreasing Atmospheric Organic Aerosol in the United States. *Proc. Natl. Acad. Sci.* **2018**, *115* (2), 290–295. https://doi.org/10.1073/pnas.1700387115.
(99) Nussbaumer, C. M.; Cohen, R. C. Impact of OA on the Temperature Dependence of PM 2.5 in the Los Angeles Basin. *Environ. Sci. Technol.* **2021**, *55* (6), 3549–3558. https://doi.org/10.1021/acs.est.0c07144.
(100) Meng, X.; Hand, J. L.; Schichtel, B. A.; Liu, Y. Space-Time Trends of $PM_{2.5}$ Constituents in the Conterminous United States Estimated by a Machine Learning Approach, 2005–2015. *Environ. Int.* **2018**, *121*, 1137–1147. https://doi.org/10.1016/j.envint.2018.10.029.

(101) Westervelt, D. M.; Horowitz, L. W.; Naik, V.; Tai, A. P. K.; Fiore, A. M.; Mauzerall, D. L. Quantifying $PM_{2.5}$-Meteorology Sensitivities in a Global Climate Model. *Atmos. Environ.* **2016**, *142*, 43–56. https://doi.org/10.1016/j.atmosenv.2016.07.040.
(102) Russell, B. T.; Wang, D.; McMahan, C. S. Spatially Modeling the Effects of Meteorological Drivers of $PM_{2.5}$ in the Eastern United States via a Local Linear Penalized Quantile Regression Estimator: Spatially Modeling the Effects of Meteorological Drivers of $PM_{2.5}$. *Environmetrics* **2017**, *28* (5), e2448. https://doi.org/10.1002/env.2448.
(103) Li, X.; Seth, A.; Zhang, C.; Feng, R.; Long, X.; Li, W.; Liu, K. Evaluation of WRF-CMAQ Simulated Climatological Mean and Extremes of Fine Particulate Matter of the United States and Its Correlation with Climate Extremes. *Atmos. Environ.* **2020**, *222*, 117181. https://doi.org/10.1016/j.atmosenv.2019.117181.
(104) Self, S. W.; McMahan, C. S.; Russell, B. T. Identifying Meteorological Drivers of $PM_{2.5}$ Levels via a Bayesian Spatial Quantile Regression. *Environmetrics* **2021**, *32* (5). https://doi.org/10.1002/env.2669.
(105) York, D.; Evensen, N. M.; Martínez, M. L.; De Basabe Delgado, J. Unified Equations for the Slope, Intercept, and Standard Errors of the Best Straight Line. *Am. J. Phys.* **2004**, *72* (3), 367–375. https://doi.org/10.1119/1.1632486.
(106) Hand, J. L.; Prenni, A. J.; Schichtel, B. A.; Malm, W. C.; Chow, J. C. Trends in Remote $PM_{2.5}$ Residual Mass across the United States: Implications for Aerosol Mass Reconstruction in the IMPROVE Network. *Atmos. Environ.* **2019**, *203*, 141–152. https://doi.org/10.1016/j.atmosenv.2019.01.049.
(107) Bürki, C.; Reggente, M.; Dillner, A. M.; Hand, J. L.; Shaw, S. L.; Takahama, S. Analysis of Functional Groups in Atmospheric Aerosols by Infrared Spectroscopy: Method Development for Probabilistic Modeling of Organic Carbon and Organic Matter Concentrations. *Atmospheric Meas. Tech.* **2020**, *13* (3), 1517–1538. https://doi.org/10.5194/amt-13-1517-2020.
(108) Bowe, B.; Xie, Y.; Yan, Y.; Al-Aly, Z. Burden of Cause-Specific Mortality Associated With PM $_{2.5}$ Air Pollution in the United States. *JAMA Netw. Open* **2019**, *2* (11), e1915834. https://doi.org/10.1001/jamanetworkopen.2019.15834.
(109) Shaffer, R. M.; Blanco, M. N.; Li, G.; Adar, S. D.; Carone, M.; Szpiro, A. A.; Kaufman, J. D.; Larson, T. V.; Larson, E. B.; Crane, P. K.; Sheppard, L. Fine Particulate Matter and Dementia Incidence in the Adult Changes in Thought Study. *Environ. Health Perspect.* **2021**, *129* (8), 087001. https://doi.org/10.1289/EHP9018.
(110) Seinfeld, J. H.; Pandis, S. N. *Atmospheric Chemistry and Physics: From Air Pollution to Climate Change*, Third edition.; Wiley: Hoboken, New Jersey, 2016.
(111) *Particulate Matter ($PM_{2.5}$) Trends*; Environmental Protection Agency. https://www.epa.gov/air-trends/particulate-matter-pm25-trends (accessed 2023-01-20).
(112) *Ambient (Outdoor) Air Pollution*; World Health Organization. https://www.who.int/news-room/fact-sheets/detail/ambient-(outdoor)-air-quality-and-health (accessed 2023-01-20).
(113) Pai, S. J.; Carter, T. S.; Heald, C. L.; Kroll, J. H. Updated World Health Organization Air Quality Guidelines Highlight the Importance of Non-Anthropogenic $PM_{2.5}$. *Environ. Sci. Technol. Lett.* **2022**, *9* (6), 501–506. https://doi.org/10.1021/acs.estlett.2c00203.
(114) Pye, H. O. T.; Appel, K. W.; Seltzer, K. M.; Ward-Caviness, C. K.; Murphy, B. N. Human-Health Impacts of Controlling Secondary Air Pollution Precursors. *Environ. Sci. Technol. Lett.* **2022**, *9* (2), 96–101. https://doi.org/10.1021/acs.estlett.1c00798.

(115) Tai, A. P. K.; Mickley, L. J.; Jacob, D. J. Correlations between Fine Particulate Matter ($PM_{2.5}$) and Meteorological Variables in the United States: Implications for the Sensitivity of $PM_{2.5}$ to Climate Change. *Atmos. Environ.* **2010**, *44* (32), 3976–3984. https://doi.org/10.1016/j.atmosenv.2010.06.060.
(116) Tai, A. P. K.; Mickley, L. J.; Jacob, D. J.; Leibensperger, E. M.; Zhang, L.; Fisher, J. A.; Pye, H. O. T. Meteorological Modes of Variability for Fine Particulate Matter ($PM_{2.5}$) Air Quality in the United States: Implications for $PM_{2.5}$; Sensitivity to Climate Change. *Atmospheric Chem. Phys.* **2012**, *12* (6), 3131–3145. https://doi.org/10.5194/acp-12-3131-2012.
(117) Farkas, C. M.; Moeller, M. D.; Felder, F. A.; Baker, K. R.; Rodgers, M.; Carlton, A. G. Temporalization of Peak Electric Generation Particulate Matter Emissions during High Energy Demand Days. *Environ. Sci. Technol.* **2015**, *49* (7), 4696–4704. https://doi.org/10.1021/es5050248.
(118) Pye, H. O. T.; Pinder, R. W.; Piletic, I. R.; Xie, Y.; Capps, S. L.; Lin, Y.-H.; Surratt, J. D.; Zhang, Z.; Gold, A.; Luecken, D. J.; Hutzell, W. T.; Jaoui, M.; Offenberg, J. H.; Kleindienst, T. E.; Lewandowski, M.; Edney, E. O. Epoxide Pathways Improve Model Predictions of Isoprene Markers and Reveal Key Role of Acidity in Aerosol Formation. *Environ. Sci. Technol.* **2013**, *47* (19), 11056–11064. https://doi.org/10.1021/es402106h.
(119) Nolte, C. G.; Dolwick, P.; Fann, N.; Horowitz, L. W.; Naik, V.; Pinder, R. W.; Spero, T. L.; Winner, D. A.; Ziska, L. H. *Chapter 13 : Air Quality. Impacts, Risks, and Adaptation in the United States: The Fourth National Climate Assessment, Volume II*; U.S. Global Change Research Program, 2018. https://doi.org/10.7930/NCA4.2018.CH13.
(120) US EPA Office Of Research And Development. CMAQ, 2022. https://doi.org/10.5281/ZENODO.7218076.
(121) Pye, H. O. T.; Place, B. K.; Murphy, B. N.; Seltzer, K. M.; D'Ambro, E. L.; Allen, C.; Piletic, I. R.; Farrell, S.; Schwantes, R. H.; Coggon, M. M.; Saunders, E.; Xu, L.; Sarwar, G.; Hutzell, W. T.; Foley, K. M.; Pouliot, G.; Bash, J.; Stockwell, W. R. *Linking Gas, Particulate, and Toxic Endpoints to Air Emissions in the Community Regional Atmospheric Chemistry Multiphase Mechanism (CRACMM) Version 1.0*; preprint; Aerosols/Atmospheric Modelling/Troposphere/Chemistry (chemical composition and reactions), 2022. https://doi.org/10.5194/acp-2022-695.
(122) *Sampling Methods for $PM_{2.5}$ Speciation Parameters*; Environmental Protection Agency. https://aqs.epa.gov/aqsweb/documents/codetables/methods_speciation.html (accessed 2023-01-20).
(123) Moch, J. M.; Dovrou, E.; Mickley, L. J.; Keutsch, F. N.; Liu, Z.; Wang, Y.; Dombek, T. L.; Kuwata, M.; Budisulistiorini, S. H.; Yang, L.; Decesari, S.; Paglione, M.; Alexander, B.; Shao, J.; Munger, J. W.; Jacob, D. J. Global Importance of Hydroxymethanesulfonate in Ambient Particulate Matter: Implications for Air Quality. *J. Geophys. Res. Atmospheres* **2020**, *125* (18). https://doi.org/10.1029/2020JD032706.
(124) Place, B. K.; Hutzell, W. T.; Appel, K. W.; Farrell, S.; Valin, L.; Murphy, B. N.; Seltzer, K. M.; Sarwar, G.; Allen, C.; Piletic, I. R.; D'Ambro, E. L.; Saunders, E.; Simon, H.; Torres-Vasquez, A.; Pleim, J.; Schwantes, R. H.; Coggon, M. M.; Xu, L.; Stockwell, W. R.; Pye, H. O. T. Sensitivity of Northeast U.S. Surface Ozone Predictions to the Representation of Atmospheric Chemistry in CRACMMv1.0. *EGUsphere* **2023**, *2023*, 1–30. https://doi.org/10.5194/egusphere-2023-288.

(125) Skamarock, W. C.; Klemp, J. B.; Dudhia, J.; Gill, D. O.; Liu, Z.; Berner, J.; Wang, W.; Powers, J. G.; Duda, M. G.; Barker, D. M.; Huang, X.-Y. *A Description of the Advanced Research WRF Model Version 4*; UCAR/NCAR, 2019. https://doi.org/10.5065/1DFH-6P97.
(126) Otte, T. L.; Pleim, J. E. The Meteorology-Chemistry Interface Processor (MCIP) for the CMAQ Modeling System: Updates through MCIPv3.4.1. *Geosci. Model Dev.* **2010**, *3* (1), 243–256. https://doi.org/10.5194/gmd-3-243-2010.
(127) Emerson, E. W.; Hodshire, A. L.; DeBolt, H. M.; Bilsback, K. R.; Pierce, J. R.; McMeeking, G. R.; Farmer, D. K. Revisiting Particle Dry Deposition and Its Role in Radiative Effect Estimates. *Proc. Natl. Acad. Sci.* **2020**, *117* (42), 26076–26082. https://doi.org/10.1073/pnas.2014761117.
(128) Foley, K. M.; Pouliot, G. A.; Eyth, A.; Aldridge, M. F.; Allen, C.; Appel, K. W.; Bash, J. O.; Beardsley, M.; Beidler, J.; Choi, D.; Farkas, C.; Gilliam, R. C.; Godfrey, J.; Henderson, B. H.; Hogrefe, C.; Koplitz, S. N.; Mason, R.; Mathur, R.; Misenis, C.; Possiel, N.; Pye, H. O. T.; Reynolds, L.; Roark, M.; Roberts, S.; Schwede, D. B.; Seltzer, K. M.; Sonntag, D.; Talgo, K.; Toro, C.; Vukovich, J.; Xing, J.; Adams, E. 2002–2017 Anthropogenic Emissions Data for Air Quality Modeling over the United States. *Data Brief* **2023**, 109022. https://doi.org/10.1016/j.dib.2023.109022.
(129) Benjey, W.G.; Houyoux, M.R.; Susick, J.W. *Implementation of the SMOKE Emission Data Processor and SMOKE Tool Input Data Processor in Models-3*; Environmental Protection Agency. https://www3.epa.gov/ttnchie1/conference/ei10/modeling/benjey2.pdf (accessed 2023-01-20).
(130) Bash, J. O.; Baker, K. R.; Beaver, M. R. Evaluation of Improved Land Use and Canopy Representation in BEIS v3.61 with Biogenic VOC Measurements in California. *Geosci. Model Dev.* **2016**, *9* (6), 2191–2207. https://doi.org/10.5194/gmd-9-2191-2016.
(131) Appel, K. W.; Gilliam, R. C.; Davis, N.; Zubrow, A.; Howard, S. C. Overview of the Atmospheric Model Evaluation Tool (AMET) v1.1 for Evaluating Meteorological and Air Quality Models. *Environ. Model. Softw.* **2011**, *26* (4), 434–443. https://doi.org/10.1016/j.envsoft.2010.09.007.
(132) Pye, H. O. T.; Murphy, B. N.; Xu, L.; Ng, N. L.; Carlton, A. G.; Guo, H.; Weber, R.; Vasilakos, P.; Appel, K. W.; Budisulistiorini, S. H.; Surratt, J. D.; Nenes, A.; Hu, W.; Jimenez, J. L.; Isaacman-VanWertz, G.; Misztal, P. K.; Goldstein, A. H. On the Implications of Aerosol Liquid Water and Phase Separation for Organic Aerosol Mass. *Atmospheric Chem. Phys.* **2017**, *17* (1), 343–369. https://doi.org/10.5194/acp-17-343-2017.
(133) Theil, H. A Rank-Invariant Method of Linear and Polynomial Regression Analysis. I, II, III. *Nederl Akad Wetensch Proc 1950 53*, 386–392.
(134) Duan, J.; Huang, R.-J.; Li, Y.; Chen, Q.; Zheng, Y.; Chen, Y.; Lin, C.; Ni, H.; Wang, M.; Ovadnevaite, J.; Ceburnis, D.; Chen, C.; Worsnop, D. R.; Hoffmann, T.; O'Dowd, C.; Cao, J. Summertime and Wintertime Atmospheric Processes of Secondary Aerosol in Beijing. *Atmospheric Chem. Phys.* **2020**, *20* (6), 3793–3807. https://doi.org/10.5194/acp-20-3793-2020.
(135) Murphy, B. N.; Nolte, C. G.; Sidi, F.; Bash, J. O.; Appel, K. W.; Jang, C.; Kang, D.; Kelly, J.; Mathur, R.; Napelenok, S.; Pouliot, G.; Pye, H. O. T. The Detailed Emissions Scaling, Isolation, and Diagnostic (DESID) Module in the Community Multiscale Air Quality (CMAQ) Modeling System Version 5.3.2. *Geosci. Model Dev.* **2021**, *14* (6), 3407–3420. https://doi.org/10.5194/gmd-14-3407-2021.

(136) Liu, T.; Chan, A. W. H.; Abbatt, J. P. D. Multiphase Oxidation of Sulfur Dioxide in Aerosol Particles: Implications for Sulfate Formation in Polluted Environments. *Environ. Sci. Technol.* **2021**, *55* (8), 4227–4242. https://doi.org/10.1021/acs.est.0c06496.
(137) Wang, S.; Liu, T.; Jang, J.; Abbatt, J. P. D.; Chan, A. W. H. Heterogeneous Interactions between SO2; and Organic Peroxides in Submicron Aerosol. *Atmospheric Chem. Phys.* **2021**, *21* (9), 6647–6661. https://doi.org/10.5194/acp-21-6647-2021.
(138) Guenther, A. B.; Jiang, X.; Heald, C. L.; Sakulyanontvittaya, T.; Duhl, T.; Emmons, L. K.; Wang, X. The Model of Emissions of Gases and Aerosols from Nature Version 2.1 (MEGAN2.1): An Extended and Updated Framework for Modeling Biogenic Emissions. *Geosci. Model Dev.* **2012**, *5* (6), 1471–1492. https://doi.org/10.5194/gmd-5-1471-2012.
(139) Epstein, S. A.; Blair, S. L.; Nizkorodov, S. A. Direct Photolysis of α-Pinene Ozonolysis Secondary Organic Aerosol: Effect on Particle Mass and Peroxide Content. *Environ. Sci. Technol.* **2014**, *48* (19), 11251–11258. https://doi.org/10.1021/es502350u.
(140) Hodzic, A.; Madronich, S.; Kasibhatla, P. S.; Tyndall, G.; Aumont, B.; Jimenez, J. L.; Lee-Taylor, J.; Orlando, J. Organic Photolysis Reactions in Tropospheric Aerosols: Effect on Secondary Organic Aerosol Formation and Lifetime. *Atmospheric Chem. Phys.* **2015**, *15* (16), 9253–9269. https://doi.org/10.5194/acp-15-9253-2015.
(141) Wong, J. P. S.; Zhou, S.; Abbatt, J. P. D. Changes in Secondary Organic Aerosol Composition and Mass Due to Photolysis: Relative Humidity Dependence. *J. Phys. Chem. A* **2015**, *119* (19), 4309–4316. https://doi.org/10.1021/jp506898c.
(142) Hodzic, A.; Kasibhatla, P. S.; Jo, D. S.; Cappa, C. D.; Jimenez, J. L.; Madronich, S.; Park, R. J. Rethinking the Global Secondary Organic Aerosol (SOA) Budget: Stronger Production, Faster Removal, Shorter Lifetime. *Atmospheric Chem. Phys.* **2016**, *16* (12), 7917–7941. https://doi.org/10.5194/acp-16-7917-2016.
(143) Zawadowicz, M. A.; Lee, B. H.; Shrivastava, M.; Zelenyuk, A.; Zaveri, R. A.; Flynn, C.; Thornton, J. A.; Shilling, J. E. Photolysis Controls Atmospheric Budgets of Biogenic Secondary Organic Aerosol. *Environ. Sci. Technol.* **2020**, *54* (7), 3861–3870. https://doi.org/10.1021/acs.est.9b07051.
(144) Zhang, H.; Yee, L. D.; Lee, B. H.; Curtis, M. P.; Worton, D. R.; Isaacman-VanWertz, G.; Offenberg, J. H.; Lewandowski, M.; Kleindienst, T. E.; Beaver, M. R.; Holder, A. L.; Lonneman, W. A.; Docherty, K. S.; Jaoui, M.; Pye, H. O. T.; Hu, W.; Day, D. A.; Campuzano-Jost, P.; Jimenez, J. L.; Guo, H.; Weber, R. J.; de Gouw, J.; Koss, A. R.; Edgerton, E. S.; Brune, W.; Mohr, C.; Lopez-Hilfiker, F. D.; Lutz, A.; Kreisberg, N. M.; Spielman, S. R.; Hering, S. V.; Wilson, K. R.; Thornton, J. A.; Goldstein, A. H. Monoterpenes Are the Largest Source of Summertime Organic Aerosol in the Southeastern United States. *Proc. Natl. Acad. Sci.* **2018**, *115* (9), 2038–2043. https://doi.org/10.1073/pnas.1717513115.
(145) Surratt, J. D.; Chan, A. W. H.; Eddingsaas, N. C.; Chan, M.; Loza, C. L.; Kwan, A. J.; Hersey, S. P.; Flagan, R. C.; Wennberg, P. O.; Seinfeld, J. H. Reactive Intermediates Revealed in Secondary Organic Aerosol Formation from Isoprene. *Proc. Natl. Acad. Sci.* **2010**, *107* (15), 6640–6645. https://doi.org/10.1073/pnas.0911114107.
(146) Krapf, M.; El Haddad, I.; Bruns, E. A.; Molteni, U.; Daellenbach, K. R.; Prévôt, A. S. H.; Baltensperger, U.; Dommen, J. Labile Peroxides in Secondary Organic Aerosol. *Chem* **2016**, *1* (4), 603–616. https://doi.org/10.1016/j.chempr.2016.09.007.

(147) Wang, Y.; Takeuchi, M.; Wang, S.; Nizkorodov, S. A.; France, S.; Eris, G.; Ng, N. L. Photolysis of Gas-Phase Atmospherically Relevant Monoterpene-Derived Organic Nitrates. *J. Phys. Chem. A* **2023**, *127* (4), 987–999. https://doi.org/10.1021/acs.jpca.2c04307.
(148) Hallquist, M.; Wängberg, I.; Ljungström, E.; Barnes, I.; Becker, K.-H. Aerosol and Product Yields from NO3 Radical-Initiated Oxidation of Selected Monoterpenes. *Environ. Sci. Technol.* **1999**, *33* (4), 553–559. https://doi.org/10.1021/es980292s.
(149) Fry, J. L.; Kiendler-Scharr, A.; Rollins, A. W.; Wooldridge, P. J.; Brown, S. S.; Fuchs, H.; Dubé, W.; Mensah, A.; Dal Maso, M.; Tillmann, R.; Dorn, H.-P.; Brauers, T.; Cohen, R. C. Organic Nitrate and Secondary Organic Aerosol Yield from NO3; Oxidation of β-Pinene Evaluated Using a Gas-Phase Kinetics/Aerosol Partitioning Model. *Atmospheric Chem. Phys.* **2009**, *9* (4), 1431–1449. https://doi.org/10.5194/acp-9-1431-2009.
(150) Fry, J. L.; Draper, D. C.; Barsanti, K. C.; Smith, J. N.; Ortega, J.; Winkler, P. M.; Lawler, M. J.; Brown, S. S.; Edwards, P. M.; Cohen, R. C.; Lee, L. Secondary Organic Aerosol Formation and Organic Nitrate Yield from NO3 Oxidation of Biogenic Hydrocarbons. *Environ. Sci. Technol.* **2014**, *48* (20), 11944–11953. https://doi.org/10.1021/es502204x.
(151) Shen, H.; Zhao, D.; Pullinen, I.; Kang, S.; Vereecken, L.; Fuchs, H.; Acir, I.-H.; Tillmann, R.; Rohrer, F.; Wildt, J.; Kiendler-Scharr, A.; Wahner, A.; Mentel, T. F. Highly Oxygenated Organic Nitrates Formed from NO $_3$ Radical-Initiated Oxidation of β-Pinene. *Environ. Sci. Technol.* **2021**, *55* (23), 15658–15671. https://doi.org/10.1021/acs.est.1c03978.
(152) Wang, Y.; Piletic, I. R.; Takeuchi, M.; Xu, T.; France, S.; Ng, N. L. Synthesis and Hydrolysis of Atmospherically Relevant Monoterpene-Derived Organic Nitrates. *Environ. Sci. Technol.* **2021**, *55* (21), 14595–14606. https://doi.org/10.1021/acs.est.1c05310.
(153) Pye, H. O. T.; Luecken, D. J.; Xu, L.; Boyd, C. M.; Ng, N. L.; Baker, K. R.; Ayres, B. R.; Bash, J. O.; Baumann, K.; Carter, W. P. L.; Edgerton, E.; Fry, J. L.; Hutzell, W. T.; Schwede, D. B.; Shepson, P. B. Modeling the Current and Future Roles of Particulate Organic Nitrates in the Southeastern United States. *Environ. Sci. Technol.* **2015**, *49* (24), 14195–14203. https://doi.org/10.1021/acs.est.5b03738.
(154) Zare, A.; Fahey, K. M.; Sarwar, G.; Cohen, R. C.; Pye, H. O. T. Vapor-Pressure Pathways Initiate but Hydrolysis Products Dominate the Aerosol Estimated from Organic Nitrates. *ACS Earth Space Chem.* **2019**, *3* (8), 1426–1437. https://doi.org/10.1021/acsearthspacechem.9b00067.
(155) Zare, A.; Romer, P. S.; Nguyen, T.; Keutsch, F. N.; Skog, K.; Cohen, R. C. A Comprehensive Organic Nitrate Chemistry: Insights into the Lifetime of Atmospheric Organic Nitrates. *Atmospheric Chem. Phys.* **2018**, *18* (20), 15419–15436. https://doi.org/10.5194/acp-18-15419-2018.
(156) Wang, S.; Zhao, Y.; Chan, A. W. H.; Yao, M.; Chen, Z.; Abbatt, J. P. D. Organic Peroxides in Aerosol: Key Reactive Intermediates for Multiphase Processes in the Atmosphere. *Chem. Rev.* **2023**, *123* (4), 1635–1679. https://doi.org/10.1021/acs.chemrev.2c00430.
(157) Riva, M.; Chen, Y.; Zhang, Y.; Lei, Z.; Olson, N. E.; Boyer, H. C.; Narayan, S.; Yee, L. D.; Green, H. S.; Cui, T.; Zhang, Z.; Baumann, K.; Fort, M.; Edgerton, E.; Budisulistiorini, S. H.; Rose, C. A.; Ribeiro, I. O.; E Oliveira, R. L.; Dos Santos, E. O.; Machado, C. M. D.; Szopa, S.; Zhao, Y.; Alves, E. G.; De Sá, S. S.; Hu, W.; Knipping, E. M.; Shaw, S. L.; Duvoisin Junior, S.; De Souza, R. A. F.; Palm, B. B.; Jimenez, J.-L.; Glasius, M.; Goldstein, A. H.; Pye, H. O. T.; Gold, A.; Turpin, B. J.; Vizuete, W.; Martin, S. T.; Thornton, J. A.; Dutcher, C. S.; Ault, A. P.; Surratt, J. D. Increasing Isoprene Epoxydiol-to-Inorganic Sulfate Aerosol Ratio Results in Extensive Conversion of Inorganic Sulfate to Organosulfur Forms:

Implications for Aerosol Physicochemical Properties. *Environ. Sci. Technol.* **2019**, *53* (15), 8682–8694. https://doi.org/10.1021/acs.est.9b01019.
(158) Huang, S.; Li, H.; Wang, M.; Qian, Y.; Steenland, K.; Caudle, W. M.; Liu, Y.; Sarnat, J.; Papatheodorou, S.; Shi, L. Long-Term Exposure to Nitrogen Dioxide and Mortality: A Systematic Review and Meta-Analysis. *Sci. Total Environ.* **2021**, *776*, 145968. https://doi.org/10.1016/j.scitotenv.2021.145968.
(159) Pusede, S. E.; Steiner, A. L.; Cohen, R. C. Temperature and Recent Trends in the Chemistry of Continental Surface Ozone. *Chem. Rev.* **2015**, *115* (10), 3898–3918. https://doi.org/10.1021/cr5006815.
(160) Pusede, S. E.; Gentner, D. R.; Wooldridge, P. J.; Browne, E. C.; Rollins, A. W.; Min, K.-E.; Russell, A. R.; Thomas, J.; Zhang, L.; Brune, W. H.; Henry, S. B.; DiGangi, J. P.; Keutsch, F. N.; Harrold, S. A.; Thornton, J. A.; Beaver, M. R.; St. Clair, J. M.; Wennberg, P. O.; Sanders, J.; Ren, X.; VandenBoer, T. C.; Markovic, M. Z.; Guha, A.; Weber, R.; Goldstein, A. H.; Cohen, R. C. On the Temperature Dependence of Organic Reactivity, Nitrogen Oxides, Ozone Production, and the Impact of Emission Controls in San Joaquin Valley, California. *Atmospheric Chem. Phys.* **2014**, *14* (7), 3373–3395. https://doi.org/10.5194/acp-14-3373-2014.
(161) Hersbach, H.; Bell, B.; Berrisford, P.; Hirahara, S.; Horányi, A.; Muñoz-Sabater, J.; Nicolas, J.; Peubey, C.; Radu, R.; Schepers, D.; Simmons, A.; Soci, C.; Abdalla, S.; Abellan, X.; Balsamo, G.; Bechtold, P.; Biavati, G.; Bidlot, J.; Bonavita, M.; Chiara, G.; Dahlgren, P.; Dee, D.; Diamantakis, M.; Dragani, R.; Flemming, J.; Forbes, R.; Fuentes, M.; Geer, A.; Haimberger, L.; Healy, S.; Hogan, R. J.; Hólm, E.; Janisková, M.; Keeley, S.; Laloyaux, P.; Lopez, P.; Lupu, C.; Radnoti, G.; Rosnay, P.; Rozum, I.; Vamborg, F.; Villaume, S.; Thépaut, J. The ERA5 Global Reanalysis. *Q. J. R. Meteorol. Soc.* **2020**, *146* (730), 1999–2049. https://doi.org/10.1002/qj.3803.
(162) *What are the WHO Air quality guidelines?* https://www.who.int/news-room/feature-stories/detail/what-are-the-who-air-quality-guidelines (accessed 2023-07-24).
(163) *2022 Air Quality Management Plan*; South Coast Air Quality Management District, 2022. http://www.aqmd.gov/home/air-quality/clean-air-plans/air-quality-mgt-plan (accessed 2023-10-18).
(164) Liu, J.; Wu, T.; Liu, Q.; Wu, S.; Chen, J.-C. Air Pollution Exposure and Adverse Sleep Health across the Life Course: A Systematic Review. *Environ. Pollut.* **2020**, *262*, 114263. https://doi.org/10.1016/j.envpol.2020.114263.
(165) Billings, M. E.; Gold, D.; Szpiro, A.; Aaron, C. P.; Jorgensen, N.; Gassett, A.; Leary, P. J.; Kaufman, J. D.; Redline, S. R. The Association of Ambient Air Pollution with Sleep Apnea: The Multi-Ethnic Study of Atherosclerosis. *Ann. Am. Thorac. Soc.* **2018**, AnnalsATS.201804-248OC. https://doi.org/10.1513/AnnalsATS.201804-248OC.
(166) Lawrence, W. R.; Yang, M.; Zhang, C.; Liu, R.-Q.; Lin, S.; Wang, S.-Q.; Liu, Y.; Ma, H.; Chen, D.-H.; Zeng, X.-W.; Yang, B.-Y.; Hu, L.-W.; Yim, S. H. L.; Dong, G.-H. Association between Long-Term Exposure to Air Pollution and Sleep Disorder in Chinese Children: The Seven Northeastern Cities Study. *Sleep* **2018**, *41* (9). https://doi.org/10.1093/sleep/zsy122.
(167) Ng, N. L.; Dillner, A. M.; Bahreini, R.; Russell, A. G.; de La Beaujardière, J.; Flynn, J.; Gentner, D. R.; Griffin, R.; Hawkins, L. N.; Jimenez, J. L.; Mao, J.; Murphy, S. M.; Nienhouse, E.; Presto, A.; Raffuse, S. M.; Robinson, A. L.; Seinfeld, J.; Surratt, J. D.; Thornton, J. A.; Thrasher, B. Atmospheric Science and Chemistry mEasurement NeTwork

(ASCENT): A New Ground-Based High Time-Resolution Air Quality Monitoring Network. **2022**, *2022*, A55R-1360.
(168) *Our Nation's Air, Trends Through 2021: Air Quality Improves as America Grows*; Environmental Protection Agency. https://gispub.epa.gov/air/trendsreport/2022/#home (accessed 2023-10-25).
(169) EPA Press Office. *EPA Proposes to Strengthen Air Quality Standards to Protect the Public from Harmful Effects of Soot*; Environmental Protection Agency. https://www.epa.gov/newsreleases/epa-proposes-strengthen-air-quality-standards-protect-public-harmful-effects-soot (accessed 2023-10-25).
(170) Lane, H. M.; Morello-Frosch, R.; Marshall, J. D.; Apte, J. S. Historical Redlining Is Associated with Present-Day Air Pollution Disparities in U.S. Cities. *Environ. Sci. Technol. Lett.* **2022**, *9* (4), 345–350. https://doi.org/10.1021/acs.estlett.1c01012.
(171) Gu, S.; Guenther, A.; Faiola, C. Effects of Anthropogenic and Biogenic Volatile Organic Compounds on Los Angeles Air Quality. *Environ. Sci. Technol.* **2021**, *55* (18), 12191–12201. https://doi.org/10.1021/acs.est.1c01481.

Appendix A: Supplement to Chapter 2

Table A.1: Summary of AQS sites queried to obtain data used in this study. Data was obtained for the period of June-August 2000-2020 whenever available with the exception of organic carbon (OC) speciation data, which was only available for the period 2016-2020.

City	Latitude	Longitude	EPA AQS Site ID	Data Collected	Years Collected
Baltimore	39.31	-76.47	24-005-3001	$PM_{2.5}$, Temperature	2000-2020
				Speciation	2001-2020
Boston	42.35	-71.10	25-025-0002	$PM_{2.5}$, Temperature	2000-2020
	42.33	-71.08	25-025-0042	Speciation	2001-2020
Buffalo	42.88	-78.81	36-029-0005	$PM_{2.5}$, Speciation, Temperature	2000-2020
New York	40.80	-73.93	36-061-0079	$PM_{2.5}$, Temperature	2000-2020
	40.74	-73.82	36-081-0124	Speciation	2001-2020
Philadelphia	39.99	-75.05	34-007-1007	$PM_{2.5}$, Temperature	2000-2020
	40.01	-75.10	42-101-0004	Speciation	2000-2005
	39.92	-75.19	42-101-0055	Speciation	2006-2020
Providence	41.84	-71.36	44-007-1010	$PM_{2.5}$, Temperature	2000-2020
				Speciation	2010-2020
	41.81	-71.41	44-007-0022	Speciation	2002-2010
Washington D.C.	38.92	-77.01	11-001-0043	$PM_{2.5}$, Speciation, Temperature, NOx	2000-2020

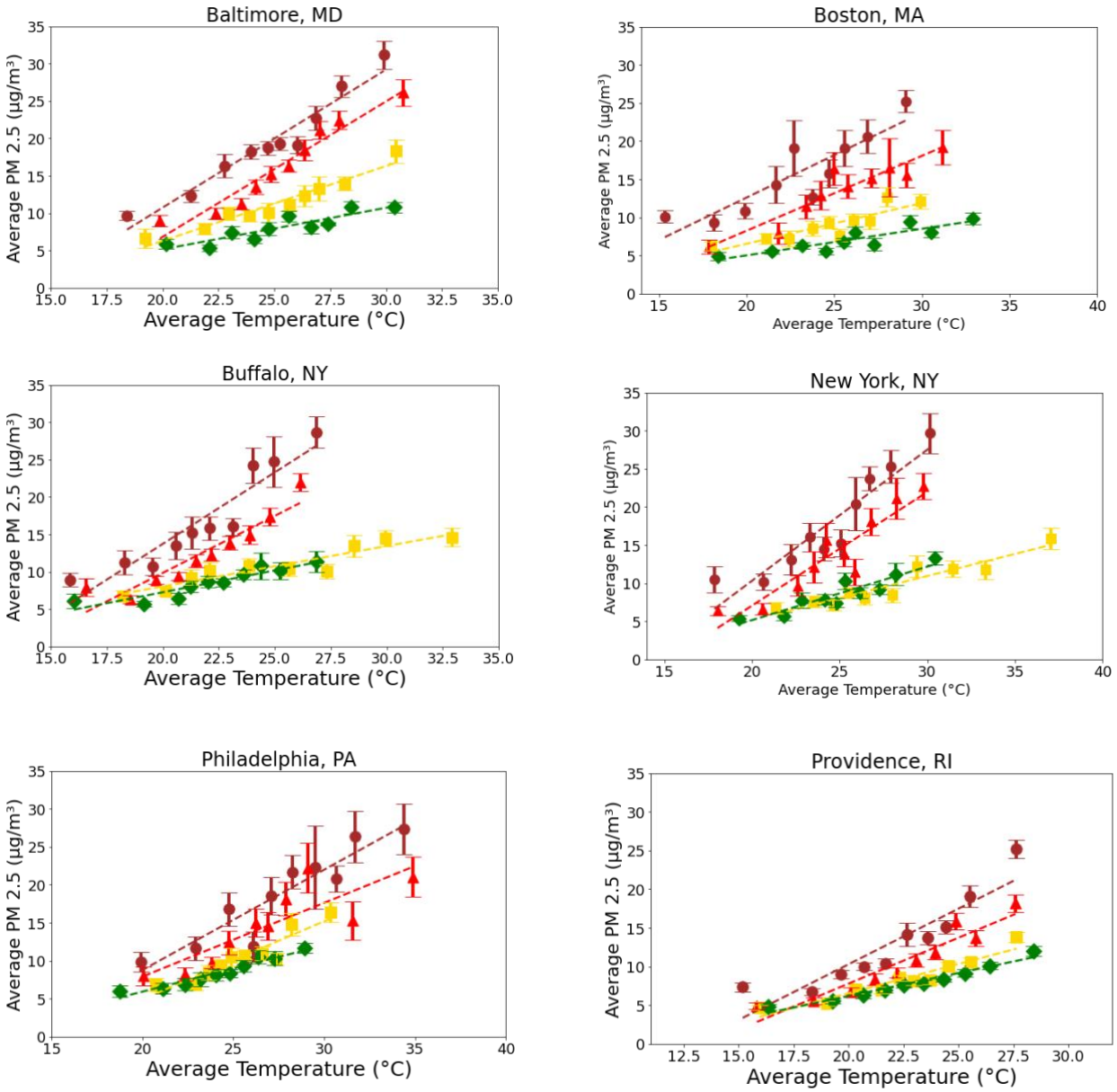

Figure A.1: Correlation between $PM_{2.5}$ and Temperature in Baltimore, MD; Boston, MA; Buffalo, NY; New York, NY; Philadelphia, PA; and Providence, RI. Error bars indicate the range of values representing 66% of the distribution within each decile bin.

● : 2000-2005; ▲ : 2006-2010; ■ : 2011-2015; ◆ : 2016-2020.

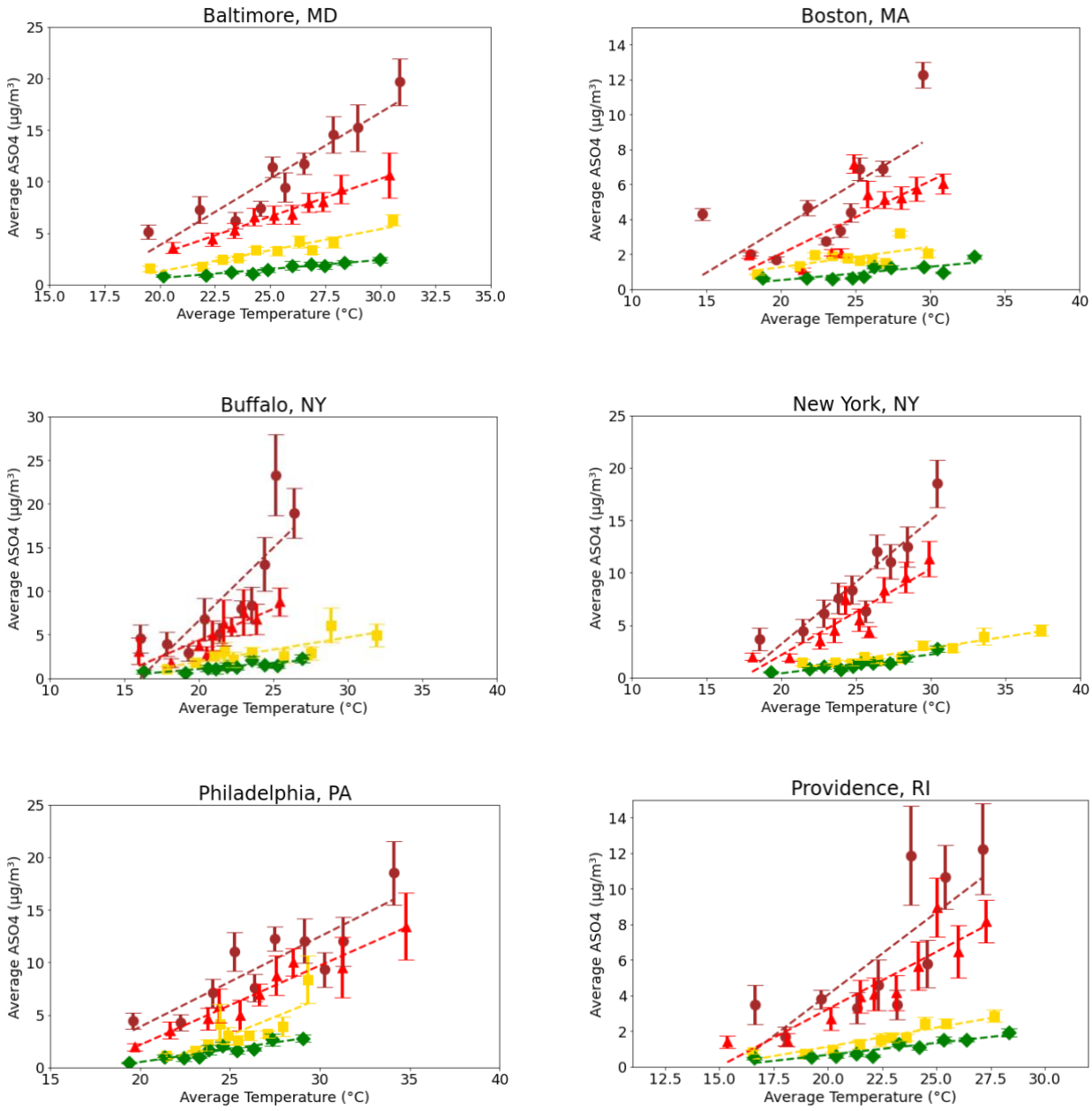

Figure A.2: Correlation between ASO_4 and Temperature in Baltimore, MD; Boston, MA; Buffalo, NY; New York, NY; Philadelphia, PA; and Providence, RI. Error bars indicate the range of values representing 66% of the distribution within each decile bin.

● : 2000-2005; ▲ : 2006-2010; ■ : 2011-2015; ◆ : 2016-2020.

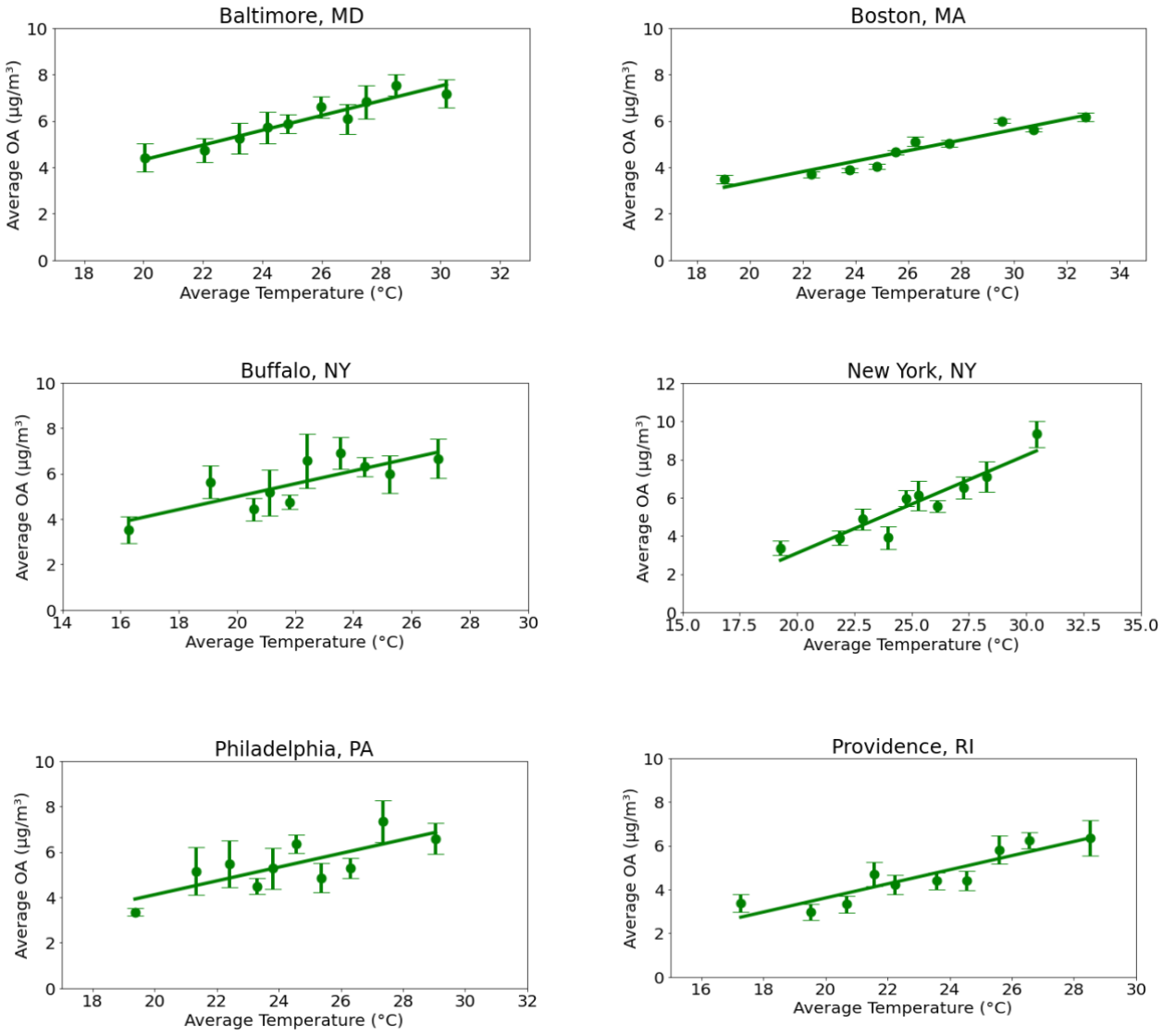

Figure A.3: Correlation between Organic Matter (OM ≡ OA = OC*2.2) and Temperature in Baltimore, MD; Boston, MA; Buffalo, NY; New York, NY; Philadelphia, PA; and Providence, RI. Error bars indicate the range of values representing 66% of the distribution within each decile bin. ◆ : 2016-2020.

Appendix B: Supplement to Chapter 3

Definitions of evaluation metrics:

The mean bias (MB) is defined as

$$\text{MB} = \frac{\sum_{i=1}^{n}(M_i - O_i)}{n} \quad \text{(S1)}$$

where the summation is over *n* data points with model values, M_i, and observed values, O_i.

The mean error (ME) (also known as the mean absolute gross error) is defined as

$$\text{ME} = \frac{\sum_{i=1}^{n}|M_i - O_i|}{n} \quad \text{(S2)}$$

where the summation is over *n* data points with model values, M_i, and observed values, O_i.

The normalized mean bias (NMB) is defined as:

$$\text{NMB} = \frac{\sum_{i=1}^{n}\frac{(M_i - O_i)}{\bar{O}}}{n} \quad \text{(S3)}$$

where the summation is over *n* data points and $\bar{O}$ represents the mean of the observed values.

The normalized mean error (NME) is defined as

$$\text{NME} = \frac{\sum_{i=1}^{n}\frac{|M_i - O_i|}{\bar{O}}}{n} \quad \text{(S4)}$$

where the summation is over *n* data points and $\bar{O}$ represents the mean of the observed values.

Specifically,

$$\bar{O} = \frac{\sum_{i=1}^{n} O_i}{n} \quad \text{(S5)}$$

The Pearson correlation coefficient is defined as

$$r = \frac{\sum_{i=1}^{n}(O_i - \bar{O})(M_i - \bar{M})}{\sqrt{\sum_{i=1}^{n}(O_i - \bar{O})^2}\sqrt{\sum_{i=1}^{n}(M_i - \bar{M})^2}} \quad \text{(S6)}$$

Table B.1: Base case model-observation summary statistics. Set represents all data points available at AQS sites across CONUS for the period June-August 2019. OC stands for organic carbon, SO_4^{2-} for sulfate, NH_4^+ for ammonium, NO_3^- for nitrate, EC for elemental carbon, NaCl for sodium chloride, "Metals" represents Fe, Al, Si, Ti, Ca, Mg, K, and Mn aerosols, O_3 is ozone, and SO_2 is sulfur dioxide gas. Note: NaCl and metals represent Aitken and accumulation mode aerosols rather than all aerosols of aerodynamic diameter smaller than 2.5 microns.

Species	Mean Observed Concentration (mg/m^3)	Mean Modeled Concentration (mg/m^3)	Mean Bias (mg/m^3)	Mean Error (mg/m^3)	Sample Size (#)
Total $PM_{2.5}$	7.29	6.06	-1.23	2.63	89,469
OC $PM_{2.5}$	1.52	1.64	0.12	0.62	7,209
SO_4^{2-} $PM_{2.5}$	0.91	0.50	-0.41	0.46	7,519
NH_4^+ $PM_{2.5}$	0.32	0.11	-0.21	0.23	7,452
NO_3^- $PM_{2.5}$	0.29	0.15	-0.14	0.18	7,479
EC $PM_{2.5}$	0.37	0.19	-0.18	0.20	7,091
NaCl	0.10	0.076	-0.03	0.07	6,103
Metals	0.45	0.33	-0.12	0.34	7,266
O_3	61.5	65.8	4.36	13.73	51,608
SO_2	3.14	1.88	-1.25	2.63	35,977

Table B.2: The same as Table B.1 but for AQS sites east of -100° Longitude.

Species	Mean Observed Concentration (mg/m^3)	Mean Modeled Concentration (mg/m^3)	Mean Bias (mg/m^3)	Mean Error (mg/m^3)	Sample Size (#)
Total $PM_{2.5}$	8.23	7.20	-1.03	2.74	52,525
OC $PM_{2.5}$	1.92	2.34	0.42	0.81	3,725
SO_4^{2-} $PM_{2.5}$	1.10	0.60	-0.50	0.56	3,911
NH_4^+ $PM_{2.5}$	0.35	0.14	-0.21	0.24	3,849
NO_3^- $PM_{2.5}$	0.30	0.15	-0.15	0.19	3,872
EC $PM_{2.5}$	0.50	0.26	-0.24	0.27	3,705
NaCl	0.09	0.07	-0.02	0.06	2,916
Metals	0.43	0.41	-0.02	0.36	3,777
O_3	57.6	64.6	7.02	12.83	38,390
SO_2	3.06	2.03	-1.03	2.53	28,191

Table B.3: Model evaluation metrics of mean bias and normalized mean bias for OC, SO_4^{2-}, and total $PM_{2.5}$, in our base case and after performing our five sensitivity simulations: (1) increasing SO_2 emissions by 40%; (2) introducing aerosol uptake of SO_2; (3) lowering the rate constant for HSO_4^-catalyzed aerosol uptake of IEPOX; (4) introducing organic aerosol photolysis; (5) altering the fate of organic nitrates to produce fewer aerosols. Set represents all data points available at AQS sites across CONUS for the period June-August 2019.

	Mean Bias (mg/m^3)			Normalized Mean Bias (%)		
	OC	**SO_4^{2-}**	**Total $PM_{2.5}$**	**OC**	**SO_4^{2-}**	**Total $PM_{2.5}$**
Base	0.12	-0.41	-1.23	7.9	-44.8	-16.8
1	0.16	-0.33	-1.03	10.8	-36.3	-14.1
2	0.33	-0.02	-0.29	21.7	-1.7	-4.0
3	-0.03	-0.30	-1.46	-2.2	-33.6	-20.0
4	-0.21	-0.40	-1.83	-13.6	-44.6	-25.0
5	-0.09	-0.40	-1.63	-6.1	-44.6	-22.4

Table B.4: The same as Table B.3 but for AQS sites east of -100° Longitude.

	Mean Bias (mg/m^3)			Normalized Mean Bias (%)		
	OC	**SO_4^{2-}**	**Total $PM_{2.5}$**	**OC**	**SO_4^{2-}**	**Total $PM_{2.5}$**
Base	0.42	-0.50	-1.03	21.7	-45.9	-12.5
1	0.51	-0.39	-0.76	26.0	-35.5	-8.7
2	0.79	-0.01	0.32	41.9	5.3	4.6
3	0.18	-0.33	-1.42	7.6	-30.0	-16.9
4	-0.002	-0.50	-1.79	-1.9	-45.6	-21.4
5	0.16	-0.50	-1.55	6.6	-45.7	-18.4

Table B.5: Model evaluation metrics of mean error and normalized mean error for OC, SO_4^{2-}, and total $PM_{2.5}$, in our base case and after performing our five sensitivity simulations: (1) increasing SO_2 emissions by 40%; (2) introducing aerosol uptake of SO_2; (3) lowering the rate constant for HSO_4^-catalyzed aerosol uptake of IEPOX; (4) introducing organic aerosol photolysis; (5) altering the fate of organic nitrates to produce fewer aerosols. Set represents all data points available at AQS sites across CONUS for the period June-August 2019.

	Mean Error (mg/m^3)			Normalized Mean Error (%)		
	OC	**SO_4^{2-}**	**Total $PM_{2.5}$**	**OC**	**SO_4^{2-}**	**Total $PM_{2.5}$**
Base	0.62	0.46	2.63	40.5	50.3	36.1
1	0.65	0.41	2.61	42.4	44.9	35.8
2	0.77	0.5	2.83	50.5	55.0	38.9
3	0.55	0.38	2.67	36.2	41.8	36.7
4	0.59	0.45	2.84	39.0	50.2	39.0
5	0.59	0.45	2.77	38.6	50.2	38.0

Table B.6: The same as Table B.5 but for AQS sites east of -100° Longitude.

	Mean Error (mg/m^3)			Normalized Mean Error (%)		
	OC	**SO_4^{2-}**	**Total $PM_{2.5}$**	**OC**	**SO_4^{2-}**	**Total $PM_{2.5}$**
Base	0.81	0.56	2.73	42.2	50.4	33.3
1	0.87	0.48	2.72	45.2	43.7	33.0
2	1.11	0.63	3.1	57.7	57.0	37.7
3	0.68	0.42	2.79	35.1	38.4	34.0
4	0.67	0.55	2.94	35.0	50.3	35.8
5	0.70	0.55	2.87	36.4	50.3	34.9

Table B.7: Pearson correlation coefficient between model predictions and observations for OC, SO_4^{2-}, and total $PM_{2.5}$, in our base case and after performing our five sensitivity simulations: (1) increasing SO_2 emissions by 40%; (2) introducing aerosol uptake of SO_2; (3) lowering the rate constant for HSO_4^- catalyzed aerosol uptake of IEPOX; (4) introducing organic aerosol photolysis; (5) altering the fate of organic nitrates to produce fewer aerosols. Set represents all data points available at AQS sites across CONUS for the period June-August 2019.

	Pearson R		
	OC	**SO_4^{2-}**	**Total $PM_{2.5}$**
Base	0.60	0.63	0.52
1	0.60	0.64	0.53
2	0.61	0.41	0.52
3	0.59	0.69	0.52
4	0.57	0.63	0.51
5	0.58	0.63	0.52

Table B.8: The same as Table B.7 but for AQS sites east of -100° Longitude.

	Pearson R		
	OC	**SO_4^{2-}**	**Total $PM_{2.5}$**
Base	0.58	0.62	0.50
1	0.57	0.63	0.50
2	0.57	0.38	0.49
3	0.59	0.70	0.50
4	0.55	0.62	0.49
5	0.57	0.62	0.49

Table B.9: Observed and modeled temperature sensitivity of OC, SO_4^{2-}, and total $PM_{2.5}$, in our base case and after performing our five sensitivity simulations: (1) increasing SO_2 emissions by 40%; (2) introducing aerosol uptake of SO_2; (3) lowering the rate constant for HSO_4^-catalyzed aerosol uptake of IEPOX; (4) introducing organic aerosol photolysis; (5) altering the fate of organic nitrates to produce fewer aerosols. Set represents data aggregated by AQS sites across CONUS for the period June-August 2019 and meeting the filtering criteria described in the Methods section.

	Observed Temperature Sensitivity ($mg/m^3/°C$)			**Modeled Temperature Sensitivity ($mg/m^3/°C$)**		
	OC	**SO_4^{2-}**	**Total $PM_{2.5}$**	**OC**	**SO_4^{2-}**	**Total $PM_{2.5}$**
Base	0.09	0.08	0.56	0.13	0.02	0.49
1				0.14	0.03	0.52
2				0.17	0.05	0.61
3				0.12	0.04	0.46
4				0.10	0.02	0.43
5				0.12	0.02	0.46

Table B.10: The same as Table B.9 but for AQS sites east of -100° Longitude.

	Observed Temperature Sensitivity ($mg/m^3/°C$)			**Modeled Temperature Sensitivity ($mg/m^3/°C$)**		
	OC	**SO_4^{2-}**	**Total $PM_{2.5}$**	**OC**	**SO_4^{2-}**	**Total $PM_{2.5}$**
Base	0.11	0.12	0.67	0.22	0.03	0.61
1				0.23	0.04	0.65
2				0.29	0.08	0.78
3				0.18	0.05	0.56
4				0.16	0.03	0.52
5				0.19	0.03	0.56

Figure B.1: Agreement between modeled and observed daily average temperatures for all data points available at AQS sites across CONUS for June to August 2019.

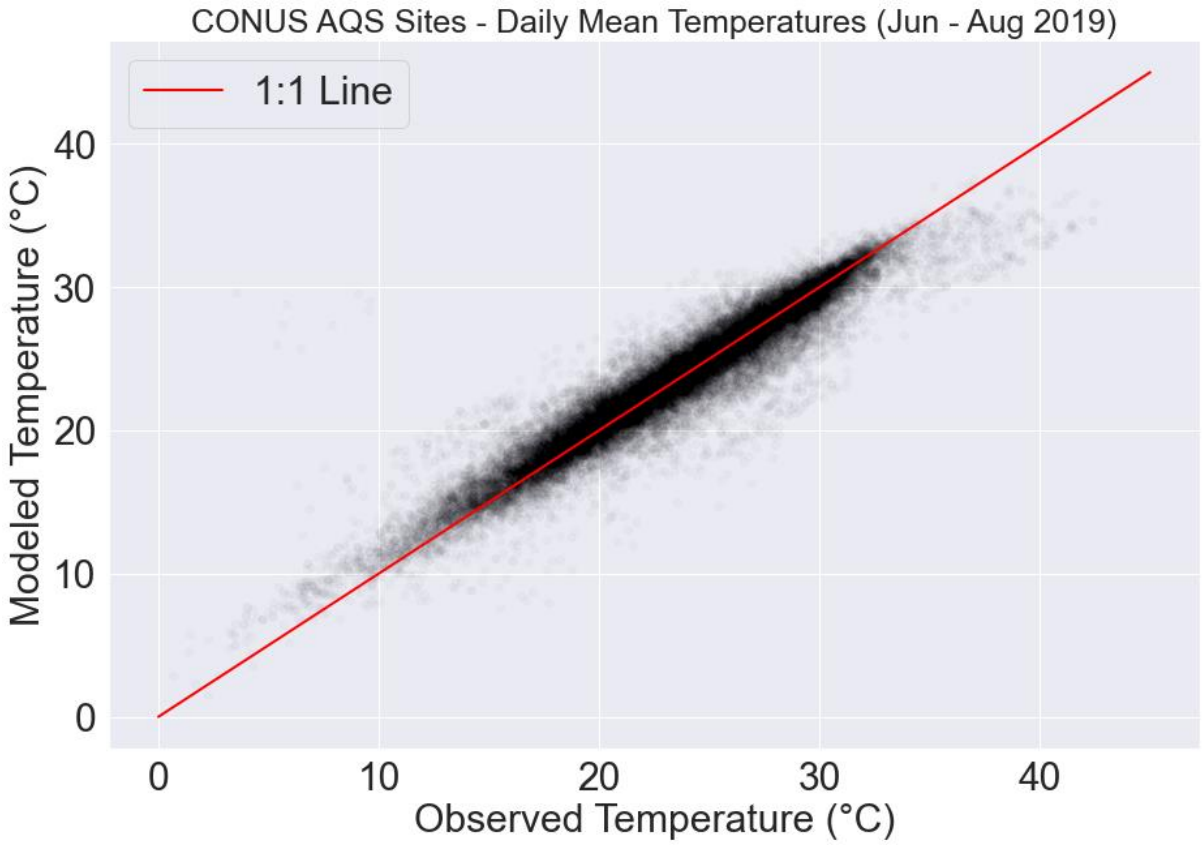

Figure B.2: Analogous to Figure 3.3 in the manuscript but featuring normalized mean error rather than normalized mean bias.

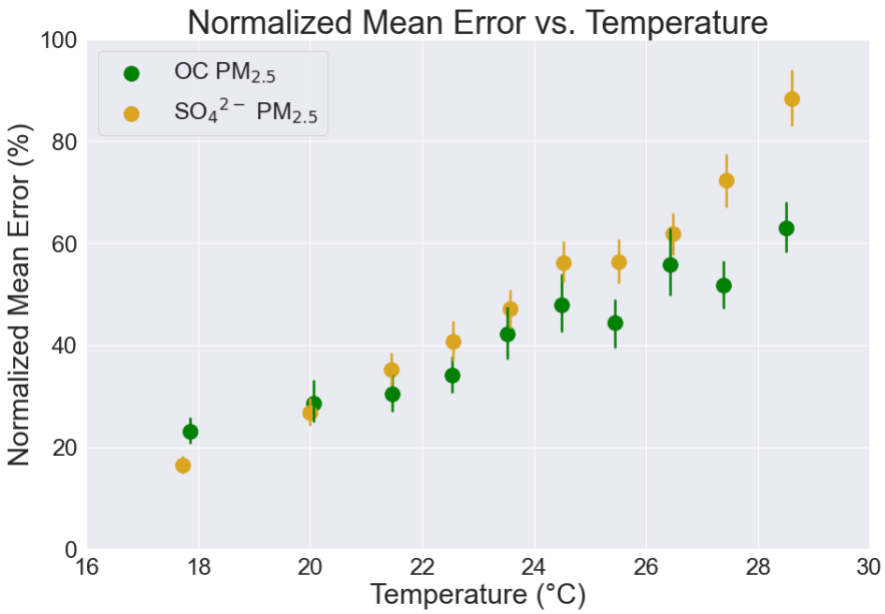

Figure B.3: Analogous to Figure 3.3 in the manuscript, showing how normalized mean bias in OC $PM_{2.5}$ with temperature increases as a result of utilizing the inline MEGAN 3.2 biogenic emissions module instead of the default BEIS module.

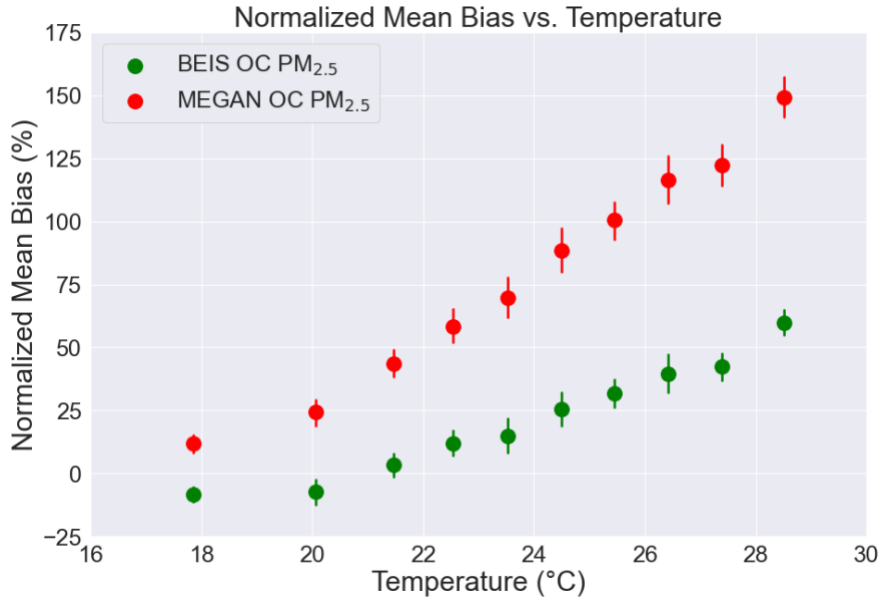

Appendix C: Supplement to Chapter 4

Table C.1: EPA AQS Sites utilized in this study. Sites were queried to obtain hourly observations of NO_2, NO_x, and CO for the period of May to September (inclusive) from 2000-2019.

EPA AQS Site ID	Latitude	Longitude
06-037-0002	34.1365	-117.92391
06-037-0113	34.05111	-118.45636
06-037-1103	34.06659	-118.22688
06-037-1201	34.19925	-118.53276
06-037-1701	34.06703	-117.7514
06-065-8001	33.99958	-117.41601
06-071-9004	34.106678	-117.274063

Table C.2: Average concentrations of all day (A = 00:00-23:00), daytime only (D = 10:00-17:00), and nighttime only (N = 22:00-05:00) NO_2, NO_x, and CO at each of the above AQS sites for the periods of 2000-2004, 2005-2009, 2010-2014, and 2015-2019. Units are in parts per billion (ppb).

AQS Site	Species	2000-2004			2005-2009			2010-2014			2015-2019		
		A	D	N	A	D	N	A	D	N	A	D	N
06-037-0002	NO_2	30.9	30.1	29.	24.0	22.1	23.4	19.7	16.7	20.7	14.7	12.1	15.6
	NO_x	44.0	36.1	43.	33.6	26.6	32.9	24.8	19.2	25.2	18.0	13.6	18.8
	CO	741	704	714	437	410	421	394	371	398	340	320	341
06-037-0113	NO_2	16.6	10.9	20.	12.6	7.9	16.2	9.4	5.2	13.2	6.4	3.4	9.1
	NO_x	25.7	13.6	36.	20.2	10.9	27.3	12.4	6.3	17.4	7.7	3.9	10.5
	CO	281	157	388	287	200	352	237	186	274	233	185	273
06-037-1103	NO_2	32.0	28.8	31.	24.0	20.6	25.3	19.1	14.9	21.0	14.6	11.1	16.7
	NO_x	50.3	34.4	58.	36.7	25.1	41.5	27.4	18.4	31.0	19.9	13.4	22.7
	CO	682	574	703	372	303	390	396	345	411	326	280	356
06-037-1201	NO_2	23.6	16.2	28.	16.8	11.0	20.6	13.1	8.1	16.8	9.0	5.5	11.4
	NO_x	31.5	17.8	40.	22.8	13.4	27.8	15.5	8.7	19.4	10.8	6.4	13.1
	CO	591	427	683	368	273	415	300	240	328	310	259	340
06-037-1701	NO_2	36.3	33.7	34.	27.9	23.2	29.8	20.6	15.4	23.6	15.3	10.5	18.4
	NO_x	61.2	42.4	69.	44.6	30.2	50.6	29.9	19.1	34.2	21.2	13.4	24.3
	CO	810	676	838	498	416	521	252	194	277	263	219	282
06-065-8001	NO_2	20.1	13.6	23.	16.8	11.2	20.5	12.2	7.2	16.0	9.8	5.3	13.1
	NO_x	31.7	14.7	42.	25.6	13.2	32.6	17.1	8.2	22.5	12.9	5.7	17.2
	CO	630	499	717	390	306	442	337	277	380	269	217	306
06-071-9004	NO_2	31.5	25.1	34.	24.4	18.2	28.7	17.7	12.0	22.2	14.2	8.8	18.5
	NO_x	44.2	30.4	52.	33.2	22.1	39.1	21.5	13.7	25.8	17.3	10.2	21.7
	CO	694	561	771	388	318	419	356	309	385	344	300	370

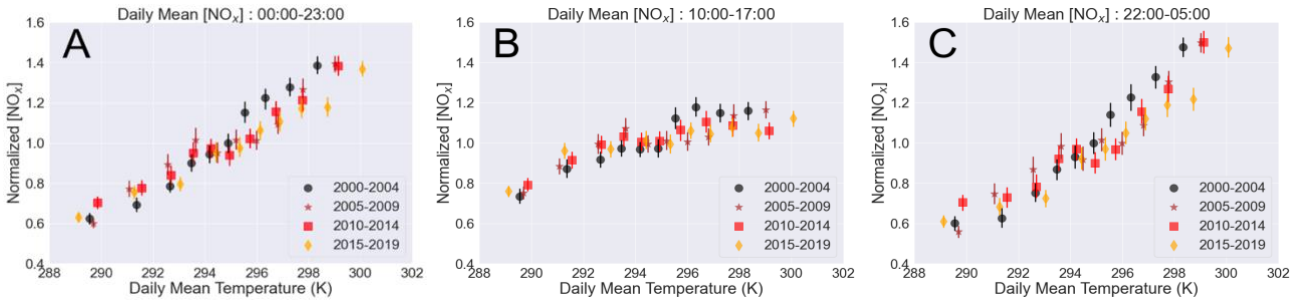

Figure C.1: Mean daily normalized concentrations of NO_x binned by temperature decile resampled from either (A) all hours of the day, (B) 10:00-17:00, and (C) 22:00-5:00. Error bars represent the bootstrapped 95% confidence interval for the median of each bin.